



Measurement of $Z\gamma\gamma$ production in pp collisions at $\sqrt{s} = 13$ TeV with the ATLAS detector

The ATLAS Collaboration

Cross-sections for the production of a Z boson in association with two photons are measured in proton–proton collisions at a centre-of-mass energy of 13 TeV. The data used correspond to an integrated luminosity of 139 fb^{-1} recorded by the ATLAS experiment during Run 2 of the LHC. The measurements use the electron and muon decay channels of the Z boson, and a fiducial phase-space region where the photons are not radiated from the leptons. The integrated $Z(\rightarrow \ell\ell)\gamma\gamma$ cross-section is measured with a precision of 12% and differential cross-sections are measured as a function of six kinematic variables of the $Z\gamma\gamma$ system. The data are compared with predictions from MC event generators which are accurate to up to next-to-leading order in QCD. The cross-section measurements are used to set limits on the coupling strengths of dimension-8 operators in the framework of an effective field theory.

arXiv:2211.14171v2 [hep-ex] 14 Jul 2023

Contents

1	Introduction	2
2	The ATLAS detector	4
3	Data and simulated event samples	4
4	Event reconstruction and selection	5
5	Backgrounds	8
5.1	$j \rightarrow \gamma$ backgrounds	8
5.2	Other backgrounds	11
6	Systematic uncertainties	12
7	Cross-section determination	13
7.1	Fiducial volume definition	13
7.2	Cross-section extraction	14
7.3	Results	15
8	EFT interpretation	20
8.1	Non-unitarised limits	21
8.2	Unitarisation treatment	21
9	Conclusions	24

1 Introduction

Processes involving the production of three electroweak (EW) gauge bosons from proton–proton collisions are typically rare. Some of these triboson processes are only just becoming accessible due to the unprecedented integrated luminosity provided during Run 2 of the CERN LHC. Measurements of such processes provide a direct probe of non-Abelian quartic gauge couplings, both those that are predicted by the Standard Model (SM) and those that could only be due to new physics. The production of a Z boson in association with two prompt photons provides an opportunity to test the electroweak sector of the SM and to constrain any potential new physics effects. Neutral quartic gauge couplings are not allowed in the SM, and hence the production of $Z\gamma\gamma$ has no tree-level contribution involving quartic couplings. In this paper, the leptonic decay channels of the Z boson, i.e. $Z \rightarrow \ell^+\ell^-$ where $\ell = e, \mu$, are considered. Despite having lower branching fractions than the quark and neutrino decay channels, the leptonic channels benefit from having a cleaner final state and smaller backgrounds. The measurement of $Z\gamma\gamma$ is also crucial for our understanding of the irreducible background to $Z(\rightarrow \ell\ell)H(\rightarrow \gamma\gamma)$ production, and for searches for resonances in the $\ell\ell\gamma\gamma$ final state.

The production of $\ell\ell\gamma\gamma$ from proton–proton collisions proceeds at leading order by diagrams of the first three types given in Figure 1. The production of $\ell\ell\gamma\gamma$ via three on-shell bosons is shown in Figure 1(a), where both of the photons are produced via initial-state radiation (ISR). In Figures 1(b) and 1(c), one or both of the photons are produced via final-state radiation (FSR). The main sources of background

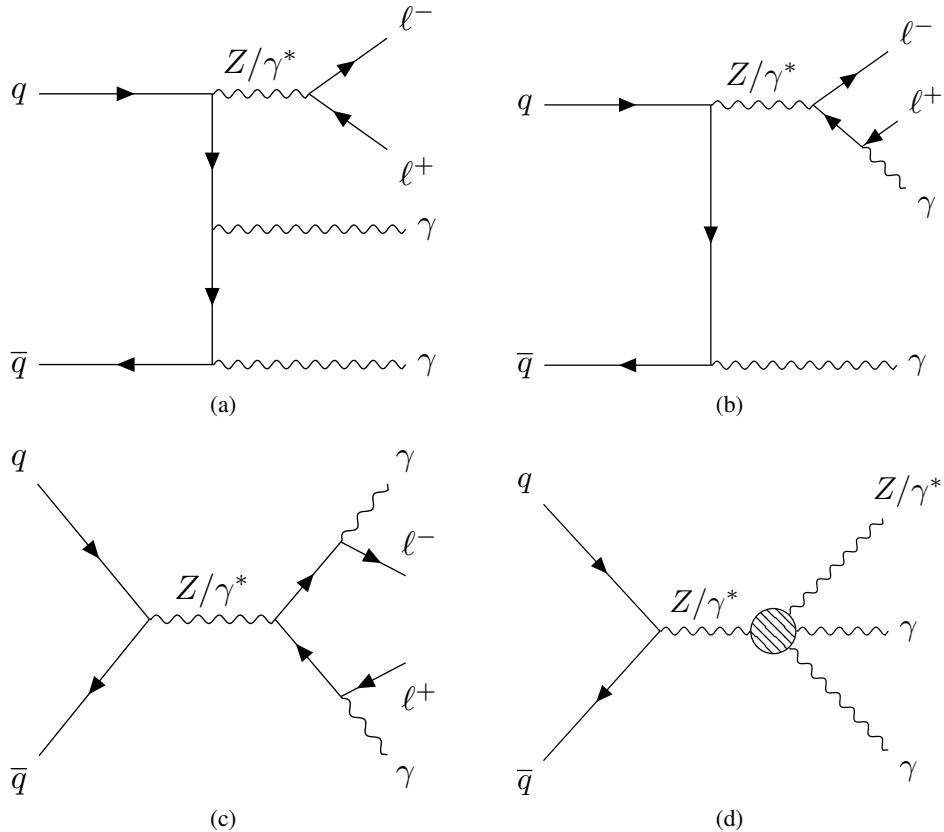


Figure 1: (a) Standard Model production of $Z(\rightarrow \ell\ell)\gamma\gamma$ at leading order. (b-c) Standard Model production of $\ell\ell\gamma\gamma$ involving final-state radiation, which is not considered as signal in this paper. (d) Production of $\ell\ell\gamma\gamma$ involving an anomalous quartic coupling between neutral EW gauge bosons.

to this signal arise from processes involving jets which are misidentified as photons. Previous studies of the $\ell\ell\gamma\gamma$ final state with the ATLAS detector at $\sqrt{s} = 8$ TeV [1], and the CMS detector at 8 TeV [2] and 13 TeV [3], were performed in phase spaces which included both the ISR and FSR production of photons. The measurement presented in this paper suppresses the FSR contribution, which allows a simpler interpretation of the measurements since the dominant signal contribution comes through the production of three on-shell bosons. The $\ell\ell\gamma\gamma$ final state is also sensitive to new physics via anomalous quartic couplings, an example of which is shown in Figure 1(d).

The measurements use $pp \rightarrow e^+e^-\gamma\gamma + X$ and $pp \rightarrow \mu^+\mu^-\gamma\gamma + X$ events recorded by the ATLAS detector at $\sqrt{s} = 13$ TeV. The ATLAS detector is described in Section 2. The full Run 2 dataset corresponding to an integrated luminosity of 139 fb^{-1} is used. It is described in Section 3 along with simulated event samples. The event selection is given in Section 4. Background processes are estimated using a combination of data-driven techniques and simulation, which are described in Section 5. The systematic uncertainties are discussed in Section 6. The yields of signal events are corrected (unfolded) to a fiducial volume where the integrated (differential) cross-section is measured; the unfolding procedures and results are described in Section 7. Differential cross-sections are measured as a function of the transverse energy $E_T^{\gamma 1}$ of the leading (highest p_T) photon, the transverse energy $E_T^{\gamma 2}$ of the subleading photon, the transverse momentum $p_T^{\ell\ell}$ of the dilepton system, the transverse momentum $p_T^{\ell\ell\gamma\gamma}$ of the four-body system, the invariant mass $m_{\gamma\gamma}$ of the diphoton system, and the invariant mass $m_{\ell\ell\gamma\gamma}$ of the four-body system. The

$E_T^{\gamma 1}$, $E_T^{\gamma 2}$ and $p_T^{\ell\ell}$ distributions measure the transverse momentum of one of the three bosons in the event. The $p_T^{\ell\ell\gamma\gamma}$ distribution is a measure of the hadrons recoiling against the $\ell\ell\gamma\gamma$ system and is hence sensitive to QCD modelling. The $m_{\gamma\gamma}$ distribution is useful for constraining backgrounds to $\gamma\gamma$ resonances in the $\ell\ell\gamma\gamma$ final state, and the $m_{\ell\ell\gamma\gamma}$ spectrum describes the scale of the full four-body system. The data are compared with predictions from Monte Carlo (MC) event generators with matrix elements calculated to up to next-to-leading order (NLO) in perturbative QCD. The differential $p_T^{\ell\ell}$ measurement is also used to constrain new physics effects arising through anomalous neutral quartic couplings. This is done via an effective field theory (EFT) approach, where limits are set on the coupling strengths of dimension-8 operators. This procedure and the measured limits are presented in Section 8. The conclusions are stated in Section 9.

2 The ATLAS detector

The ATLAS experiment [4] at the LHC is a multipurpose particle detector with a forward–backward symmetric cylindrical geometry and a near 4π coverage in solid angle.¹ It consists of an inner tracking detector (ID) surrounded by a thin superconducting solenoid providing a 2 T axial magnetic field, electromagnetic and hadron calorimeters, and a muon spectrometer. The inner tracking detector covers the pseudorapidity range $|\eta| < 2.5$. It consists of silicon pixel, silicon microstrip, and transition radiation tracking detectors. Lead/liquid-argon (LAr) sampling calorimeters provide electromagnetic (EM) energy measurements with high granularity. A steel/scintillator-tile hadron calorimeter covers the central pseudorapidity range (referred to as the barrel), covering $|\eta| < 1.7$. The endcap and forward regions are instrumented with LAr calorimeters for both the EM and hadronic energy measurements up to $|\eta| = 4.9$. The muon spectrometer surrounds the calorimeters and is based on three large superconducting air-core toroidal magnets with eight coils each. The field integral of the toroids ranges between 2.0 and 6.0 T m across most of the detector. The muon spectrometer (MS) includes a system of precision tracking chambers and fast detectors for triggering. A two-level trigger system is used to select events. The first-level trigger is implemented in hardware and uses a subset of the detector information to accept events at a rate below 100 kHz. This is followed by a software-based trigger that reduces the accepted event rate to 1 kHz on average depending on the data-taking conditions. An extensive software suite [5] is used in data simulation, in the reconstruction and analysis of real and simulated data, in detector operations, and in the trigger and data acquisition systems of the experiment.

3 Data and simulated event samples

The data used in this analysis were collected in proton–proton collisions at $\sqrt{s} = 13$ TeV from 2015 to 2018. After applying criteria to ensure normal ATLAS detector operation [6], the total integrated luminosity useful for data analysis is 139 fb^{-1} . The uncertainty in the total Run 2 integrated luminosity is 1.7% [7], obtained using the LUCID-2 detector [8] for the primary luminosity measurements. The average number of inelastic pp interactions produced per bunch-crossing for the dataset considered is $\langle\mu\rangle = 33.7$.

¹ ATLAS uses a right-handed coordinate system with its origin at the nominal interaction point (IP) in the centre of the detector and the z -axis along the beam pipe. The x -axis points from the IP to the centre of the LHC ring, and the y -axis points upwards. Cylindrical coordinates (r, ϕ) are used in the transverse plane, ϕ being the azimuthal angle around the z -axis. The pseudorapidity is defined in terms of the polar angle θ as $\eta = -\ln \tan(\theta/2)$. Angular distance is measured in units of $\Delta R \equiv \sqrt{(\Delta\eta)^2 + (\Delta\phi)^2}$.

Simulated event samples are used to correct the background-subtracted data yield for detector effects and to estimate several background contributions. The simulated samples were produced with various MC event generators, processed through a full ATLAS detector simulation [9] based on GEANT4 [10], and reconstructed using the same algorithms as used for data. All simulated samples were corrected with data-driven correction factors to account for differences in trigger, reconstruction, identification and isolation performance between data and simulation. Additional pp interactions (pile-up) occurring in the same or neighbouring bunch-crossings were modelled by overlaying each simulated event with minimum-bias events generated using PYTHIA 8.186 [11] with the A3 set of tuned parameters [12] and the NNPDF2.3LO [13] set of parton distribution functions (PDFs). The simulated events were then reweighted to reproduce the distribution of the number of pp interactions per bunch-crossing observed in the data.

Samples of simulated $e^+e^-\gamma\gamma$ and $\mu^+\mu^-\gamma\gamma$ events were generated using SHERPA 2.2.10 [14] at NLO accuracy in QCD for zero additional partons and LO accuracy for up to two additional partons. Matrix elements were matched and merged with the SHERPA parton shower [15] based on Catani–Seymour dipole factorisation [15, 16] using the MEPS@NLO prescription [17–20]. The NNPDF3.0NNLO [21] set of PDFs were used.

For studies of systematic uncertainties and cross-checks, an alternative signal sample is considered. It was produced with the MADGRAPH5_AMC@NLO 2.7.3 [22] generator with up to one additional final-state parton at NLO accuracy, using the NNPDF3.0NLO PDF set. Events were interfaced to PYTHIA 8.244 [23], via the FxFx merging procedure [24], for modelling of the parton shower, hadronisation and underlying event. Both the baseline and alternative signal samples utilise smooth-cone photon isolation [25], with the parameters $\delta_0 = 0.1$, $\epsilon = 0.1$ and $n = 2$, to remove contributions from fragmentation photons.

The $Z\gamma$ + jets (Z + jets) samples used in the estimation of misidentified-photon backgrounds were generated with SHERPA 2.2.4 (POWHEG BOX v1 [26–29]). Truth-level selections on the photon candidates and their parent particles are used to separate these two samples into three distinct misidentified-photon background components. The $t\bar{t}\gamma$ sample used in the estimation of the background where the leptons originate from top quark decays was generated with MADGRAPH5_AMC@NLO 2.3.3. The backgrounds arising from electrons misidentified as photons were modelled with SHERPA 2.2.2 ($ZZ \rightarrow \ell\ell\ell$) and SHERPA 2.2.5 ($WZ\gamma \rightarrow \ell\nu\ell\ell\gamma$). The contribution from $Z(\rightarrow \ell\ell)H(\rightarrow \gamma\gamma)$ was generated with POWHEG BOX v2. The single-photon and diphoton samples used in the estimation of the pile-up overlay backgrounds were modelled using SHERPA 2.2.2. Further details are given in Table 1, along with a summary of the signal samples.

4 Event reconstruction and selection

Events are selected in the electron and muon channels using unrescaled single-lepton triggers [31, 32] with the lowest p_T threshold available. From 2016 to 2018, this was 26 GeV for both electrons and muons, and in 2015 it was 24 GeV for electrons and 20 GeV for muons. The low- p_T triggers are supplemented by higher ones with relaxed identification and isolation requirements which improve the overall trigger efficiency. Reconstructed tracks in the ID and clusters of energy deposits in the EM calorimeter are used as inputs in the reconstruction of electrons and photons [33]. Reconstructed track segments in the ID and MS are used as inputs in the reconstruction of muons [34].

Electron candidates are seeded by EM calorimeter energy clusters and must have $p_T > 20$ GeV, $|\eta| < 2.47$, and a matching ID track. The transition region between the barrel and endcap of the EM calorimeter

Table 1: Summary of simulated MC event samples for the $ll\gamma\gamma$ signal process and those used in the estimation of backgrounds. The third and fourth columns give the order in perturbative QCD and the PDF set used in the hard-scattering matrix element calculations. The rightmost column specifies the generator used to model parton showering, hadronisation, the underlying event and multiple parton interactions.

	Process	Generator	Order	PDF Set	PS/UE/MPI
Signal	$ll\gamma\gamma$	SHERPA 2.2.10	NLO	NNPDF3.0NNLO	SHERPA 2.2.10
	$ll\gamma\gamma$	MADGRAPH5_AMC@NLO 2.7.3	NLO	NNPDF3.0NLO	PYTHIA 8.244
Background	$Z\gamma$ + jets	SHERPA 2.2.4	LO	NNPDF3.0NNLO	SHERPA 2.2.4
	Z + jets	POWHEG BOX v1	NLO	CT10NLO [30]	PYTHIA 8.186
	$t\bar{t}\gamma$	MADGRAPH5_AMC@NLO 2.3.3	LO	NNPDF2.3LO	PYTHIA 8.212
	$ZZ \rightarrow llll$	SHERPA 2.2.2	NLO	NNPDF3.0NNLO	SHERPA 2.2.2
	$WZ\gamma \rightarrow l\nu ll\gamma$	SHERPA 2.2.5	NLO	NNPDF3.0NNLO	SHERPA 2.2.5
	$Z(\rightarrow ll)H(\rightarrow \gamma\gamma)$	POWHEG BOX v2	NLO	NNPDF3.0NLO	PYTHIA 8.212
	γ + jets	SHERPA 2.2.2	NLO	NNPDF3.0NNLO	SHERPA 2.2.2
	$\gamma\gamma$ + jets	SHERPA 2.2.2	NLO	NNPDF3.0NNLO	SHERPA 2.2.2

($1.37 < |\eta| < 1.52$) is excluded. Electrons are identified using a likelihood discriminant formed from shower shape variables, track variables and a measure of how well the track matches the cluster. All electron candidates must satisfy the *Medium* identification working point [33]. To suppress the contribution from jets misidentified as electrons, the electron candidates must be isolated from other activity in the tracking and calorimeter systems. The calorimeter and tracking isolation variables are constructed, respectively, from the sums of cluster energies and track momenta falling within a cone of size $\Delta R = 0.2$ around the electron, which are then required to satisfy the *Loose* working point described in Ref. [33].

Muon candidates are formed from tracks and must have $p_T > 20$ GeV and $|\eta| < 2.5$. Identification requirements comprise selections on track quality and a measure of how well the ID track matches the MS track. Muon candidates must pass the *Medium* identification working point [34]. The muon candidates are also required to be isolated in the tracking and calorimeter systems using variables similar to those for electrons, in a variable-sized cone up to a maximum of $\Delta R = 0.3$. The *Loose* isolation working point is used and is similar to that described in Ref. [34].

Reconstructed tracks matched to common points of origin along the beam axis serve as candidates for the location of proton–proton collisions (vertices). The vertex with the largest sum of the track p_T^2 is chosen as the primary vertex (PV). Electrons and muons must be consistent with originating from the PV, requiring that their transverse impact parameter significance satisfies $|d_0|/\sigma_{d_0} < 3$ (5) for muons (electrons) and the longitudinal distance z_0 from the PV to the point where d_0 is measured satisfies $|z_0 \sin(\theta)| < 0.5$ mm.

Photon candidates are seeded by EM calorimeter energy clusters which have $p_T > 20$ GeV and $|\eta| < 2.37$. The transition region between the barrel and endcap of the EM calorimeter ($1.37 < |\eta| < 1.52$) is excluded. Converted photon candidates are formed from clusters which are matched to a conversion vertex. The conversion vertices are formed from one or two tracks which are consistent with a massless particle converting within the ID volume. Unconverted photon candidates are formed from clusters which are not matched to an electron track or conversion vertex. Photon candidates are required to pass a number of selections on shower shape variables which correspond to the *Loose* identification working point [33].

Overlap removal requirements are applied to the preliminarily selected objects to prevent the same particle

from being reconstructed as two separate physics objects. Photons are removed if they are within $\Delta R = 0.4$ of a selected electron or muon. Electrons are removed if they are within $\Delta R = 0.2$ of a selected muon.

Correction factors are applied to the selected objects to account for object trigger, reconstruction, identification and isolation efficiency differences between data and simulation.

Candidate events are considered further if they contain at least one opposite-sign same-flavour lepton pair and at least two photons. One of the leptons must be matched to the trigger object which fired the event, and the highest- p_T (leading) lepton must have $p_T > 30$ GeV to be well above the trigger threshold. If an electron (muon) pair is selected, the leading electron (muon) must pass the *Tight* identification [33] (*Tight* isolation) requirement. The invariant mass of the dilepton pair must be above 40 GeV in order to remove contributions from low-mass resonances.

The two highest- p_T photons in the event that pass the *Tight* identification and *Loose* isolation [33] requirements are selected. The two selected photons must be separated from each other by at least $\Delta R = 0.4$. Finally, the contribution from FSR photons is suppressed by requiring that the sum of the dilepton invariant mass and the smaller of the two three-body invariant masses, formed from the dilepton system and each of the two photons, is greater than twice the Z boson rest mass. The selection criterion ($m_{\ell\ell} + \min(m_{\ell\ell\gamma_1}, m_{\ell\ell\gamma_2}) > 2m_Z$) is motivated by the fact that, at the generator level, it provides absolute distinction between ISR and FSR events when the Z boson is on-shell. The effect of this selection at the detector level is illustrated in Figure 2.

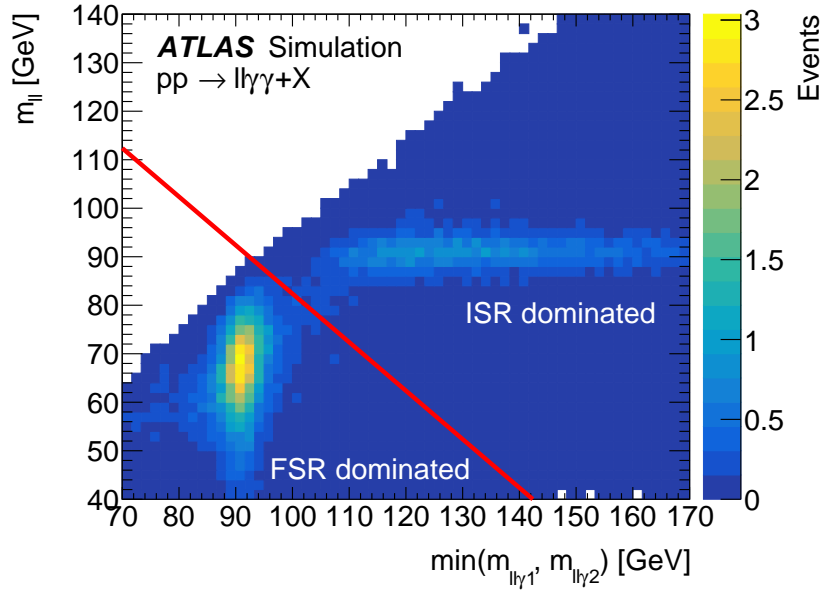


Figure 2: The predicted detector-level distribution in SHERPA 2.2.10 simulation of the dilepton invariant mass versus the smaller of the two three-body masses formed from the dilepton system and each of the two photons. The events are subject to the full set of signal region requirements, with the exception of the FSR removal selection ($m_{\ell\ell} + \min(m_{\ell\ell\gamma_1}, m_{\ell\ell\gamma_2}) > 2m_Z$). The cut value is indicated by the red line.

5 Backgrounds

The dominant background contributions to $\ell\ell\gamma\gamma$ arise from processes involving jets misidentified as photons (referred to as $j \rightarrow \gamma$ backgrounds), and are estimated using a data-driven method. These backgrounds account for approximately 20% of the data yield in the signal region. A small contribution is expected from electrons misidentified as photons (referred to as $e \rightarrow \gamma$ backgrounds), and is estimated from simulation. The remaining backgrounds, which are small, come from processes involving prompt photons, and are also estimated from simulation. The largest of the prompt-photon backgrounds arises from $t\bar{t}\gamma\gamma$ events, which contribute approximately 5% of the events selected in the signal region.

The number of data events selected in each channel is given in Table 2 along with the estimated background yields. The data yield in the muon channel is higher than in the electron channel because the muons have a higher reconstruction efficiency than electrons, and also a larger detector acceptance. Table 2 also shows the extracted number of signal events in data (i.e. data minus background), which is compared with predictions from both signal event generators for each channel. The detector-level $E_T^{\gamma 1}$, $E_T^{\gamma 2}$ and $m_{\ell\ell\gamma\gamma}$ data distributions, in both the electron and muon channels, are compared with the signal-plus-background predictions in Figure 3. The estimation of the different backgrounds is described in the following subsections.

Table 2: The observed data yield, background composition and estimated signal yield is given for each channel. The signal yield predictions from both of the MC event generators are also given. The statistical uncertainty of the signal predictions and all backgrounds besides the $j \rightarrow \gamma$ background (second row) is due to the limited number of generated simulation events.

	$e^+e^-\gamma\gamma$	$\mu^+\mu^-\gamma\gamma$
Data	148	171
Background predictions		
$Z\gamma j + Zj\gamma + Zjj$	29.8 ± 5.7 (stat.) ± 5.5 (sys.)	34.4 ± 6.6 (stat.) ± 6.3 (sys.)
$t\bar{t}\gamma\gamma$	6.4 ± 0.4 (stat.) ± 1.4 (sys.)	8.4 ± 0.5 (stat.) ± 1.8 (sys.)
$ZZ \rightarrow \ell\ell\ell\ell$	1.03 ± 0.10 (stat.) ± 0.51 (sys.)	1.24 ± 0.11 (stat.) ± 0.62 (sys.)
$WZ\gamma \rightarrow \ell\nu\ell\ell\gamma$	0.69 ± 0.06 (stat.) ± 0.35 (sys.)	0.52 ± 0.05 (stat.) ± 0.26 (sys.)
$Z(\rightarrow \ell\ell)H(\rightarrow \gamma\gamma)$	1.08 ± 0.01 (stat.) ± 0.22 (sys.)	1.38 ± 0.01 (stat.) ± 0.28 (sys.)
$Z\gamma + \gamma$	2.07 ± 0.16 (stat.) ± 0.72 (sys.)	2.74 ± 0.21 (stat.) ± 0.96 (sys.)
$Z + \gamma\gamma$	1.44 ± 0.04 (stat.) ± 0.39 (sys.)	1.90 ± 0.05 (stat.) ± 0.51 (sys.)
Data – background	105.5 ± 12.2 (stat.) ± 8.1 (sys.)	120.4 ± 13.1 (stat.) ± 9.4 (sys.)
Signal predictions		
SHERPA NLO	91.5 ± 0.9 (stat.)	119.5 ± 1.0 (stat.)
MADGRAPH5_AMC@NLO	91.0 ± 1.0 (stat.)	118.1 ± 1.2 (stat.)

5.1 $j \rightarrow \gamma$ backgrounds

Processes involving jets misidentified as prompt photons populate the $\ell\ell\gamma\gamma$ signal region. They typically involve light-hadron decays into a pair of photons within jets. In these processes, one or both of the photon candidates are misidentified jets; these are divided into $Z\gamma j$, $Zj\gamma$ and Zjj categories, the first two

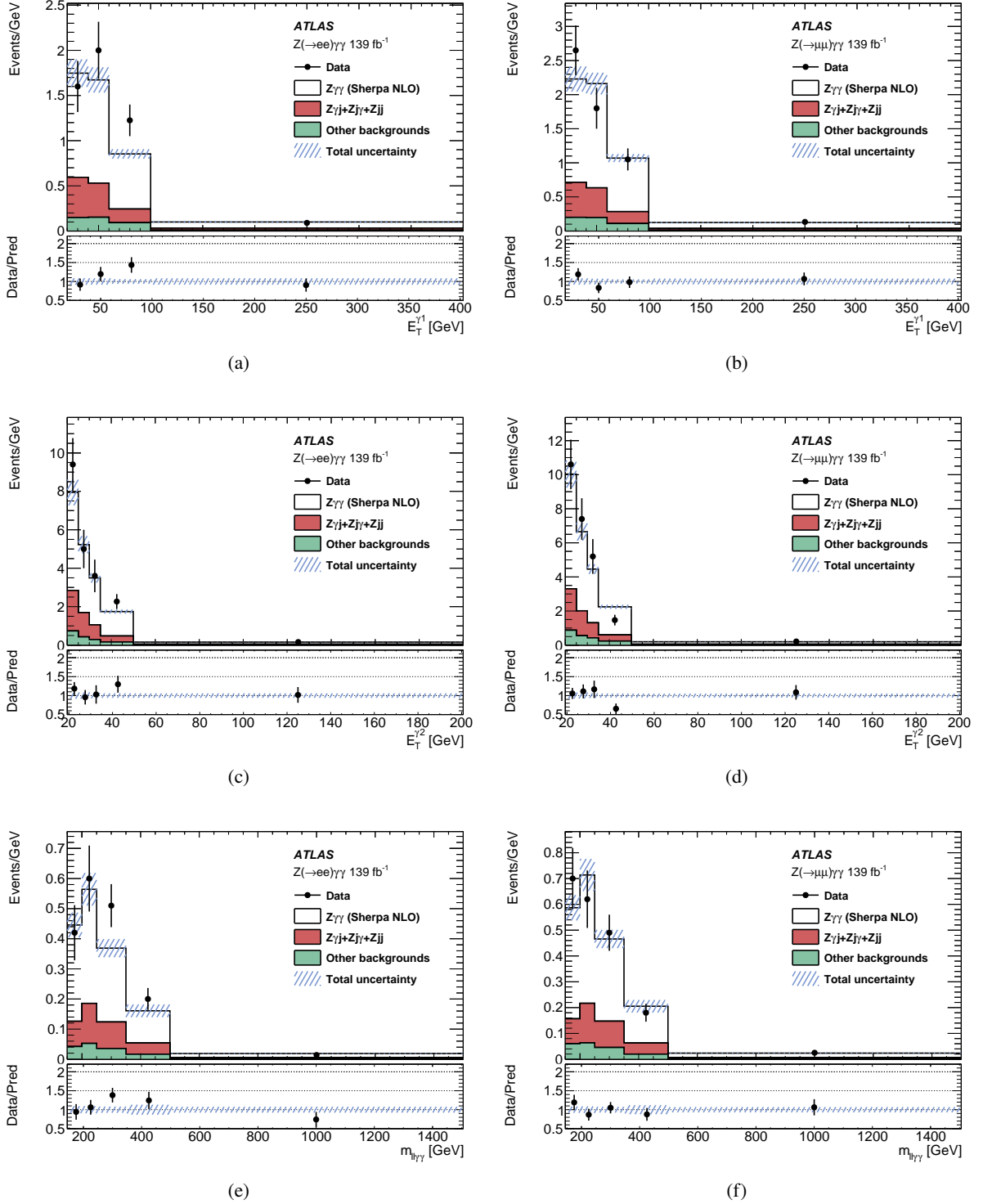


Figure 3: The detector-level distributions in data compared with signal-plus-background predictions in the electron and muon channels for (a)–(b) $E_T^{\gamma 1}$, (c)–(d) $E_T^{\gamma 2}$ and (e)–(f) $m_{\ell\ell\gamma\gamma}$. The lower panels show the ratio of the data to the total prediction.

according to whether the lower- or higher- p_T photon candidate is a misidentified jet. The probability of a jet being misidentified as a photon is poorly modelled in simulation, so a data-driven method is used. Such methods utilise jet-enriched control regions, defined by using photon candidates which fail either the photon identification or isolation selections, or both. A loosened data sample is used, where two photons are selected with a loose identification requirement and with no isolation requirement. Each of the two photons in an event can be assigned to one of four categories defined by the signal region's photon identification and isolation requirements: pass identification and pass isolation (A), pass identification and fail isolation (B), fail identification and pass isolation (C), or fail identification and fail isolation (D). The signal region is hence denoted by AA, and the other 15 combinations define the control regions. In the following, the number of data (signal) events falling into each control region is denoted by N_{data}^{XY} (N_{signal}^{XY}) where $X, Y = A, B, C, D$.

The number of events involving jets misidentified as photons in the signal region can be computed from the relevant yields in the control regions using a matrix method that has been employed in previous diphoton analyses [1, 35]. The method uses as inputs the prompt-photon isolation efficiencies (ϵ_1, ϵ_2), which are the probabilities for *Tight* identified photons to be isolated, and the jet-to-photon fake rates (f_1, f_2), which are the probabilities for photon candidates which fail the *Tight* identification selection to be isolated. The real photon efficiencies are measured in simulation and the jet-to-photon fake rates are calculated in data as

$$f_1 = \frac{(N_{\text{data}}^{\text{CA}} - N_{\text{signal}}^{\text{CA}})R}{(N_{\text{data}}^{\text{CA}} - N_{\text{signal}}^{\text{CA}})R + N_{\text{data}}^{\text{DA}} - N_{\text{signal}}^{\text{DA}}}, \quad f_2 = \frac{(N_{\text{data}}^{\text{AC}} - N_{\text{signal}}^{\text{AC}})R}{(N_{\text{data}}^{\text{AC}} - N_{\text{signal}}^{\text{AC}})R + N_{\text{data}}^{\text{AD}} - N_{\text{signal}}^{\text{AD}}},$$

where the indices 1 and 2 refer respectively to the leading and subleading photons and $R = N_{\text{A}}N_{\text{D}}/N_{\text{B}}N_{\text{C}}$ is a correlation parameter which accounts for the bias due to requiring the photon candidate to fail the identification requirement. The values of $\epsilon_1 = 94 \pm 3\%$ and $\epsilon_2 = 91 \pm 4\%$ are used where the uncertainty is systematic and calculated by looking at the variation of the isolation efficiencies with E_T^γ in the signal simulations. The parameter R is determined from simulation for each of the photon candidates, and the combined average of $R = 1.18 \pm 0.18$ is used for the calculated values of both fake rates. The systematic uncertainty on R is assigned such that it conservatively covers the values predicted for both fake photon candidates by the $Z\gamma$ + jets and Z + jets simulations. The signal leakage into the jet-enriched control regions is corrected for by subtracting from data the number of signal events predicted by the simulation to fall in the control region.

The number of events from each process in the loosened sample (W_{Zxy} where $x, y = \gamma, j$) can be mapped onto the signal region (AA) and the control regions AB, BA and BB by using the matrix

$$\begin{pmatrix} N^{\text{AA}} \\ N^{\text{AB}} \\ N^{\text{BA}} \\ N^{\text{BB}} \end{pmatrix} = \begin{pmatrix} \epsilon_1 \epsilon_2 & \epsilon_1 f_2 & f_1 \epsilon_2 & f_1 f_2 \\ \epsilon_1 (1 - \epsilon_2) & \epsilon_1 (1 - f_2) & f_1 (1 - \epsilon_2) & f_1 (1 - f_2) \\ (1 - \epsilon_1) \epsilon_2 & (1 - \epsilon_1) f_2 & (1 - f_1) \epsilon_2 & (1 - f_1) f_2 \\ (1 - \epsilon_1)(1 - \epsilon_2) & (1 - \epsilon_1)(1 - f_2) & (1 - f_1)(1 - \epsilon_2) & (1 - f_1)(1 - f_2) \end{pmatrix} \begin{pmatrix} W_{Z\gamma\gamma} \\ W_{Z\gamma j} \\ W_{Zj\gamma} \\ W_{Zjj} \end{pmatrix}. \quad (1)$$

The matrix can then be inverted to determine the unknown yields, W_{Zxy} . The contributions of the four processes to the signal region are determined from the first row of the matrix in Eq. (1):

$$N^{\text{AA}} = N_{Z\gamma\gamma} + N_{Z\gamma j} + N_{Zj\gamma} + N_{Zjj} = W_{Z\gamma\gamma} \epsilon_1 \epsilon_2 + W_{Z\gamma j} \epsilon_1 f_2 + W_{Zj\gamma} f_1 \epsilon_2 + W_{Zjj} f_1 f_2.$$

The $j \rightarrow \gamma$ background fractions are determined using the signal region events in the $e^+e^-\gamma\gamma$ and $\mu^+\mu^-\gamma\gamma$ channels combined. These fractions, and their statistical uncertainties, are found to be: $8.2 \pm 2.6\%$ for $Z\gamma j$, $9.1 \pm 2.3\%$ for $Zj\gamma$ and $2.8 \pm 1.1\%$ for Zjj . The statistical uncertainties are derived using 1000 sets of ‘toy’ data. For each set, the data yield in each region is randomly drawn from a Poisson distribution with a mean value equal to the observed data yield in that region. Each set of toy data is propagated through the matrix inversion, and the standard deviation of the 1000 extracted background fractions is taken as the statistical uncertainty.

The uncertainties on the extracted yields related to the fixed parameters ϵ_1 , ϵ_2 and R are investigated by varying these parameters within their systematic uncertainties. Two sources of systematic uncertainty related to the choice of jet-enriched control regions are considered. The dependence of the photon candidates on shower shape variables used in the photon identification definition is tested by varying the selections placed on these variables. An additional requirement is added to the nominal photon isolation requirement in order to reduce the amount of signal which leaks into regions B and D. A systematic uncertainty for this effect is calculated from the difference in extracted yields when not including this requirement. The largest contribution to the total uncertainty on the $j \rightarrow \gamma$ background yield comes from the data statistical uncertainty, but is similar in size to the total systematic uncertainty.

The method is validated on a ‘pseudo-dataset’ formed from the signal and $j \rightarrow \gamma$ background simulation samples, where the fractions of the four contributing processes are known. The extracted total normalisation of the $j \rightarrow \gamma$ background agrees with the expected value within one standard deviation.

There are insufficient events to perform the matrix method in each of the differential measurement bins, therefore the shapes of the $j \rightarrow \gamma$ backgrounds are taken from simulation and normalised to the overall fractions found in data. The shapes are derived in a slightly loosened signal region where one of the two photons is allowed to fail either the *Tight* identification or *Loose* isolation requirements, in order to increase the number of events selected from simulation. The ability of the simulation to describe the shapes in data is checked in a jet-enriched control region. Two sources of uncertainty affecting these shape templates are considered. The first is related to differences between data and simulation, and is estimated by testing the ability of the simulation to model the data distributions in a jet-enriched control region. This uncertainty is typically below 5% of the measured cross-section per bin, but can be as large as 15% in the most poorly modelled regions. The second source of shape uncertainty is related to the choice of control region in which the shapes are derived, and is evaluated by reweighting the shapes to a harder p_T spectrum because the photons which fail the identification or isolation requirements are typically softer ones. The uncertainty is below 2% across all the differential measurement bins.

5.2 Other backgrounds

The second largest background contribution comes from $t\bar{t}\gamma\gamma$ events where the top quarks decay leptonically. The normalisation factor for this background is determined in a control region with the same selection requirements as the signal region, except that an opposite-sign $e\mu$ lepton pair is selected. The $t\bar{t}\gamma\gamma$ process dominates in this region, but the contribution from $j \rightarrow \gamma$ events is also considered using the matrix method described above. The ratio of data, with the $j \rightarrow \gamma$ background subtracted, to the $t\bar{t}$ simulation in the $e\mu$ control region is used to define a normalisation factor which is applied to $t\bar{t}$ simulation events entering the signal region. The considered sources of systematic uncertainty are the same as for the signal. The normalisation factor is 0.81 ± 0.17 , where the dominant uncertainty is due to the limited number of data events in the $e\mu$ control region.

As there are no vertex requirements placed on photons, a source of background arises when two proton–proton interactions in the same bunch-crossing overlap to produce a combined $\ell\ell\gamma\gamma$ system. A data-driven method, such as the one described in Ref. [36], is not possible due to the limited number of signal region events, so these backgrounds are estimated using simulation only. Two processes contribute at first order: $Z\gamma + \gamma$ and $Z + \gamma\gamma$. Random events from each sample are combined and subjected to the fiducial selection (described later in Section 7.1). The resulting particle-level distributions of the six kinematic variables listed in Section 1 are corrected to the detector level using bin-by-bin factors determined from the simulated signal events. A systematic uncertainty is assigned to account for the different p_T distributions of signal events and pile-up background events. It is estimated by recalculating the bin-by-bin factors after reweighting the signal simulation to the pile-up background photon p_T spectra. The uncertainties in the predicted cross-section of the single-photon [37] and diphoton [38] samples are significant and hence are also included as systematic uncertainties. The total systematic uncertainty is 35% (27%) for the $Z\gamma + \gamma$ ($Z + \gamma\gamma$) pile-up background processes.

Another source of background is misidentification of electrons as photons. This $e \rightarrow \gamma$ background is modelled by ZZ and $WZ\gamma$ simulations. The modelling of electron-to-photon misidentification rates has been tested [39] and is found to disagree with data at a level of up to 50% in some regions. Therefore, a conservative systematic uncertainty of 50% is applied to the ZZ and $WZ\gamma$ yields in the signal region.

The contribution from $Z(\rightarrow \ell\ell)H(\rightarrow \gamma\gamma)$ is estimated directly from simulation. The contribution from $Z(\rightarrow \tau^+\tau^-)\gamma\gamma$ is estimated from simulation and is found to be negligible.

6 Systematic uncertainties

Systematic uncertainties in the measured cross-sections are related to the background estimation, the detector-to-fiducial acceptance correction factors (both inclusively and through the unfolding, as described in Section 7.1) and the integrated luminosity. The uncertainties in the backgrounds are discussed in Section 5. The correction factor and response matrix used for the unfolding are affected by the selection efficiency, and therefore variations of the different object reconstruction efficiencies are considered.

The performance of the electron and photon reconstruction, and their associated systematic uncertainties, are studied in Ref. [33]. For electrons, the reconstruction, identification and isolation efficiencies and their uncertainties are measured by applying tag-and-probe methods to events containing $Z \rightarrow e^+e^-$ or $J/\psi \rightarrow e^+e^-$ decays [40]. For photons, the corresponding efficiencies are measured using samples of $Z \rightarrow \ell^+\ell^-\gamma$ decays, and an inclusive photon sample collected using single-photon triggers. The energy scale and resolution for electrons and photons, and their uncertainties, are obtained from a sample of $Z \rightarrow e^+e^-$ events. For muons, the efficiencies, the momentum scale and resolution, and their uncertainties, are obtained using samples of $Z \rightarrow \mu^+\mu^-$ or $J/\psi \rightarrow \mu^+\mu^-$ decays [34].

The uncertainty due to the pile-up reweighting procedure discussed in Section 3 is estimated by varying the amount of pile-up in the signal simulation to cover the uncertainty in the ratio of the predicted and measured inelastic cross-sections [41].

The statistical uncertainty due to the limited number of generated signal events is considered.

Various sources of theoretical uncertainty are considered. The uncertainty due to the choice of PDF is estimated from the standard deviation of the mean of 100 variations of the nominal PDF set (NNPDF3.0_{NNLO}). The renormalisation and factorisation scales are each varied by factors of 0.5 and 2.0, except for shifts

Table 3: Relative systematic uncertainties in the integrated fiducial cross-section measurements in each channel using 139 fb^{-1} of Run 2 data. Systematic uncertainty sources that contribute less than 0.1% are not shown. Systematic sources labelled with an asterisk are treated as correlated between the two channels.

Source	Relative uncertainty [%]	
	$e^+e^-\gamma\gamma$	$\mu^+\mu^-\gamma\gamma$
Photon identification efficiency*	2.5	2.6
Photon isolation efficiency*	2.0	2.0
Electron–photon energy resolution*	0.2	0.1
Electron–photon energy scale*	0.8	0.6
Electron identification efficiency	2.0	-
Electron reconstruction efficiency	0.3	-
Muon isolation efficiency	-	0.4
Muon reconstruction efficiency	-	0.4
Muon trigger efficiency	-	0.3
Muon momentum scale	-	0.2
Pile-up reweighting*	2.8	2.9
Monte Carlo signal statistics	1.1	1.0
Signal modelling*	1.1	1.1
Integrated luminosity*	1.7	1.7
$j \rightarrow \gamma$ backgrounds*	7.5	7.6
Other backgrounds*	1.7	1.9
Total systematic uncertainty	9.3	9.3
Data statistical uncertainty	11.5	10.9
Total uncertainty	14.8	14.3

in opposite directions, and the envelope of the effects of these scale variations is taken as an estimate of the uncertainty due to missing higher order corrections. The assumed value of the strong coupling constant, $\alpha_s(m_Z) = 0.118$, is varied by ± 0.001 and the average effect is taken as the α_s contribution to the uncertainty. The effect of these theoretical uncertainties is accounted for in the integrated fiducial cross-section measurements and in the predicted cross-sections from the MC event generators. For the differential cross-section measurements, the theoretical uncertainties are determined to be negligible with respect to the total uncertainty.

The systematic uncertainties in the integrated cross-section in the fiducial region are summarised in Table 3. The measurement in each channel is dominated by the data statistical uncertainty, and the largest systematic uncertainty comes from the $j \rightarrow \gamma$ background estimation.

7 Cross-section determination

7.1 Fiducial volume definition

The measured yields for the signal process in data are corrected to a fiducial volume which accounts for detector inefficiency, geometry and resolution. The fiducial volume is defined using particle-level objects

Table 4: Definition of the $Z(\rightarrow \ell\ell)\gamma\gamma$ fiducial phase space.

Photons	Leptons
$p_T^\gamma > 20 \text{ GeV}$	$p_T^{\ell^1} > 30 \text{ GeV}, p_T^{\ell^2} > 20 \text{ GeV}$
$ \eta^\gamma < 2.37$	$ \eta^\ell < 2.47$
$E_T^{\text{iso}}/p_T^\gamma < 0.07$	dressed leptons
Event	
$\Delta R(\gamma, \ell) > 0.4, \Delta R(\gamma, \gamma) > 0.4$	
$m_{\ell\ell} > 40 \text{ GeV}$	
$m_{\ell\ell} + \min(m_{\ell\ell\gamma_1}, m_{\ell\ell\gamma_2}) > 2m_Z$	

in simulation which have a proper decay length longer than 10 mm. To correct for bremsstrahlung, each particle-level lepton is ‘dressed’ by vectorially adding to its four-momentum the four-momenta of any nearby photons, except those from hadron decays, within a cone of size $\Delta R = 0.1$ around the lepton.

To minimise the model-dependence of the procedure to correct the data from detector level to particle level, also known as unfolding, the selection requirements placed on the particle-level objects are as close as possible to the detector-level selection outlined in Section 4. An exception is the calorimeter transition region, which is included in the selection of particle-level electrons and photons. The detector-to-fiducial-level correction procedure includes an extrapolation, over a few percent of the total phase space, which accounts for the loss of detector-level acceptance in this region. The particle-level photons must pass an isolation selection which requires E_T^{iso} , defined as the summed transverse energy of all particles except muons, neutrinos and the photon itself within a cone of size $\Delta R = 0.2$ around the photon, to be less than 7% of the photon p_T . This value is chosen as it best replicates the performance of the *Loose* isolation working point used in the detector-level selection. The complete set of requirements is listed in Table 4.

7.2 Cross-section extraction

The integrated fiducial cross-section, σ_{fid} , is calculated from the observed yield in data (N_{data}), the expected background yield (N_{bkg}) and the total integrated luminosity (L)

$$\sigma_{\text{fid}} = \frac{N_{\text{data}} - N_{\text{bkg}}}{C \times L}.$$

The correction factor (C) is defined as the ratio of the number of signal simulation events passing the detector-level selection to the number which pass the fiducial-level selection. The value of C is 0.286 ± 0.014 in the electron channel and 0.379 ± 0.017 in the muon channel where the uncertainties include the systematic sources discussed in Section 6. The dominant contributions come from the photon identification efficiency and pile-up reweighting systematic uncertainties.

For the differential cross-section measurements, the detector-to-fiducial-level correction is instead done via an iterative Bayesian unfolding procedure [42] which accounts for bin migrations. The procedure takes as input the background-subtracted data distributions and a response matrix produced from the nominal signal simulation. The bin migrations are typically below 5% but can be as large as 18% in the regions with the finest binning. After accounting for migrations the unfolded yields are corrected for out-of-fiducial

events which corresponds to a reduction of 5-10% per bin. Two iterations are used which is chosen as the central values do not change significantly, less than 3%, with a larger number of iterations. The statistical uncertainties related to both the finite number of events in data and in the signal simulation are assessed using Poisson distributed ‘toys’. The systematic uncertainties related to the signal selection efficiency are propagated through the unfolding by constructing new response matrices for the upwards and downwards shifts of one standard deviation and taking the average effect as the uncertainty on the unfolded yield. The background systematic uncertainties are assessed by varying each background expectation up and down by one standard deviation and taking the average effect as the uncertainty on the unfolded yield. The reliability of the unfolding procedure is tested by unfolding the detector-level signal distribution from simulation, reweighted such that it better describes the data. The difference between the resulting unfolded distribution and the reweighted fiducial distribution is assigned as an uncertainty of the differential measurements. The uncertainty is negligible in most bins, up to 8% in one bin, but overall has a very small effect on the measurements.

The bins used for the differential distributions were chosen such that there are sufficient events in each bin to perform the unfolding. The uppermost bin edges were chosen using the expected distributions from the signal simulation to exclude regions which are not sensitive to $Z\gamma\gamma$ production.

The integrated and differential cross-section measurements are performed separately in each channel. The results are combined into $Z(\rightarrow \ell\ell)\gamma\gamma$ measurements via an averaging procedure which accounts for statistical and systematic uncertainties, and their correlations between the two channels. The technique uses a χ^2 minimisation procedure which is documented in Ref. [43].

7.3 Results

The measured integrated cross-sections in each channel and the combined average are

$$\sigma_{\text{fid}}^{Z(\rightarrow ee)\gamma\gamma} = 2.65 \pm 0.31(\text{stat}) \pm 0.24(\text{syst}) \pm 0.05(\text{lumi}) \text{ fb} ,$$

$$\sigma_{\text{fid}}^{Z(\rightarrow \mu\mu)\gamma\gamma} = 2.29 \pm 0.25(\text{stat}) \pm 0.21(\text{syst}) \pm 0.04(\text{lumi}) \text{ fb} ,$$

$$\sigma_{\text{fid}}^{Z(\rightarrow \ell\ell)\gamma\gamma} = 2.45 \pm 0.20(\text{stat}) \pm 0.22(\text{syst}) \pm 0.04(\text{lumi}) \text{ fb} .$$

The integrated $Z(\rightarrow \ell\ell)\gamma\gamma$ cross-section is measured with an overall precision of 12% and is compared with the MC event generator predictions in Figure 4, where good agreement between data and both predictions is seen. The SHERPA prediction suffers from larger scale uncertainties due to the matrix element NLO accuracy being at the 0-jet level, whereas it includes 1-jet contributions in the MADGRAPH5_AMC@NLO prediction.

The measured $Z(\rightarrow \ell\ell)\gamma\gamma$ differential cross-sections are compared with the predictions from SHERPA and MADGRAPH5_AMC@NLO in Figures 5, 6 and 7.

The photon transverse energy ($E_T^{\gamma 1}, E_T^{\gamma 2}$) distributions displayed in Figure 5 are well described by the predictions. The $p_T^{\ell\ell}$ distribution in Figure 6(a) describes the transverse momentum of the Z boson, which typically recoils against the two photons. This distribution is therefore sculpted by the minimum transverse

momentum selections imposed on the two photons, which results in the peak around 40 GeV. The $p_T^{\ell\ell\gamma\gamma}$ distribution in Figure 6(b) probes the QCD modelling of the transverse momentum of the $Z\gamma\gamma$ system. The description by the MC event generator predictions is good across all measurement bins except for a discrepancy in the high- $p_T^{\ell\ell\gamma\gamma}$ region. The $m_{\gamma\gamma}$ distribution is important in the context of diphoton resonance searches in $\ell\ell\gamma\gamma$ channels. The measured distribution is shown in Figure 7(a) and the simulations provide a good description, particularly in the fourth bin, which is most relevant for $Z(\rightarrow \ell\ell)H(\rightarrow \gamma\gamma)$ measurements. The $m_{\ell\ell\gamma\gamma}$ distribution (Figure 7(b)) provides a measure of the hard scale of the system, and is described well by the predictions, even for $m_{\ell\ell\gamma\gamma} > 500$ GeV.

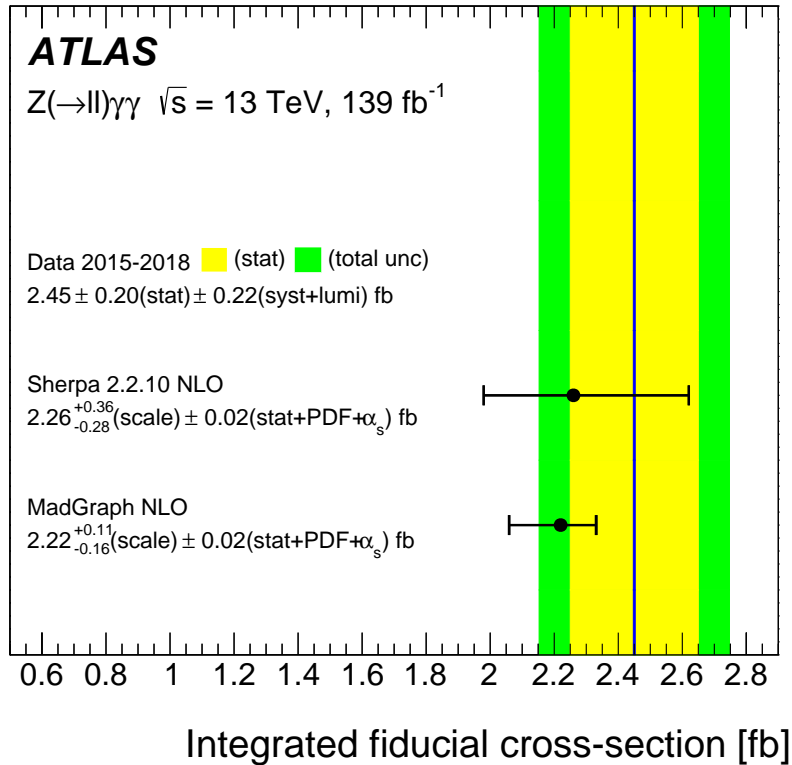
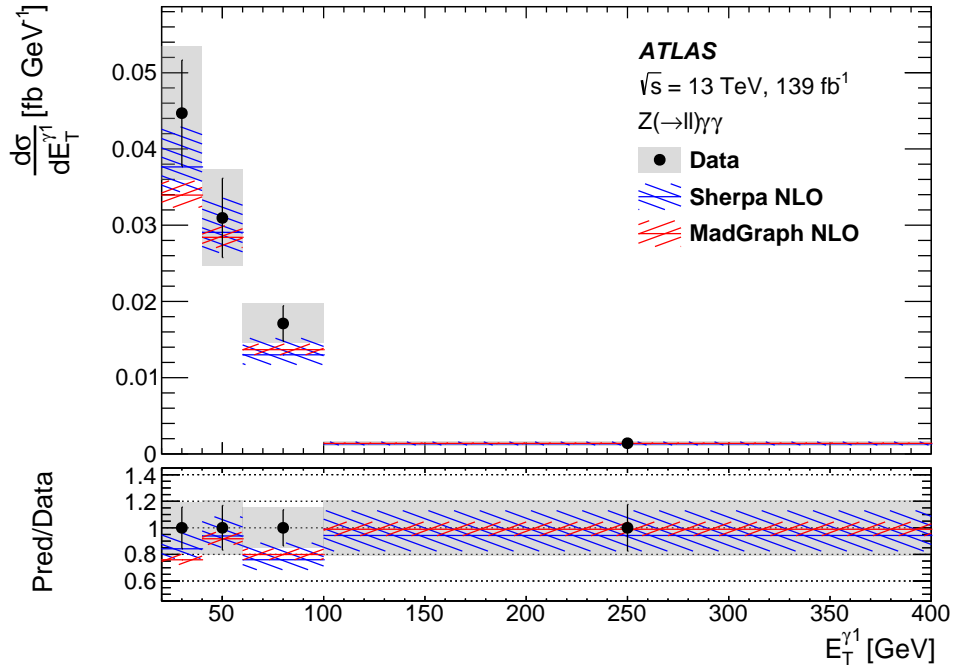
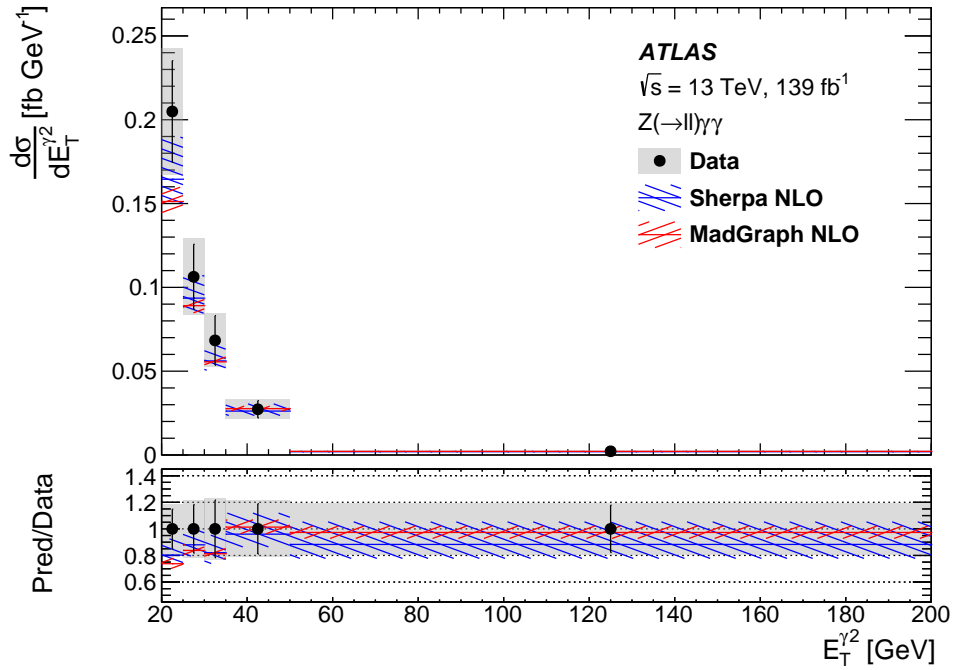


Figure 4: The $Z(\rightarrow \ell\ell)\gamma\gamma$ integrated cross-section, measured in a fiducial region corresponding to the production of three on-shell electroweak bosons. The measurement is compared with both the signal event generator predictions.

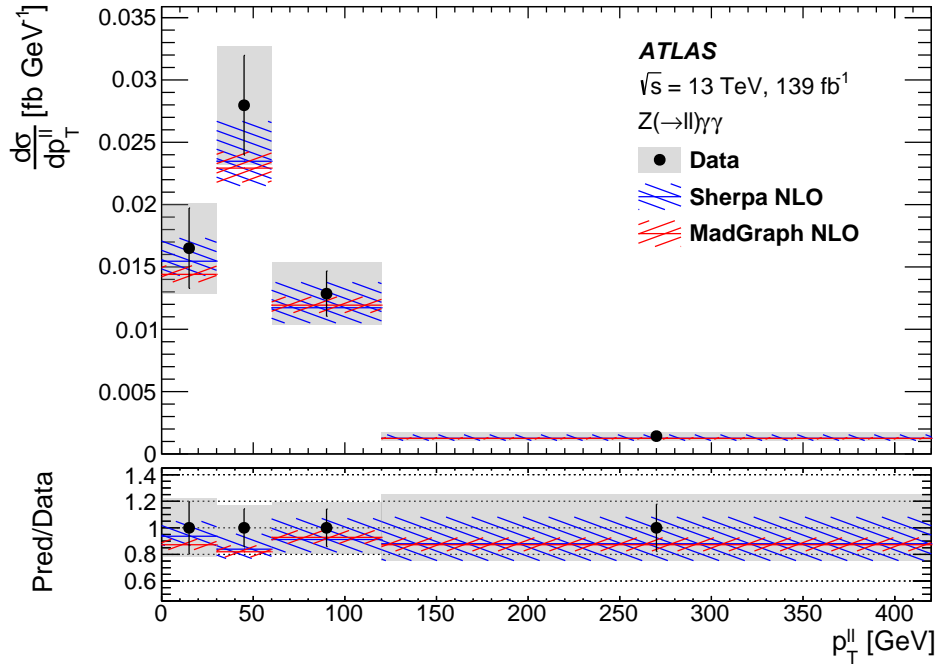


(a)

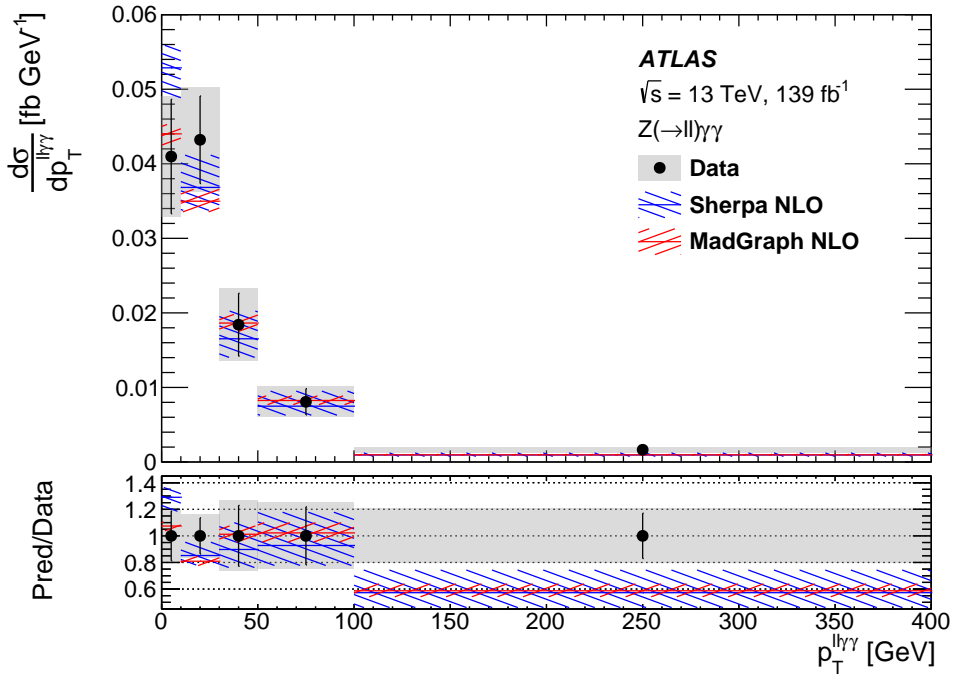


(b)

Figure 5: The unfolded differential cross-sections as a function of (a) the leading photon transverse energy and (b) the subleading photon transverse energy are compared with NLO predictions from SHERPA and MADGRAPH5_AMC@NLO. The black uncertainty bar on the data represents the statistical uncertainty, whereas the slightly taller grey uncertainty band represents the total uncertainty. The uncertainty in the predictions includes both the statistical and theoretical uncertainties. The lower panels show the ratios of the predictions to data, as well as the fractional uncertainty of the data.

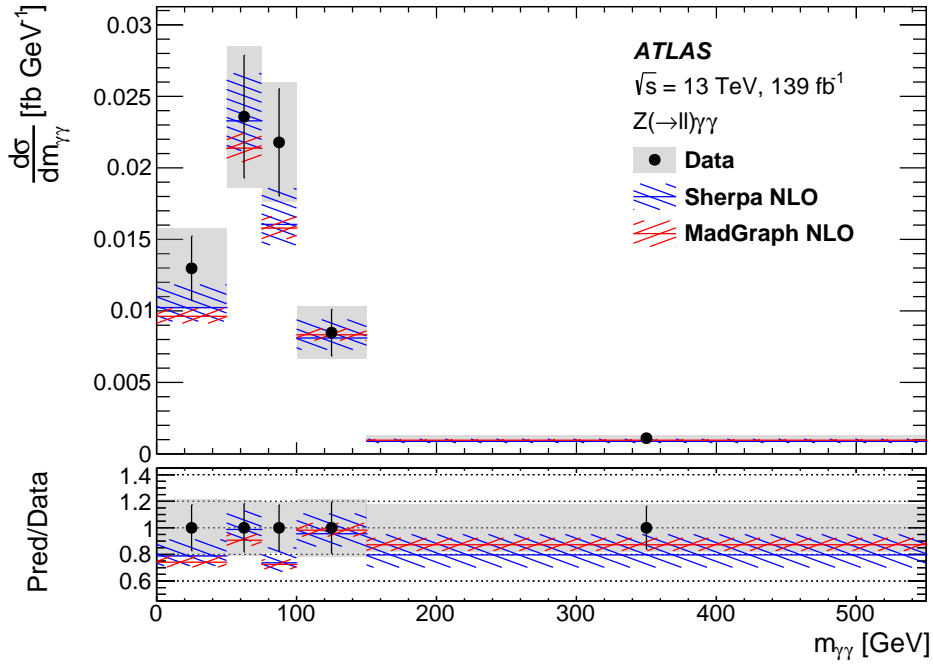


(a)

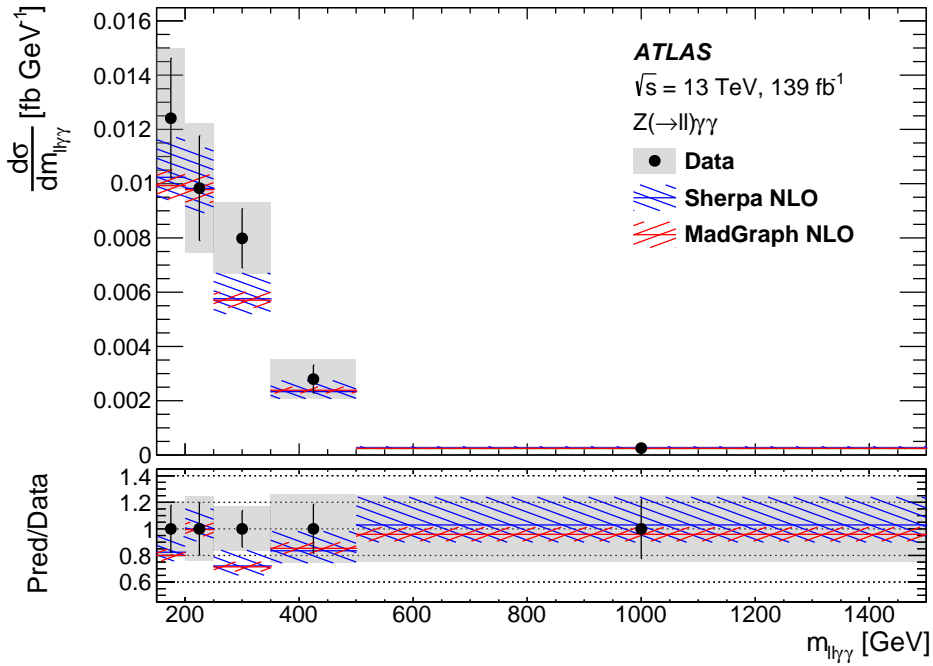


(b)

Figure 6: The unfolded differential cross-sections as a function of (a) the dilepton transverse momentum and (b) the four-body transverse momentum are compared with NLO predictions from SHERPA and MADGRAPH5_AMC@NLO. The black uncertainty bar on the data represents the statistical uncertainty, whereas the slightly taller grey uncertainty band represents the total uncertainty. The uncertainty in the predictions includes both the statistical and theoretical uncertainties. The lower panels show the ratios of the predictions to data, as well as the fractional uncertainty of the data.



(a)



(b)

Figure 7: The unfolded differential cross-sections as a function of (a) the diphoton invariant mass and (b) the four-body invariant mass are compared with NLO predictions from SHERPA and MADGRAPH5_AMC@NLO. The black uncertainty bar on the data represents the statistical uncertainty, whereas the slightly taller grey uncertainty band represents the total uncertainty. The uncertainty in the predictions includes both the statistical and theoretical uncertainties. The lower panels show the ratios of the predictions to data, as well as the fractional uncertainty of the data.

8 EFT interpretation

The $\ell\ell\gamma\gamma$ final state can probe the non-Abelian structure of the $SU(2)_L \times U(1)_Y$ symmetry of the Standard Model, which gives rise to gauge boson self-interactions. Modifications of the self-interactions arising through new physics (NP) are investigated using an effective field theory approach [44]. The SM Lagrangian \mathcal{L}_{SM} is expanded with operators of dimension $d > 4$, which are suppressed by the energy scale Λ of NP:

$$\mathcal{L}_{\text{EFT}} = \mathcal{L}_{\text{SM}} + \sum_{d>4} \sum_i \frac{f_i^d}{\Lambda^{d-4}} \mathcal{O}_i^d.$$

The dimensionless Wilson coefficient of operator \mathcal{O}_i^d , where i runs over all operators of dimension d , is given by f_i^d . The production of $\ell\ell\gamma\gamma$ events is altered by modifying the SM coupling between four gauge bosons. These so-called ‘anomalous quartic gauge couplings’ introduce new contributions via the SM-forbidden vertices between four neutral EW gauge bosons. The lowest-dimension operators which give rise to $ZZ\gamma\gamma$, $Z\gamma\gamma\gamma$, and $\gamma\gamma\gamma\gamma$ interactions are of dimension 8.

Constraints are placed on the subset of dimension-8 operators from Ref. [45] which are constructed using only field strength tensors. They are typically referred to as transverse operators, in the following abbreviated by $\mathcal{O}_{T,j}^8$, with $j \in \{0, 1, 2, 5, 6, 7, 8, 9\}$, and can introduce the aforementioned interactions between neutral EW gauge bosons. The contributions were simulated in MADGRAPH5_AMC@NLO 2.8.1 at LO in QCD with the NNPDF3.0_{NLO} PDF set, and PYTHIA 8.244 was used to perform parton showering. The full fiducial phase-space selection defined in Section 7.1 is applied. The transverse momentum of the dilepton system $p_T^{\ell\ell}$ provides the highest sensitivity to NP effects in the fiducial volume. It is thus used to constrain the $\mathcal{O}_{T,j}^8$ coupling parameters defined by dividing the Wilson coefficients by the NP scale, $f_{T,j}/\Lambda^4$.

The measured differential cross-section is compared with the SHERPA 2.2.10 $Z\gamma\gamma$ prediction and the EFT prediction of transverse operator $\mathcal{O}_{T,8}^8$ in Figure 8. The SM $Z\gamma\gamma$ contribution estimated by a MADGRAPH5_AMC@NLO simulation at LO is also shown and this can be compared with the NLO prediction to investigate the impact of NLO QCD corrections. A slightly softer $p_T^{\ell\ell}$ spectrum is observed at LO. The predicted differential cross-section at LO is used in Section 8.1 in the estimation of NLO QCD corrections for the EFT prediction.

Limits are placed on the coupling parameters $f_{T,j}/\Lambda^4$ by constructing and scanning a profile likelihood ratio, taking as input the baseline SHERPA 2.2.10 $Z\gamma\gamma$ production (expected limits) and Run 2 data (observed limits), the contributions of the transverse operators, and all sources of uncertainty. The limits are calculated for the combination of the electron and muon channels. In the fit, the likelihood function is represented by a multivariate Gaussian distribution, where theory uncertainties are modelled by additional Gaussian constraints. All experimental uncertainties are encoded in the covariance matrix accounting for $p_T^{\ell\ell}$ bin correlations. A description of the experimental uncertainties is given in Section 6. The bin-to-bin correlation of the statistical uncertainty, which can be present after unfolding, is found to be negligible and is not considered further. The shift of each systematic uncertainty is applied consistently in the same direction for all $p_T^{\ell\ell}$ bins; correlations between different sources of systematic uncertainty are not considered. Theory uncertainties, consisting of renormalisation and factorisation scale, PDF, and α_s uncertainties, are included for SM $Z\gamma\gamma$ production and all transverse operators. Gaussian constraints for the limited size of the SHERPA 2.2.10 $Z\gamma\gamma$ sample and the EFT samples are also added. The largest experimental uncertainties stem from the limited size of the data sample and the estimation of the fake-photon contribution, reaching 18% and 14%, respectively, in certain $p_T^{\ell\ell}$ bins. The renormalisation and factorisation scales are the

sources of the largest theory uncertainties, which reach values of 23% in the last $p_T^{\ell\ell}$ bin. Limits at 95% confidence level are constructed from the profile likelihood ratio by applying Wilks' theorem [46] and thus assuming that the test statistic is χ^2 -distributed. The effect of one transverse operator at a time is studied while all other Wilson coefficients are set to zero.

8.1 Non-unitarised limits

The expected and observed limits are displayed in Figure 9. Constraints arising from unitarity conservation are not considered. The observed limits are typically 11%–12% less stringent than those expected. This is driven by the larger contribution of fake photons in data and the corresponding uncertainties in the fake-photon normalisation and shape.

Higher-order QCD corrections are not available for the EFT prediction. In order to study the impact of such corrections on the constraints that can be placed on couplings of dimension-8 operators, a test fit was performed assuming that the EFT scales similarly to the SM with respect to higher-order corrections. In this test, the MADGRAPH5_AMC@NLO 2.7.3 differential cross-section at NLO (see Table 1) was divided by the MADGRAPH5_AMC@NLO LO prediction displayed in Figure 8 to obtain bin-wise correction factors. The parameter settings for the LO simulation were identical to those chosen for the generation of the EFT contributions, except that all Wilson coefficients were set to zero. The differential cross-sections predicted by $\mathcal{O}_{T,j}^8$ were then multiplied by the correction factors. The results of this study show that the expected and observed constraints on the coupling parameters $f_{T,j}/\Lambda^4$ are 13%–15% more stringent. Although such higher-order QCD corrections result in a sizeable impact on the limits, the underlying assumption cannot be validated with the available theoretical calculations in the EFT formalism, therefore the nominal confidence intervals, as shown in Figure 9, are calculated without the bin-wise correction factors.

The confidence intervals presented for the four transverse operators $\mathcal{O}_{T,1}^8$, $\mathcal{O}_{T,2}^8$, $\mathcal{O}_{T,6}^8$, $\mathcal{O}_{T,7}^8$ are the first published by the ATLAS experiment at a centre-of-mass energy of 13 TeV and are up to two orders of magnitude more stringent than the limits extracted at 8 TeV. The non-unitarised limits derived in this analysis are less stringent than those published by CMS in their $W^\pm\gamma\gamma$ and $Z\gamma\gamma$ analysis at 13 TeV [3], but differ by less than a factor of two. This difference is primarily driven by binning requirements on $p_T^{\ell\ell}$. The binning was optimised to have sufficient events in the unfolding procedure. This results in a reduced sensitivity to EFT effects, particularly in the final bin.

8.2 Unitarisation treatment

Limits for all transverse operators are also derived as functions of an energy scale cut-off which prevents the violation of unitarity at large energy scales. Various techniques make use of a truncation of the EFT contribution to restore unitarity. This analysis uses a method which is typically referred to as *clipping* [47]. Any EFT contribution is suppressed above an energy scale E_c . The $\ell\ell\gamma\gamma$ invariant mass is used to select various thresholds for the clipping energy. Technically, this is achieved by scanning the simulated events at parton level before the parton showering is performed and suppressing any EFT contribution of events in which $m_{\ell\ell\gamma\gamma} > E_c$. The SM $Z\gamma\gamma$ contribution is not truncated and is allowed to reach arbitrary energy scales. The evolution of the expected and observed confidence intervals as a function of E_c for the coupling parameter of transverse operator $\mathcal{O}_{T,8}^8$ is shown in Figure 10. A similar evolution is observed for the remaining dimension-8 operators, where the confidence intervals become 4–5 more stringent between $E_c = 1.1$ TeV and $E_c = \infty$.

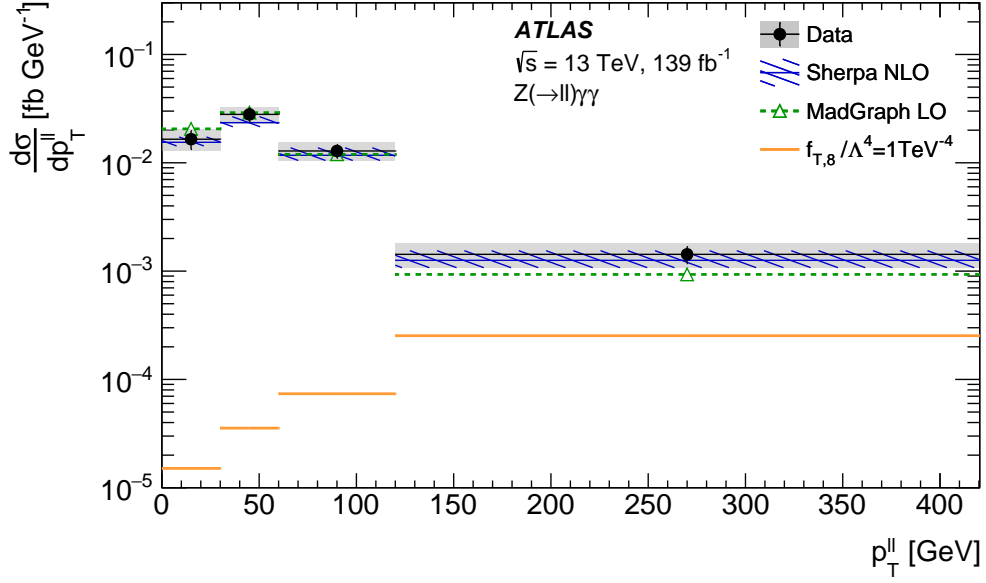


Figure 8: Comparison of the differential cross-section at particle level as a function of the dilepton transverse momentum between the observation in full Run 2 data, the NLO prediction from SHERPA, the LO prediction from MADGRAPH5_AMC@NLO, and the EFT prediction of one dimension-8 operator. The black uncertainty line on the data represents the statistical uncertainty, whereas the slightly taller grey uncertainty band represents the total uncertainty. The uncertainty in the SHERPA prediction includes both the statistical and theoretical uncertainties. The coupling parameter $f_{T,8}/\Lambda^4$ for the NP contribution of transverse operator $\mathcal{O}_{T,8}^8$ is set to $1/\text{TeV}^4$. The NP contribution contains interference effects between the SM $Z\gamma\gamma$ production and the contribution of transverse operator $\mathcal{O}_{T,8}^8$.

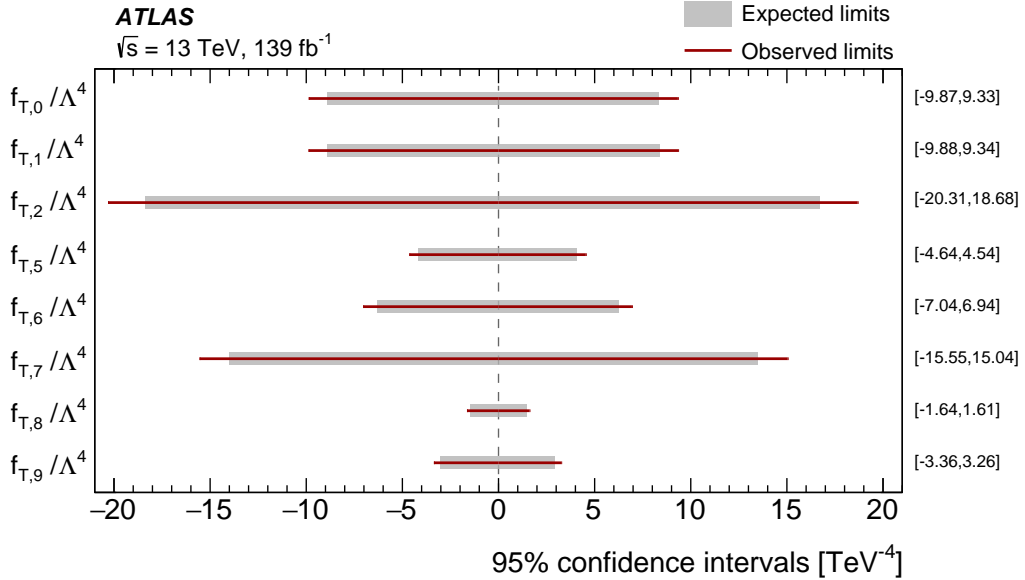


Figure 9: Expected and observed 95% confidence intervals for the coupling parameters $f_{T,j}/\Lambda^4$ of transverse dimension-8 operators $\mathcal{O}_{T,j}^8$. All parameter values outside of the shown range are excluded at the chosen confidence level. No unitarity constraints are applied. The numeric values of the observed confidence intervals are displayed at the right border of the figure.

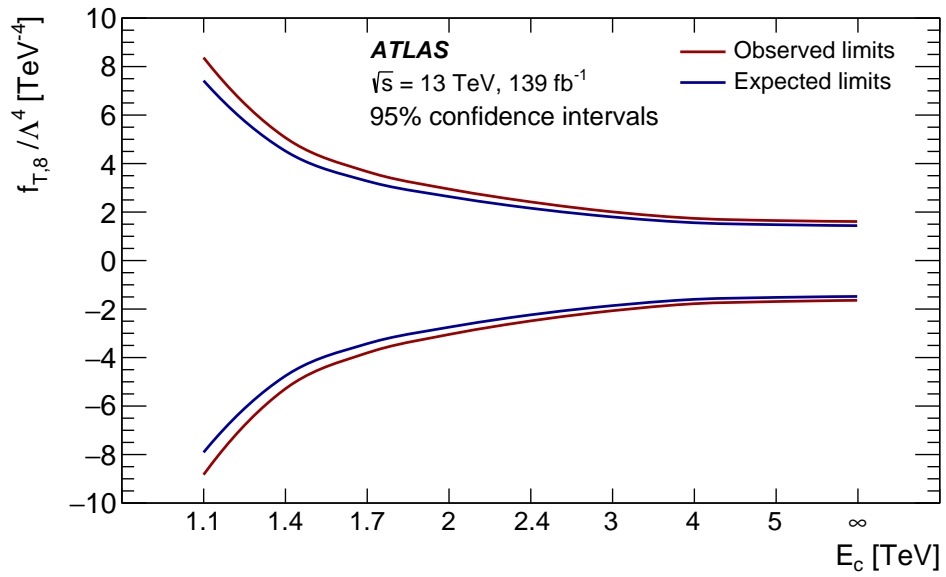


Figure 10: Expected and observed unitarised 95% confidence intervals for the coupling parameter $f_{T,8}/\Lambda^4$ in the clipping energy range between 1.1 and 5 TeV. The non-unitarised limits ($E_c = \infty$) are also displayed. All parameter values above the upper or below the lower observed and expected limits are excluded at the chosen confidence level.

9 Conclusions

The production of a Z boson in association with two photons in a phase-space region dominated by the ISR production of photons is studied in proton–proton collisions. The measurements are performed using 139 fb^{-1} of 13 TeV proton–proton collision data recorded by the ATLAS detector at the LHC. The electron and muon decay channels of the Z boson are used, and events where either photon is radiated from one of the final-state leptons are rejected.

The integrated $Z(\rightarrow \ell^+ \ell^-) \gamma \gamma$ cross-section is measured with a precision of 12%, with approximately equal contributions from statistical and systematic uncertainties. The cross-section is also measured differentially for the first time, and is used to test Standard Model predictions at up to next-to-leading-order accuracy from SHERPA and MADGRAPH5_AMC@NLO. The description by the MC event generator predictions is good across all measurement bins.

The measurements are also used to set limits on the Wilson coefficients, divided by the new physics scale Λ , of dimension-8 EFT operators. The constraints on four of the eight operators under consideration are tightened by up to two orders of magnitude with respect to previous ATLAS analyses using 8 TeV data.

Acknowledgements

We thank CERN for the very successful operation of the LHC, as well as the support staff from our institutions without whom ATLAS could not be operated efficiently.

We acknowledge the support of ANPCyT, Argentina; YerPhI, Armenia; ARC, Australia; BMWFW and FWF, Austria; ANAS, Azerbaijan; CNPq and FAPESP, Brazil; NSERC, NRC and CFI, Canada; CERN; ANID, Chile; CAS, MOST and NSFC, China; Minciencias, Colombia; MEYS CR, Czech Republic; DNRf and DNSRC, Denmark; IN2P3-CNRS and CEA-DRF/IRFU, France; SRNSFG, Georgia; BMBF, HGF and MPG, Germany; GSRI, Greece; RGC and Hong Kong SAR, China; ISF and Benoziyo Center, Israel; INFN, Italy; MEXT and JSPS, Japan; CNRST, Morocco; NWO, Netherlands; RCN, Norway; MEiN, Poland; FCT, Portugal; MNE/IFA, Romania; MESTD, Serbia; MSSR, Slovakia; ARRS and MIZŠ, Slovenia; DSI/NRF, South Africa; MICINN, Spain; SRC and Wallenberg Foundation, Sweden; SERI, SNSF and Cantons of Bern and Geneva, Switzerland; MOST, Taiwan; TENMAK, Türkiye; STFC, United Kingdom; DOE and NSF, United States of America. In addition, individual groups and members have received support from BCKDF, CANARIE, Compute Canada and CRC, Canada; PRIMUS 21/SCI/017 and UNCE SCI/013, Czech Republic; COST, ERC, ERDF, Horizon 2020 and Marie Skłodowska-Curie Actions, European Union; Investissements d’Avenir Labex, Investissements d’Avenir IDEX and ANR, France; DFG and AvH Foundation, Germany; Herakleitos, Thales and Aristeia programmes co-financed by EU-ESF and the Greek NSRF, Greece; BSF-NSF and MINERVA, Israel; Norwegian Financial Mechanism 2014–2021, Norway; NCN and NAWA, Poland; La Caixa Banking Foundation, CERCA Programme Generalitat de Catalunya and PROMETEO and GenT Programmes Generalitat Valenciana, Spain; Göran Gustafssons Stiftelse, Sweden; The Royal Society and Leverhulme Trust, United Kingdom.

The crucial computing support from all WLCG partners is acknowledged gratefully, in particular from CERN, the ATLAS Tier-1 facilities at TRIUMF (Canada), NDGF (Denmark, Norway, Sweden), CC-IN2P3 (France), KIT/GridKA (Germany), INFN-CNAF (Italy), NL-T1 (Netherlands), PIC (Spain), ASGC (Taiwan), RAL (UK) and BNL (USA), the Tier-2 facilities worldwide and large non-WLCG resource providers. Major contributors of computing resources are listed in Ref. [48].

References

- [1] ATLAS Collaboration, *Measurements of $Z\gamma$ and $Z\gamma\gamma$ production in pp collisions at $\sqrt{s} = 8$ TeV with the ATLAS detector*, *Phys. Rev. D* **93** (2016) 112002, arXiv: [1604.05232 \[hep-ex\]](#).
- [2] CMS Collaboration, *Measurements of the $pp \rightarrow W\gamma\gamma$ and $pp \rightarrow Z\gamma\gamma$ cross sections and limits on anomalous quartic gauge couplings at $\sqrt{s} = 8$ TeV*, *JHEP* **10** (2017) 072, arXiv: [1704.00366 \[hep-ex\]](#).
- [3] CMS Collaboration, *Measurements of the $pp \rightarrow W^\pm\gamma\gamma$ and $pp \rightarrow Z\gamma\gamma$ cross sections at $\sqrt{s} = 13$ TeV and limits on anomalous quartic gauge couplings*, *JHEP* **10** (2021) 174, arXiv: [2105.12780 \[hep-ex\]](#).
- [4] ATLAS Collaboration, *The ATLAS Experiment at the CERN Large Hadron Collider*, *JINST* **3** (2008) S08003.
- [5] ATLAS Collaboration, *The ATLAS Collaboration Software and Firmware*, ATL-SOFT-PUB-2021-001, 2021, URL: <https://cds.cern.ch/record/2767187>.
- [6] ATLAS Collaboration, *ATLAS data quality operations and performance for 2015–2018 data-taking*, *JINST* **15** (2020) P04003, arXiv: [1911.04632 \[physics.ins-det\]](#).
- [7] ATLAS Collaboration, *Luminosity determination in pp collisions at $\sqrt{s} = 13$ TeV using the ATLAS detector at the LHC*, ATL-CONF-2019-021, 2019, URL: <https://cds.cern.ch/record/2677054>.
- [8] G. Avoni et al., *The new LUCID-2 detector for luminosity measurement and monitoring in ATLAS*, *JINST* **13** (2018) P07017.
- [9] ATLAS Collaboration, *The ATLAS Simulation Infrastructure*, *Eur. Phys. J. C* **70** (2010) 823, arXiv: [1005.4568 \[physics.ins-det\]](#).
- [10] S. Agostinelli et al., *GEANT4 – a simulation toolkit*, *Nucl. Instrum. Meth. A* **506** (2003) 250.
- [11] T. Sjöstrand, S. Mrenna and P. Skands, *A brief introduction to PYTHIA 8.1*, *Comput. Phys. Commun.* **178** (2008) 852, arXiv: [0710.3820 \[hep-ph\]](#).
- [12] ATLAS Collaboration, *The Pythia 8 A3 tune description of ATLAS minimum bias and inelastic measurements incorporating the Donnachie–Landshoff diffractive model*, ATL-PHYS-PUB-2016-017, 2016, URL: <https://cds.cern.ch/record/2206965>.
- [13] NNPDF Collaboration, R. D. Ball et al., *Parton distributions with LHC data*, *Nucl. Phys. B* **867** (2013) 244, arXiv: [1207.1303 \[hep-ph\]](#).
- [14] E. Bothmann et al., *Event generation with Sherpa 2.2*, *SciPost Phys.* **7** (2019) 034, arXiv: [1905.09127 \[hep-ph\]](#).
- [15] S. Schumann and F. Krauss, *A parton shower algorithm based on Catani–Seymour dipole factorisation*, *JHEP* **03** (2008) 038, arXiv: [0709.1027 \[hep-ph\]](#).
- [16] T. Gleisberg and S. Höche, *Comix, a new matrix element generator*, *JHEP* **12** (2008) 039, arXiv: [0808.3674 \[hep-ph\]](#).
- [17] S. Höche, F. Krauss, M. Schönherr and F. Siegert, *A critical appraisal of NLO+PS matching methods*, *JHEP* **09** (2012) 049, arXiv: [1111.1220 \[hep-ph\]](#).

- [18] S. Höche, F. Krauss, M. Schönherr and F. Siegert, *QCD matrix elements + parton showers. The NLO case*, *JHEP* **04** (2013) 027, arXiv: [1207.5030 \[hep-ph\]](#).
- [19] S. Catani, F. Krauss, B. R. Webber and R. Kuhn, *QCD Matrix Elements + Parton Showers*, *JHEP* **11** (2001) 063, arXiv: [hep-ph/0109231](#).
- [20] S. Höche, F. Krauss, S. Schumann and F. Siegert, *QCD matrix elements and truncated showers*, *JHEP* **05** (2009) 053, arXiv: [0903.1219 \[hep-ph\]](#).
- [21] The NNPDF Collaboration, R. D. Ball et al., *Parton distributions for the LHC run II*, *JHEP* **04** (2015) 040, arXiv: [1410.8849 \[hep-ph\]](#).
- [22] J. Alwall et al., *The automated computation of tree-level and next-to-leading order differential cross sections, and their matching to parton shower simulations*, *JHEP* **07** (2014) 079, arXiv: [1405.0301 \[hep-ph\]](#).
- [23] T. Sjöstrand et al., *An introduction to PYTHIA 8.2*, *Comput. Phys. Commun.* **191** (2015) 159, arXiv: [1410.3012 \[hep-ph\]](#).
- [24] R. Frederix and S. Frixione, *Merging meets matching in MC@NLO*, *JHEP* **12** (2012) 061, arXiv: [1209.6215 \[hep-ph\]](#).
- [25] S. Frixione, *Isolated photons in perturbative QCD*, *Phys. Lett. B* **429** (1998) 369, arXiv: [hep-ph/9801442](#).
- [26] P. Nason, *A new method for combining NLO QCD with shower Monte Carlo algorithms*, *JHEP* **11** (2004) 040, arXiv: [hep-ph/0409146](#).
- [27] S. Frixione, P. Nason and C. Oleari, *Matching NLO QCD computations with parton shower simulations: the POWHEG method*, *JHEP* **11** (2007) 070, arXiv: [0709.2092 \[hep-ph\]](#).
- [28] S. Alioli, P. Nason, C. Oleari and E. Re, *A general framework for implementing NLO calculations in shower Monte Carlo programs: the POWHEG BOX*, *JHEP* **06** (2010) 043, arXiv: [1002.2581 \[hep-ph\]](#).
- [29] S. Alioli, P. Nason, C. Oleari and E. Re, *NLO vector-boson production matched with shower in POWHEG*, *JHEP* **07** (2008) 060, arXiv: [0805.4802 \[hep-ph\]](#).
- [30] H.-L. Lai et al., *New parton distributions for collider physics*, *Phys. Rev. D* **82** (2010) 074024, arXiv: [1007.2241 \[hep-ph\]](#).
- [31] ATLAS Collaboration, *Performance of electron and photon triggers in ATLAS during LHC Run 2*, *Eur. Phys. J. C* **80** (2020) 47, arXiv: [1909.00761 \[hep-ex\]](#).
- [32] ATLAS Collaboration, *Performance of the ATLAS muon triggers in Run 2*, *JINST* **15** (2020) P09015, arXiv: [2004.13447 \[hep-ex\]](#).
- [33] ATLAS Collaboration, *Electron and photon performance measurements with the ATLAS detector using the 2015–2017 LHC proton–proton collision data*, *JINST* **14** (2019) P12006, arXiv: [1908.00005 \[hep-ex\]](#).
- [34] ATLAS Collaboration, *Muon reconstruction performance of the ATLAS detector in proton–proton collision data at $\sqrt{s} = 13$ TeV*, *Eur. Phys. J. C* **76** (2016) 292, arXiv: [1603.05598 \[hep-ex\]](#).
- [35] ATLAS Collaboration, *Measurement of isolated-photon pair production in pp collisions at $\sqrt{s} = 7$ TeV with the ATLAS detector*, *JHEP* **01** (2013) 086, arXiv: [1211.1913 \[hep-ex\]](#).

- [36] ATLAS Collaboration, *Measurement of the $Z(\rightarrow \ell^+\ell^-)\gamma$ production cross-section in pp collisions at $\sqrt{s} = 13$ TeV with the ATLAS detector*, *JHEP* **03** (2020) 054, arXiv: [1911.04813 \[hep-ex\]](#).
- [37] ATLAS Collaboration, *Measurement of the inclusive isolated-photon cross section in pp collisions at $\sqrt{s} = 13$ TeV using 36fb^{-1} of ATLAS data*, *JHEP* **10** (2019) 203, arXiv: [1908.02746 \[hep-ex\]](#).
- [38] ATLAS Collaboration, *Measurement of the production cross section of pairs of isolated photons in pp collisions at 13 TeV with the ATLAS detector*, *JHEP* **11** (2021) 169, arXiv: [2107.09330 \[hep-ex\]](#).
- [39] ATLAS Collaboration, *Measurement of the photon identification efficiencies with the ATLAS detector using LHC Run 2 data collected in 2015 and 2016*, *Eur. Phys. J. C* **79** (2019) 205, arXiv: [1810.05087 \[hep-ex\]](#).
- [40] ATLAS Collaboration, *Electron reconstruction and identification in the ATLAS experiment using the 2015 and 2016 LHC proton–proton collision data at $\sqrt{s} = 13$ TeV*, *Eur. Phys. J. C* **79** (2019) 639, arXiv: [1902.04655 \[hep-ex\]](#).
- [41] ATLAS Collaboration, *Measurement of the Inelastic Proton–Proton Cross Section at $\sqrt{s} = 13$ TeV with the ATLAS Detector at the LHC*, *Phys. Rev. Lett.* **117** (2016) 182002, arXiv: [1606.02625 \[hep-ex\]](#).
- [42] G. D’Agostini, *A multidimensional unfolding method based on Bayes’ theorem*, *Nucl. Instrum. Meth. A* **362** (1995) 487.
- [43] H1 Collaboration, *Measurement of the Inclusive ep Scattering Cross Section at Low Q^2 and x at HERA*, *Eur. Phys. J. C* **63** (2009) 625, arXiv: [0904.0929 \[hep-ph\]](#).
- [44] C. Degrande et al., *Effective field theory: A modern approach to anomalous couplings*, *Annals Phys.* **335** (2013) 21, arXiv: [1205.4231 \[hep-ph\]](#).
- [45] O. J. P. Éboli and M. C. Gonzalez-Garcia, *Classifying the bosonic quartic couplings*, *Phys. Rev. D* **93** (2016) 093013, arXiv: [1604.03555 \[hep-ph\]](#).
- [46] S. S. Wilks, *The Large-Sample Distribution of the Likelihood Ratio for Testing Composite Hypotheses*, *Ann. Math. Stat.* **9** (1938) 60.
- [47] CMS Collaboration, *Measurements of production cross sections of WZ and same-sign WW boson pairs in association with two jets in proton–proton collisions at $\sqrt{s} = 13$ TeV*, *Phys. Lett. B* **809** (2020) 135710, arXiv: [2005.01173 \[hep-ex\]](#).
- [48] ATLAS Collaboration, *ATLAS Computing Acknowledgements*, ATL-SOFT-PUB-2021-003, 2021, URL: <https://cds.cern.ch/record/2776662>.

The ATLAS Collaboration

G. Aad ¹⁰², B. Abbott ¹²⁰, D.C. Abbott ¹⁰³, K. Abeling ⁵⁵, S.H. Abidi ²⁹, A. Aboulhorma ^{35e}, H. Abramowicz ¹⁵¹, H. Abreu ¹⁵⁰, Y. Abulaiti ¹¹⁷, A.C. Abusleme Hoffman ^{137a}, B.S. Acharya ^{69a,69b,q}, C. Adam Bourdarios ⁴, L. Adamczyk ^{85a}, L. Adamek ¹⁵⁵, S.V. Addepalli ²⁶, J. Adelman ¹¹⁵, A. Adiguzel ^{21c}, S. Adorni ⁵⁶, T. Adye ¹³⁴, A.A. Affolder ¹³⁶, Y. Afik ³⁶, M.N. Agaras ¹³, J. Agarwala ^{73a,73b}, A. Aggarwal ¹⁰⁰, C. Agheorghiesei ^{27c}, J.A. Aguilar-Saavedra ^{130f}, A. Ahmad ³⁶, F. Ahmadov ^{38,ac}, W.S. Ahmed ¹⁰⁴, S. Ahuja ⁹⁵, X. Ai ⁴⁸, G. Aielli ^{76a,76b}, M. Ait Tamlihat ^{35e}, B. Aitbenkikh ^{35a}, I. Aizenberg ¹⁶⁹, M. Akbiyik ¹⁰⁰, T.P.A. Åkesson ⁹⁸, A.V. Akimov ³⁷, K. Al Houry ⁴¹, G.L. Alberghi ^{23b}, J. Albert ¹⁶⁵, P. Albicocco ⁵³, S. Alderweireldt ⁵², M. Aleksa ³⁶, I.N. Aleksandrov ³⁸, C. Alexa ^{27b}, T. Alexopoulos ¹⁰, A. Alfonsi ¹¹⁴, F. Alfonsi ^{23b}, M. Alhroob ¹²⁰, B. Ali ¹³², S. Ali ¹⁴⁸, M. Aliev ³⁷, G. Alimonti ^{71a}, W. Alkakh ⁵⁵, C. Allaire ⁶⁶, B.M.M. Allbrooke ¹⁴⁶, C.A. Allendes Flores ^{137f}, P.P. Allport ²⁰, A. Aloisio ^{72a,72b}, F. Alonso ⁹⁰, C. Alpigiani ¹³⁸, M. Alvarez Estevez ⁹⁹, M.G. Alviggi ^{72a,72b}, M. Aly ¹⁰¹, Y. Amaral Coutinho ^{82b}, A. Ambler ¹⁰⁴, C. Amelung ³⁶, M. Amerl ¹, C.G. Ames ¹⁰⁹, D. Amidei ¹⁰⁶, S.P. Amor Dos Santos ^{130a}, K.R. Amos ¹⁶³, V. Ananiev ¹²⁵, C. Anastopoulos ¹³⁹, T. Andeen ¹¹, J.K. Anders ³⁶, S.Y. Andrean ^{47a,47b}, A. Andreazza ^{71a,71b}, S. Angelidakis ⁹, A. Angerami ^{41,af}, A.V. Anisenkov ³⁷, A. Annovi ^{74a}, C. Antel ⁵⁶, M.T. Anthony ¹³⁹, E. Antipov ¹²¹, M. Antonelli ⁵³, D.J.A. Antrim ^{17a}, F. Anulli ^{75a}, M. Aoki ⁸³, T. Aoki ¹⁵³, J.A. Aparisi Pozo ¹⁶³, M.A. Aparo ¹⁴⁶, L. Aperio Bella ⁴⁸, C. Appelt ¹⁸, N. Aranzabal ³⁶, V. Araujo Ferraz ^{82a}, C. Arcangeletti ⁵³, A.T.H. Arce ⁵¹, E. Arena ⁹², J-F. Arguin ¹⁰⁸, S. Argyropoulos ⁵⁴, J.-H. Arling ⁴⁸, A.J. Armbruster ³⁶, O. Arnaez ¹⁵⁵, H. Arnold ¹¹⁴, Z.P. Arrubarrena Tame ¹⁰⁹, G. Artoni ^{75a,75b}, H. Asada ¹¹¹, K. Asai ¹¹⁸, S. Asai ¹⁵³, N.A. Asbah ⁶¹, J. Assahsah ^{35d}, K. Assamagan ²⁹, R. Astalos ^{28a}, R.J. Atkin ^{33a}, M. Atkinson ¹⁶², N.B. Atlay ¹⁸, H. Atmani ^{62b}, P.A. Atmasiddha ¹⁰⁶, K. Augsten ¹³², S. Auricchio ^{72a,72b}, A.D. Auriol ²⁰, V.A. Austrup ¹⁷¹, G. Avner ¹⁵⁰, G. Avolio ³⁶, K. Axiotis ⁵⁶, M.K. Ayoub ^{14c}, G. Azuelos ^{108,ak}, D. Babal ^{28a}, H. Bachacou ¹³⁵, K. Bachas ^{152,t}, A. Bachiu ³⁴, F. Backman ^{47a,47b}, A. Badea ⁶¹, P. Bagnaia ^{75a,75b}, M. Bahmani ¹⁸, A.J. Bailey ¹⁶³, V.R. Bailey ¹⁶², J.T. Baines ¹³⁴, C. Bakalis ¹⁰, O.K. Baker ¹⁷², P.J. Bakker ¹¹⁴, E. Bakos ¹⁵, D. Bakshi Gupta ⁸, S. Balaji ¹⁴⁷, R. Balasubramanian ¹¹⁴, E.M. Baldin ³⁷, P. Balek ¹³³, E. Ballabene ^{71a,71b}, F. Balli ¹³⁵, L.M. Baltes ^{63a}, W.K. Balunas ³², J. Balz ¹⁰⁰, E. Banas ⁸⁶, M. Bandieramonte ¹²⁹, A. Bandyopadhyay ²⁴, S. Bansal ²⁴, L. Barak ¹⁵¹, E.L. Barberio ¹⁰⁵, D. Barberis ^{57b,57a}, M. Barbero ¹⁰², G. Barbour ⁹⁶, K.N. Barends ^{33a}, T. Barillari ¹¹⁰, M-S. Barisits ³⁶, T. Barklow ¹⁴³, R.M. Barnett ^{17a}, P. Baron ¹²², D.A. Baron Moreno ¹⁰¹, A. Baroncelli ^{62a}, G. Barone ²⁹, A.J. Barr ¹²⁶, L. Barranco Navarro ^{47a,47b}, F. Barreiro ⁹⁹, J. Barreiro Guimarães da Costa ^{14a}, U. Barron ¹⁵¹, M.G. Barros Teixeira ^{130a}, S. Barsov ³⁷, F. Bartels ^{63a}, R. Bartoldus ¹⁴³, A.E. Barton ⁹¹, P. Bartos ^{28a}, A. Basalae ⁴⁸, A. Basan ¹⁰⁰, M. Baselga ⁴⁹, I. Bashta ^{77a,77b}, A. Bassalat ^{66,b}, M.J. Basso ¹⁵⁵, C.R. Basson ¹⁰¹, R.L. Bates ⁵⁹, S. Batlamous ^{35e}, J.R. Batley ³², B. Batool ¹⁴¹, M. Battaglia ¹³⁶, D. Battulga ¹⁸, M. Baucé ^{75a,75b}, P. Bauer ²⁴, A. Bayirli ^{21a}, J.B. Beacham ⁵¹, T. Beau ¹²⁷, P.H. Beauchemin ¹⁵⁸, F. Becherer ⁵⁴, P. Bechtel ²⁴, H.P. Beck ^{19,s}, K. Becker ¹⁶⁷, A.J. Beddall ^{21d}, V.A. Bednyakov ³⁸, C.P. Bee ¹⁴⁵, L.J. Beemster ¹⁵, T.A. Beermann ³⁶, M. Begalli ^{82d}, M. Begel ²⁹, A. Behera ¹⁴⁵, J.K. Behr ⁴⁸, C. Beirao Da Cruz E Silva ³⁶, J.F. Beirer ^{55,36}, F. Beisiegel ²⁴, M. Belfkir ¹⁵⁹, G. Bella ¹⁵¹, L. Bellagamba ^{23b}, A. Bellerive ³⁴, P. Bellos ²⁰, K. Beloborodov ³⁷, K. Belotskiy ³⁷, N.L. Belyaev ³⁷, D. Benckekroun ^{35a}, F. Bendebba ^{35a}, Y. Benhammou ¹⁵¹, D.P. Benjamin ²⁹,

M. Benoit ²⁹, J.R. Bensinger ²⁶, S. Bentvelsen ¹¹⁴, L. Beresford ³⁶, M. Beretta ⁵³,
E. Bergeaas Kuutmann ¹⁶¹, N. Berger ⁴, B. Bergmann ¹³², J. Beringer ^{17a}, S. Berlendis ⁷,
G. Bernardi ⁵, C. Bernius ¹⁴³, F.U. Bernlochner ²⁴, T. Berry ⁹⁵, P. Berta ¹³³, A. Berthold ⁵⁰,
I.A. Bertram ⁹¹, S. Bethke ¹¹⁰, A. Betti ^{75a,75b}, A.J. Bevan ⁹⁴, M. Bhamjee ^{33c}, S. Bhatta ¹⁴⁵,
D.S. Bhattacharya ¹⁶⁶, P. Bhattarai ²⁶, V.S. Bhopatkar ¹²¹, R. Bi ^{29,an}, R.M. Bianchi ¹²⁹,
O. Biebel ¹⁰⁹, R. Bielski ¹²³, M. Biglietti ^{77a}, T.R.V. Billoud ¹³², M. Bindi ⁵⁵, A. Bingul ^{21b},
C. Bini ^{75a,75b}, A. Biondini ⁹², C.J. Birch-sykes ¹⁰¹, G.A. Bird ^{20,134}, M. Birman ¹⁶⁹,
M. Biros ¹³³, T. Bisanz ³⁶, E. Bisceglie ^{43b,43a}, D. Biswas ^{170,m}, A. Bitadze ¹⁰¹, K. Bjørke ¹²⁵,
I. Bloch ⁴⁸, C. Blocker ²⁶, A. Blue ⁵⁹, U. Blumenschein ⁹⁴, J. Blumenthal ¹⁰⁰, G.J. Bobbink ¹¹⁴,
V.S. Bobrovnikov ³⁷, M. Boehler ⁵⁴, D. Bogavac ³⁶, A.G. Bogdanchikov ³⁷, C. Bohm ^{47a},
V. Boisvert ⁹⁵, P. Bokan ⁴⁸, T. Bold ^{85a}, M. Bomben ⁵, M. Bona ⁹⁴, M. Boonekamp ¹³⁵,
C.D. Booth ⁹⁵, A.G. Borbély ⁵⁹, H.M. Borecka-Bielska ¹⁰⁸, L.S. Borgna ⁹⁶, G. Borissov ⁹¹,
D. Bortoletto ¹²⁶, D. Boscherini ^{23b}, M. Bosman ¹³, J.D. Bossio Sola ³⁶, K. Bouaouda ^{35a},
N. Bouchhar ¹⁶³, J. Boudreau ¹²⁹, E.V. Bouhova-Thacker ⁹¹, D. Boumediene ⁴⁰, R. Bouquet ⁵,
A. Boveia ¹¹⁹, J. Boyd ³⁶, D. Boye ²⁹, I.R. Boyko ³⁸, J. Bracinik ²⁰, N. Brahimi ^{62d},
G. Brandt ¹⁷¹, O. Brandt ³², F. Braren ⁴⁸, B. Brau ¹⁰³, J.E. Brau ¹²³, K. Brendlinger ⁴⁸,
R. Brenner ¹⁶⁹, L. Brenner ¹¹⁴, R. Brenner ¹⁶¹, S. Bressler ¹⁶⁹, D. Britton ⁵⁹, D. Britzger ¹¹⁰,
I. Brock ²⁴, G. Brooijmans ⁴¹, W.K. Brooks ^{137f}, E. Brost ²⁹, T.L. Bruckler ¹²⁶,
P.A. Bruckman de Renstrom ⁸⁶, B. Brüers ⁴⁸, D. Bruncko ^{28b,*}, A. Bruni ^{23b}, G. Bruni ^{23b},
M. Bruschi ^{23b}, N. Bruscinò ^{75a,75b}, T. Buanes ¹⁶, Q. Buat ¹³⁸, P. Buchholz ¹⁴¹,
A.G. Buckley ⁵⁹, I.A. Budagov ^{38,*}, M.K. Bugge ¹²⁵, O. Bulekov ³⁷, B.A. Bullard ¹⁴³,
S. Burdin ⁹², C.D. Burgard ⁴⁹, A.M. Burger ⁴⁰, B. Burghgrave ⁸, J.T.P. Burr ³², C.D. Burton ¹¹,
J.C. Burzynski ¹⁴², E.L. Busch ⁴¹, V. Büscher ¹⁰⁰, P.J. Bussey ⁵⁹, J.M. Butler ²⁵, C.M. Buttar ⁵⁹,
J.M. Butterworth ⁹⁶, W. Buttinger ¹³⁴, C.J. Buxo Vazquez ¹⁰⁷, A.R. Buzykaev ³⁷, G. Cabras ^{23b},
S. Cabrera Urbán ¹⁶³, D. Caforio ⁵⁸, H. Cai ¹²⁹, Y. Cai ^{14a,14d}, V.M.M. Cairo ³⁶, O. Cakir ^{3a},
N. Calace ³⁶, P. Calafiura ^{17a}, G. Calderini ¹²⁷, P. Calfayan ⁶⁸, G. Callea ⁵⁹, L.P. Caloba ^{82b},
D. Calvet ⁴⁰, S. Calvet ⁴⁰, T.P. Calvet ¹⁰², M. Calvetti ^{74a,74b}, R. Camacho Toro ¹²⁷,
S. Camarda ³⁶, D. Camarero Munoz ²⁶, P. Camarri ^{76a,76b}, M.T. Camerlingo ^{72a,72b},
D. Cameron ¹²⁵, C. Camincher ¹⁶⁵, M. Campanelli ⁹⁶, A. Camplani ⁴², V. Canale ^{72a,72b},
A. Canesse ¹⁰⁴, M. Cano Bret ⁸⁰, J. Cantero ¹⁶³, Y. Cao ¹⁶², F. Capocasa ²⁶, M. Capua ^{43b,43a},
A. Carbone ^{71a,71b}, R. Cardarelli ^{76a}, J.C.J. Cardenas ⁸, F. Cardillo ¹⁶³, T. Carli ³⁶,
G. Carlino ^{72a}, J.I. Carlotto ¹³, B.T. Carlson ^{129,u}, E.M. Carlson ^{165,156a}, L. Carminati ^{71a,71b},
M. Carnesale ^{75a,75b}, S. Caron ¹¹³, E. Carquin ^{137f}, S. Carrá ^{71a,71b}, G. Carratta ^{23b,23a},
F. Carrio Argos ^{33g}, J.W.S. Carter ¹⁵⁵, T.M. Carter ⁵², M.P. Casado ^{13j}, A.F. Casha ¹⁵⁵,
E.G. Castiglia ¹⁷², F.L. Castillo ^{63a}, L. Castillo Garcia ¹³, V. Castillo Gimenez ¹⁶³,
N.F. Castro ^{130a,130e}, A. Catinaccio ³⁶, J.R. Catmore ¹²⁵, V. Cavaliere ²⁹, N. Cavalli ^{23b,23a},
V. Cavasinni ^{74a,74b}, E. Celebi ^{21a}, F. Celli ¹²⁶, M.S. Centonze ^{70a,70b}, K. Cerny ¹²²,
A.S. Cerqueira ^{82a}, A. Cerri ¹⁴⁶, L. Cerrito ^{76a,76b}, F. Cerutti ^{17a}, A. Cervelli ^{23b}, S.A. Cetin ^{21d},
Z. Chadi ^{35a}, D. Chakraborty ¹¹⁵, M. Chala ^{130f}, J. Chan ¹⁷⁰, W.Y. Chan ¹⁵³, J.D. Chapman ³²,
B. Chargeishvili ^{149b}, D.G. Charlton ²⁰, T.P. Charman ⁹⁴, M. Chatterjee ¹⁹, S. Chekanov ⁶,
S.V. Chekulaev ^{156a}, G.A. Chelkov ^{38,a}, A. Chen ¹⁰⁶, B. Chen ¹⁵¹, B. Chen ¹⁶⁵, H. Chen ^{14c},
H. Chen ²⁹, J. Chen ^{62c}, J. Chen ¹⁴², S. Chen ¹⁵³, S.J. Chen ^{14c}, X. Chen ^{62c}, X. Chen ^{14b,aj},
Y. Chen ^{62a}, C.L. Cheng ¹⁷⁰, H.C. Cheng ^{64a}, S. Cheong ¹⁴³, A. Cheplakov ³⁸,
E. Cheremushkina ⁴⁸, E. Cherepanova ¹¹⁴, R. Cherkaoui El Moursli ^{35e}, E. Cheu ⁷, K. Cheung ⁶⁵,
L. Chevalier ¹³⁵, V. Chiarella ⁵³, G. Chiarelli ^{74a}, N. Chiedde ¹⁰², G. Chiodini ^{70a},
A.S. Chisholm ²⁰, A. Chitan ^{27b}, M. Chitishvili ¹⁶³, Y.H. Chiu ¹⁶⁵, M.V. Chizhov ³⁸, K. Choi ¹¹,
A.R. Chomont ^{75a,75b}, Y. Chou ¹⁰³, E.Y.S. Chow ¹¹⁴, T. Chowdhury ^{33g}, L.D. Christopher ^{33g},

K.L. Chu^{64a}, M.C. Chu^{64a}, X. Chu^{14a,14d}, J. Chudoba¹³¹, J.J. Chwastowski⁸⁶, D. Cieri¹¹⁰,
 K.M. Ciesla^{85a}, V. Cindro⁹³, A. Ciocio^{17a}, F. Cirotto^{72a,72b}, Z.H. Citron^{169,n}, M. Citterio^{71a},
 D.A. Ciubotaru^{27b}, B.M. Ciungu¹⁵⁵, A. Clark⁵⁶, P.J. Clark⁵², J.M. Clavijo Columbie⁴⁸,
 S.E. Clawson¹⁰¹, C. Clement^{47a,47b}, J. Clercx⁴⁸, L. Clissa^{23b,23a}, Y. Coadou¹⁰²,
 M. Cobal^{69a,69c}, A. Cocco^{57b}, R.F. Coelho Barrue^{130a}, R. Coelho Lopes De Sa¹⁰³,
 S. Coelli^{71a}, H. Cohen¹⁵¹, A.E.C. Coimbra^{71a,71b}, B. Cole⁴¹, J. Collot⁶⁰,
 P. Conde Muiño^{130a,130g}, M.P. Connell^{33c}, S.H. Connell^{33c}, I.A. Connelly⁵⁹, E.I. Conroy¹²⁶,
 F. Conventi^{72a,al}, H.G. Cooke²⁰, A.M. Cooper-Sarkar¹²⁶, F. Cormier¹⁶⁴, L.D. Corpe³⁶,
 M. Corradi^{75a,75b}, E.E. Corrigan⁹⁸, F. Corriveau^{104,aa}, A. Cortes-Gonzalez¹⁸, M.J. Costa¹⁶³,
 F. Costanza⁴, D. Costanzo¹³⁹, B.M. Cote¹¹⁹, G. Cowan⁹⁵, J.W. Cowley³², K. Cranmer¹¹⁷,
 S. Crépe-Renaudin⁶⁰, F. Crescioli¹²⁷, M. Cristinziani¹⁴¹, M. Cristoforetti^{78a,78b,d}, V. Croft¹⁵⁸,
 G. Crosetti^{43b,43a}, A. Cueto³⁶, T. Cuhadar Donszelmann¹⁶⁰, H. Cui^{14a,14d}, Z. Cui⁷,
 W.R. Cunningham⁵⁹, F. Curcio^{43b,43a}, P. Czodrowski³⁶, M.M. Czurylo^{63b},
 M.J. Da Cunha Sargedas De Sousa^{62a}, J.V. Da Fonseca Pinto^{82b}, C. Da Via¹⁰¹, W. Dabrowski^{85a},
 T. Dado⁴⁹, S. Dahbi^{33g}, T. Dai¹⁰⁶, C. Dallapiccola¹⁰³, M. Dam⁴², G. D'amen²⁹,
 V. D'Amico¹⁰⁹, J. Damp¹⁰⁰, J.R. Dandoy¹²⁸, M.F. Daneri³⁰, M. Danninger¹⁴², V. Dao³⁶,
 G. Darbo^{57b}, S. Darmora⁶, S.J. Das^{29,an}, S. D'Auria^{71a,71b}, C. David^{156b}, T. Davidek¹³³,
 D.R. Davis⁵¹, B. Davis-Purcell³⁴, I. Dawson⁹⁴, K. De⁸, R. De Asmundis^{72a},
 M. De Beurs¹¹⁴, N. De Biase⁴⁸, S. De Castro^{23b,23a}, N. De Groot¹¹³, P. de Jong¹¹⁴,
 H. De la Torre¹⁰⁷, A. De Maria^{14c}, A. De Salvo^{75a}, U. De Sanctis^{76a,76b}, A. De Santo¹⁴⁶,
 J.B. De Vivie De Regie⁶⁰, D.V. Dedovich³⁸, J. Degens¹¹⁴, A.M. Deiana⁴⁴, F. Del Corso^{23b,23a},
 J. Del Peso⁹⁹, F. Del Rio^{63a}, F. Deliot¹³⁵, C.M. Delitzsch⁴⁹, M. Della Pietra^{72a,72b},
 D. Della Volpe⁵⁶, A. Dell'Acqua³⁶, L. Dell'Asta^{71a,71b}, M. Delmastro⁴, P.A. Delsart⁶⁰,
 S. Demers¹⁷², M. Demichev³⁸, S.P. Denisov³⁷, L. D'Eramo¹¹⁵, D. Derendarz⁸⁶,
 F. Derue¹²⁷, P. Dervan⁹², K. Desch²⁴, K. Dette¹⁵⁵, C. Deutsch²⁴, F.A. Di Bello^{57b,57a},
 A. Di Ciaccio^{76a,76b}, L. Di Ciaccio⁴, A. Di Domenico^{75a,75b}, C. Di Donato^{72a,72b},
 A. Di Girolamo³⁶, G. Di Gregorio⁵, A. Di Luca^{78a,78b}, B. Di Micco^{77a,77b}, R. Di Nardo^{77a,77b},
 C. Diaconu¹⁰², F.A. Dias¹¹⁴, T. Dias Do Vale¹⁴², M.A. Diaz^{137a,137b}, F.G. Diaz Capriles²⁴,
 M. Didenko¹⁶³, E.B. Diehl¹⁰⁶, L. Diehl⁵⁴, S. Díez Cornell⁴⁸, C. Díez Pardos¹⁴¹,
 C. Dimitriadi^{24,161}, A. Dimitrievska^{17a}, J. Dingfelder²⁴, I-M. Dinu^{27b}, S.J. Dittmeier^{63b},
 F. Dittus³⁶, F. Djama¹⁰², T. Djobava^{149b}, J.I. Djuvsland¹⁶, C. Doglioni^{101,98}, J. Dolejsi¹³³,
 Z. Dolezal¹³³, M. Donadelli^{82c}, B. Dong¹⁰⁷, J. Donini⁴⁰, A. D'Onofrio^{77a,77b},
 M. D'Onofrio⁹², J. Dopke¹³⁴, A. Doria^{72a}, M.T. Dova⁹⁰, A.T. Doyle⁵⁹, M.A. Draguet¹²⁶,
 E. Drechsler¹⁴², E. Dreyer¹⁶⁹, I. Drivas-koulouris¹⁰, A.S. Drobac¹⁵⁸, M. Drozdova⁵⁶,
 D. Du^{62a}, T.A. du Pree¹¹⁴, F. Dubinin³⁷, M. Dubovsky^{28a}, E. Duchovni¹⁶⁹, G. Duckeck¹⁰⁹,
 O.A. Ducu^{27b}, D. Duda¹¹⁰, A. Dudarev³⁶, M. D'uffizi¹⁰¹, L. Duflot⁶⁶, M. Dührssen³⁶,
 C. Dülsen¹⁷¹, A.E. Dumitriu^{27b}, M. Dunford^{63a}, S. Dungs⁴⁹, K. Dunne^{47a,47b},
 A. Duperrin¹⁰², H. Duran Yildiz^{3a}, M. Düren⁵⁸, A. Durglishvili^{149b}, B.L. Dwyer¹¹⁵,
 G.I. Dyckes^{17a}, M. Dyndal^{85a}, S. Dysch¹⁰¹, B.S. Dziedzic⁸⁶, Z.O. Earnshaw¹⁴⁶,
 B. Eckerova^{28a}, S. Eggebrecht⁵⁵, M.G. Eggleston⁵¹, E. Egidio Purcino De Souza¹²⁷,
 L.F. Ehrke⁵⁶, G. Eigen¹⁶, K. Einsweiler^{17a}, T. Ekelof¹⁶¹, P.A. Ekman⁹⁸, Y. El Ghazali^{35b},
 H. El Jarrari^{35e,148}, A. El Moussaouy^{35a}, V. Ellajosyula¹⁶¹, M. Ellert¹⁶¹, F. Ellinghaus¹⁷¹,
 A.A. Elliot⁹⁴, N. Ellis³⁶, J. Elmsheuser²⁹, M. Elsing³⁶, D. Emelianov¹³⁴, A. Emerman⁴¹,
 Y. Enari¹⁵³, I. Ene^{17a}, S. Epari¹³, J. Erdmann^{49,ah}, A. Ereditato¹⁹, P.A. Erland⁸⁶,
 M. Errenst¹⁷¹, M. Escalier⁶⁶, C. Escobar¹⁶³, E. Etzion¹⁵¹, G. Evans^{130a}, H. Evans⁶⁸,
 M.O. Evans¹⁴⁶, A. Ezhilov³⁷, S. Ezzarqtouni^{35a}, F. Fabbri⁵⁹, L. Fabbri^{23b,23a}, G. Facini⁹⁶,
 V. Fadeyev¹³⁶, R.M. Fakhrutdinov³⁷, S. Falciano^{75a}, L.F. Falda Ulhoa Coelho³⁶, P.J. Falke²⁴,

S. Falke ³⁶, J. Faltova ¹³³, Y. Fan ^{14a}, Y. Fang ^{14a,14d}, G. Fanourakis ⁴⁶, M. Fanti ^{71a,71b},
 M. Faraj ^{69a,69b}, Z. Farazpay ⁹⁷, A. Farbin ⁸, A. Farilla ^{77a}, T. Farooque ¹⁰⁷, S.M. Farrington ⁵²,
 F. Fassi ^{35e}, D. Fassouliotis ⁹, M. Faucci Giannelli ^{76a,76b}, W.J. Fawcett ³², L. Fayard ⁶⁶,
 P. Federicova ¹³¹, O.L. Fedin ^{37,a}, G. Fedotov ³⁷, M. Feickert ¹⁷⁰, L. Feligioni ¹⁰², A. Fell ¹³⁹,
 D.E. Fellers ¹²³, C. Feng ^{62b}, M. Feng ^{14b}, Z. Feng ¹¹⁴, M.J. Fenton ¹⁶⁰, A.B. Fenyuk ³⁷,
 L. Ferencz ⁴⁸, R.A.M. Ferguson ⁹¹, J. Ferrando ⁴⁸, A. Ferrari ¹⁶¹, P. Ferrari ^{114,113},
 R. Ferrari ^{73a}, D. Ferrere ⁵⁶, C. Ferretti ¹⁰⁶, F. Fiedler ¹⁰⁰, A. Filipčič ⁹³, E.K. Filmer ¹,
 F. Filthaut ¹¹³, M.C.N. Fiolhais ^{130a,130c,c}, L. Fiorini ¹⁶³, F. Fischer ¹⁴¹, W.C. Fisher ¹⁰⁷,
 T. Fitschen ¹⁰¹, I. Fleck ¹⁴¹, P. Fleischmann ¹⁰⁶, T. Flick ¹⁷¹, L. Flores ¹²⁸, M. Flores ^{33d,ag},
 L.R. Flores Castillo ^{64a}, F.M. Follega ^{78a,78b}, N. Fomin ¹⁶, J.H. Foo ¹⁵⁵, B.C. Forland ⁶⁸,
 A. Formica ¹³⁵, A.C. Forti ¹⁰¹, E. Fortin ¹⁰², A.W. Fortman ⁶¹, M.G. Foti ^{17a}, L. Fountas ^{9,k},
 D. Fournier ⁶⁶, H. Fox ⁹¹, P. Francavilla ^{74a,74b}, S. Francescato ⁶¹, S. Franchellucci ⁵⁶,
 M. Franchini ^{23b,23a}, S. Franchino ^{63a}, D. Francis ³⁶, L. Franco ¹¹³, L. Franconi ¹⁹, M. Franklin ⁶¹,
 G. Frattari ²⁶, A.C. Freegard ⁹⁴, P.M. Freeman ²⁰, W.S. Freund ^{82b}, N. Fritzsche ⁵⁰, A. Froch ⁵⁴,
 D. Froidevaux ³⁶, J.A. Frost ¹²⁶, Y. Fu ^{62a}, M. Fujimoto ¹¹⁸, E. Fullana Torregrosa ^{163,*},
 J. Fuster ¹⁶³, A. Gabrielli ^{23b,23a}, A. Gabrielli ¹⁵⁵, P. Gadow ⁴⁸, G. Gagliardi ^{57b,57a},
 L.G. Gagnon ^{17a}, G.E. Gallardo ¹²⁶, E.J. Gallas ¹²⁶, B.J. Gallop ¹³⁴, R. Gamboa Goni ⁹⁴,
 K.K. Gan ¹¹⁹, S. Ganguly ¹⁵³, J. Gao ^{62a}, Y. Gao ⁵², F.M. Garay Walls ^{137a,137b}, B. Garcia ^{29,an},
 C. García ¹⁶³, J.E. García Navarro ¹⁶³, M. Garcia-Sciveres ^{17a}, R.W. Gardner ³⁹, D. Garg ⁸⁰,
 R.B. Garg ^{143,r}, C.A. Garner ¹⁵⁵, V. Garonne ²⁹, S.J. Gasiorowski ¹³⁸, P. Gaspar ^{82b},
 G. Gaudio ^{73a}, V. Gautam ¹³, P. Gauzzi ^{75a,75b}, I.L. Gavrilenko ³⁷, A. Gavrilyuk ³⁷, C. Gay ¹⁶⁴,
 G. Gaycken ⁴⁸, E.N. Gazis ¹⁰, A.A. Geanta ^{27b,27e}, C.M. Gee ¹³⁶, J. Geisen ⁹⁸, C. Gemme ^{57b},
 M.H. Genest ⁶⁰, S. Gentile ^{75a,75b}, S. George ⁹⁵, W.F. George ²⁰, T. Gerialis ⁴⁶, L.O. Gerlach ⁵⁵,
 P. Gessinger-Befurt ³⁶, M. Ghasemi Bostanabad ¹⁶⁵, M. Ghneimat ¹⁴¹, K. Ghorbanian ⁹⁴,
 A. Ghosal ¹⁴¹, A. Ghosh ¹⁶⁰, A. Ghosh ⁷, B. Giacobbe ^{23b}, S. Giagu ^{75a,75b}, P. Giannetti ^{74a},
 A. Giannini ^{62a}, S.M. Gibson ⁹⁵, M. Gignac ¹³⁶, D.T. Gil ^{85b}, A.K. Gilbert ^{85a}, B.J. Gilbert ⁴¹,
 D. Gillberg ³⁴, G. Gilles ¹¹⁴, N.E.K. Gillwald ⁴⁸, L. Ginabat ¹²⁷, D.M. Gingrich ^{2,ak},
 M.P. Giordani ^{69a,69c}, P.F. Giraud ¹³⁵, G. Giugliarelli ^{69a,69c}, D. Giugni ^{71a}, F. Giuli ³⁶,
 I. Gkialas ^{9,k}, L.K. Gladilin ³⁷, C. Glasman ⁹⁹, G.R. Gledhill ¹²³, M. Glisic ¹²³, I. Gnesi ^{43b,g},
 Y. Go ^{29,an}, M. Goblirsch-Kolb ²⁶, B. Gocke ⁴⁹, D. Godin ¹⁰⁸, B. Gokturk ^{21a}, S. Goldfarb ¹⁰⁵,
 T. Golling ⁵⁶, M.G.D. Gololo ^{33g}, D. Golubkov ³⁷, J.P. Gombas ¹⁰⁷, A. Gomes ^{130a,130b},
 G. Gomes Da Silva ¹⁴¹, A.J. Gomez Delegido ¹⁶³, R. Goncalves Gama ⁵⁵, R. Gonçalves ^{130a,130c},
 G. Gonella ¹²³, L. Gonella ²⁰, A. Gongadze ³⁸, F. Gonnella ²⁰, J.L. Gonski ⁴¹,
 R.Y. González Andana ⁵², S. González de la Hoz ¹⁶³, S. Gonzalez Fernandez ¹³,
 R. Gonzalez Lopez ⁹², C. Gonzalez Renteria ^{17a}, R. Gonzalez Suarez ¹⁶¹, S. Gonzalez-Sevilla ⁵⁶,
 G.R. Gonzalvo Rodriguez ¹⁶³, L. Goossens ³⁶, N.A. Gorasia ²⁰, P.A. Gorbounov ³⁷, B. Gorini ³⁶,
 E. Gorini ^{70a,70b}, A. Gorišek ⁹³, A.T. Goshaw ⁵¹, M.I. Gostkin ³⁸, S. Goswami ¹²¹,
 C.A. Gottardo ³⁶, M. Goughri ^{35b}, V. Goumarre ⁴⁸, A.G. Goussiou ¹³⁸, N. Govender ^{33c},
 C. Goy ⁴, I. Grabowska-Bold ^{85a}, K. Graham ³⁴, E. Gramstad ¹²⁵, S. Grancagnolo ¹⁸,
 M. Grandi ¹⁴⁶, V. Gratchev ^{37,*}, P.M. Gravila ^{27f}, F.G. Gravili ^{70a,70b}, H.M. Gray ^{17a},
 M. Greco ^{70a,70b}, C. Grefe ²⁴, I.M. Gregor ⁴⁸, P. Grenier ¹⁴³, C. Grieco ¹³, A.A. Grillo ¹³⁶,
 K. Grimm ^{31,o}, S. Grinstein ^{13,w}, J.-F. Grivaz ⁶⁶, E. Gross ¹⁶⁹, J. Grosse-Knetter ⁵⁵, C. Grud ¹⁰⁶,
 A. Grummer ¹¹², J.C. Grundy ¹²⁶, L. Guan ¹⁰⁶, W. Guan ¹⁷⁰, C. Gubbels ¹⁶⁴,
 J.G.R. Guerrero Rojas ¹⁶³, G. Guerrieri ^{69a,69b}, F. Guescini ¹¹⁰, R. Gugel ¹⁰⁰, J.A.M. Guhit ¹⁰⁶,
 A. Guida ⁴⁸, T. Guillemain ⁴, E. Guilloton ^{167,134}, S. Guindon ³⁶, F. Guo ^{14a,14d}, J. Guo ^{62c},
 L. Guo ⁶⁶, Y. Guo ¹⁰⁶, R. Gupta ⁴⁸, S. Gurbuz ²⁴, S.S. Gurdasani ⁵⁴, G. Gustavino ³⁶,
 M. Guth ⁵⁶, P. Gutierrez ¹²⁰, L.F. Gutierrez Zagazeta ¹²⁸, C. Gutschow ⁹⁶, C. Guyot ¹³⁵,

C. Gwenlan ^{id126}, C.B. Gwilliam ^{id92}, E.S. Haaland ^{id125}, A. Haas ^{id117}, M. Habedank ^{id48},
 C. Haber ^{id17a}, H.K. Hadavand ^{id8}, A. Hadeif ^{id100}, S. Hadzic ^{id110}, E.H. Haines ^{id96}, M. Haleem ^{id166},
 J. Haley ^{id121}, J.J. Hall ^{id139}, G.D. Hallewell ^{id102}, L. Halser ^{id19}, K. Hamano ^{id165}, H. Hamdaoui ^{id35e},
 M. Hamer ^{id24}, G.N. Hamity ^{id52}, J. Han ^{id62b}, K. Han ^{id62a}, L. Han ^{id14c}, L. Han ^{id62a}, S. Han ^{id17a},
 Y.F. Han ^{id155}, K. Hanagaki ^{id83}, M. Hance ^{id136}, D.A. Hangal ^{id41.af}, H. Hanif ^{id142}, M.D. Hank ^{id39},
 R. Hankache ^{id101}, J.B. Hansen ^{id42}, J.D. Hansen ^{id42}, P.H. Hansen ^{id42}, K. Hara ^{id157}, D. Harada ^{id56},
 T. Harenberg ^{id171}, S. Harkusha ^{id37}, Y.T. Harris ^{id126}, N.M. Harrison ^{id119}, P.F. Harrison ^{id167},
 N.M. Hartman ^{id143}, N.M. Hartmann ^{id109}, Y. Hasegawa ^{id140}, A. Hasib ^{id52}, S. Haug ^{id19},
 R. Hauser ^{id107}, M. Havranek ^{id132}, C.M. Hawkes ^{id20}, R.J. Hawkins ^{id36}, S. Hayashida ^{id111},
 D. Hayden ^{id107}, C. Hayes ^{id106}, R.L. Hayes ^{id164}, C.P. Hays ^{id126}, J.M. Hays ^{id94}, H.S. Hayward ^{id92},
 F. He ^{id62a}, Y. He ^{id154}, Y. He ^{id127}, M.P. Heath ^{id52}, V. Hedberg ^{id98}, A.L. Heggelund ^{id125},
 N.D. Hehir ^{id94}, C. Heidegger ^{id54}, K.K. Heidegger ^{id54}, W.D. Heidorn ^{id81}, J. Heilman ^{id34},
 S. Heim ^{id48}, T. Heim ^{id17a}, J.G. Heinlein ^{id128}, J.J. Heinrich ^{id123}, L. Heinrich ^{id110.ai}, J. Hejbal ^{id131},
 L. Helary ^{id48}, A. Held ^{id170}, S. Hellesund ^{id125}, C.M. Helling ^{id164}, S. Hellman ^{id47a.47b}, C. Helsens ^{id36},
 R.C.W. Henderson ^{id91}, L. Henkelmann ^{id32}, A.M. Henriques Correia ^{id36}, H. Herde ^{id98},
 Y. Hernández Jiménez ^{id145}, L.M. Herrmann ^{id24}, M.G. Herrmann ^{id109}, T. Herrmann ^{id50}, G. Herten ^{id54},
 R. Hertenberger ^{id109}, L. Hervas ^{id36}, N.P. Hesse ^{id156a}, H. Hibi ^{id84}, E. Higón-Rodríguez ^{id163},
 S.J. Hillier ^{id20}, I. Hinchliffe ^{id17a}, F. Hinterkeuser ^{id24}, M. Hirose ^{id124}, S. Hirose ^{id157},
 D. Hirschbuehl ^{id171}, T.G. Hitchings ^{id101}, B. Hiti ^{id93}, J. Hobbs ^{id145}, R. Hobincu ^{id27e}, N. Hod ^{id169},
 M.C. Hodgkinson ^{id139}, B.H. Hodgkinson ^{id32}, A. Hoecker ^{id36}, J. Hofer ^{id48}, D. Hohn ^{id54}, T. Holm ^{id24},
 M. Holzbock ^{id110}, L.B.A.H. Hommels ^{id32}, B.P. Honan ^{id101}, J. Hong ^{id62c}, T.M. Hong ^{id129},
 J.C. Honig ^{id54}, A. Hönle ^{id110}, B.H. Hooberman ^{id162}, W.H. Hopkins ^{id6}, Y. Horii ^{id111}, S. Hou ^{id148},
 A.S. Howard ^{id93}, J. Howarth ^{id59}, J. Hoya ^{id6}, M. Hrabovsky ^{id122}, A. Hrynevich ^{id48}, T. Hryn'ova ^{id4},
 P.J. Hsu ^{id65}, S.-C. Hsu ^{id138}, Q. Hu ^{id41}, Y.F. Hu ^{id14a.14d.am}, D.P. Huang ^{id96}, S. Huang ^{id64b},
 X. Huang ^{id14c}, Y. Huang ^{id62a}, Y. Huang ^{id14a}, Z. Huang ^{id101}, Z. Hubacek ^{id132}, M. Huebner ^{id24},
 F. Huegging ^{id24}, T.B. Huffman ^{id126}, M. Huhtinen ^{id36}, S.K. Huiberts ^{id16}, R. Hulsken ^{id104},
 N. Huseynov ^{id12.a}, J. Huston ^{id107}, J. Huth ^{id61}, R. Hyneman ^{id143}, S. Hyrych ^{id28a}, G. Iacobucci ^{id56},
 G. Iakovidis ^{id29}, I. Ibragimov ^{id141}, L. Iconomidou-Fayard ^{id66}, P. Iengo ^{id72a.72b}, R. Iguchi ^{id153},
 T. Iizawa ^{id56}, Y. Ikegami ^{id83}, A. Ilg ^{id19}, N. Ilic ^{id155}, H. Imam ^{id35a}, T. Ingebretsen Carlson ^{id47a.47b},
 G. Introzzi ^{id73a.73b}, M. Iodice ^{id77a}, V. Ippolito ^{id75a.75b}, M. Ishino ^{id153}, W. Islam ^{id170}, C. Issever ^{id18.48},
 S. Istin ^{id21a.ap}, H. Ito ^{id168}, J.M. Iturbe Ponce ^{id64a}, R. Iuppa ^{id78a.78b}, A. Ivina ^{id169}, J.M. Izen ^{id45},
 V. Izzo ^{id72a}, P. Jacka ^{id131.132}, P. Jackson ^{id1}, R.M. Jacobs ^{id48}, B.P. Jaeger ^{id142}, C.S. Jagfeld ^{id109},
 P. Jain ^{id54}, G. Jäkel ^{id171}, K. Jakobs ^{id54}, T. Jakoubek ^{id169}, J. Jamieson ^{id59}, K.W. Janas ^{id85a},
 G. Jarlskog ^{id98}, A.E. Jaspán ^{id92}, M. Javurkova ^{id103}, F. Jeanneau ^{id135}, L. Jeanty ^{id123},
 J. Jejelava ^{id149a.ad}, P. Jenni ^{id54.h}, C.E. Jessiman ^{id34}, S. Jézéquel ^{id4}, J. Jia ^{id145}, X. Jia ^{id61},
 X. Jia ^{id14a.14d}, Z. Jia ^{id14c}, Y. Jiang ^{id62a}, S. Jiggins ^{id52}, J. Jimenez Pena ^{id110}, S. Jin ^{id14c}, A. Jinaru ^{id27b},
 O. Jinnouchi ^{id154}, P. Johansson ^{id139}, K.A. Johns ^{id7}, J.W. Johnson ^{id136}, D.M. Jones ^{id32}, E. Jones ^{id167},
 P. Jones ^{id32}, R.W.L. Jones ^{id91}, T.J. Jones ^{id92}, R. Joshi ^{id119}, J. Jovicevic ^{id15}, X. Ju ^{id17a},
 J.J. Junggeburth ^{id36}, T. Junkermann ^{id63a}, A. Juste Rozas ^{id13.w}, S. Kabana ^{id137e}, A. Kaczmarek ^{id86},
 M. Kado ^{id75a.75b}, H. Kagan ^{id119}, M. Kagan ^{id143}, A. Kahn ^{id41}, A. Kahn ^{id128}, C. Kahra ^{id100}, T. Kaji ^{id168},
 E. Kajomovitz ^{id150}, N. Kakati ^{id169}, C.W. Kalderon ^{id29}, A. Kamenshchikov ^{id155}, S. Kanayama ^{id154},
 N.J. Kang ^{id136}, D. Kar ^{id33g}, K. Karava ^{id126}, M.J. Kareem ^{id156b}, E. Karentzos ^{id54}, I. Karkanas ^{id152.f},
 S.N. Karpov ^{id38}, Z.M. Karpova ^{id38}, V. Kartvelishvili ^{id91}, A.N. Karyukhin ^{id37}, E. Kasimi ^{id152.f},
 C. Kato ^{id62d}, J. Katzy ^{id48}, S. Kaur ^{id34}, K. Kawade ^{id140}, K. Kawagoe ^{id89}, T. Kawamoto ^{id135},
 G. Kawamura ^{id55}, E.F. Kay ^{id165}, F.I. Kaya ^{id158}, S. Kazakos ^{id13}, V.F. Kazanin ^{id37}, Y. Ke ^{id145},
 J.M. Keaveney ^{id33a}, R. Keeler ^{id165}, G.V. Kehris ^{id61}, J.S. Keller ^{id34}, A.S. Kelly ^{id96}, D. Kelsey ^{id146},
 J.J. Kempster ^{id20}, K.E. Kennedy ^{id41}, P.D. Kennedy ^{id100}, O. Kepka ^{id131}, B.P. Kerridge ^{id167},

S. Kersten ¹⁷¹, B.P. Kerševan ⁹³, S. Keshri ⁶⁶, L. Keszeghova ^{28a}, S. Ketabchi Haghighat ¹⁵⁵,
 M. Khandoga ¹²⁷, A. Khanov ¹²¹, A.G. Kharlamov ³⁷, T. Kharlamova ³⁷, E.E. Khoda ¹³⁸,
 T.J. Khoo ¹⁸, G. Khoriali ¹⁶⁶, J. Khubua ^{149b}, Y.A.R. Khwaira ⁶⁶, M. Kiehn ³⁶,
 A. Kilgallon ¹²³, D.W. Kim ^{47a,47b}, E. Kim ¹⁵⁴, Y.K. Kim ³⁹, N. Kimura ⁹⁶, A. Kirchhoff ⁵⁵,
 D. Kirchmeier ⁵⁰, C. Kirfel ²⁴, J. Kirk ¹³⁴, A.E. Kiryunin ¹¹⁰, T. Kishimoto ¹⁵³, D.P. Kisliuk ¹⁵⁵,
 C. Kitsaki ¹⁰, O. Kivernyk ²⁴, M. Klassen ^{63a}, C. Klein ³⁴, L. Klein ¹⁶⁶, M.H. Klein ¹⁰⁶,
 M. Klein ⁹², S.B. Klein ⁵⁶, U. Klein ⁹², P. Klimek ³⁶, A. Klimentov ²⁹, F. Klimpel ¹¹⁰,
 T. Klioutchnikova ³⁶, P. Kluit ¹¹⁴, S. Kluth ¹¹⁰, E. Kneringer ⁷⁹, T.M. Knight ¹⁵⁵, A. Knue ⁵⁴,
 D. Kobayashi ⁸⁹, R. Kobayashi ⁸⁷, M. Kocian ¹⁴³, P. Kodyš ¹³³, D.M. Koeck ¹⁴⁶, P.T. Koenig ²⁴,
 T. Koffas ³⁴, M. Kolb ¹³⁵, I. Koletsou ⁴, T. Komarek ¹²², K. Köneke ⁵⁴, A.X.Y. Kong ¹,
 T. Kono ¹¹⁸, N. Konstantinidis ⁹⁶, B. Konya ⁹⁸, R. Kopeliansky ⁶⁸, S. Koperny ^{85a}, K. Korcyl ⁸⁶,
 K. Kordas ^{152,f}, G. Koren ¹⁵¹, A. Korn ⁹⁶, S. Korn ⁵⁵, I. Korolkov ¹³, N. Korotkova ³⁷,
 B. Kortman ¹¹⁴, O. Kortner ¹¹⁰, S. Kortner ¹¹⁰, W.H. Kostecka ¹¹⁵, V.V. Kostyukhin ¹⁴¹,
 A. Kotsokechagia ¹³⁵, A. Kotwal ⁵¹, A. Koulouris ³⁶, A. Kourkoumeli-Charalampidi ^{73a,73b},
 C. Kourkoumelis ⁹, E. Kourlitis ⁶, O. Kovanda ¹⁴⁶, R. Kowalewski ¹⁶⁵, W. Kozanecki ¹³⁵,
 A.S. Kozhin ³⁷, V.A. Kramarenko ³⁷, G. Kramberger ⁹³, P. Kramer ¹⁰⁰, M.W. Krasny ¹²⁷,
 A. Krasznahorkay ³⁶, J.A. Kremer ¹⁰⁰, T. Kresse ⁵⁰, J. Kretschmar ⁹², K. Kreul ¹⁸,
 P. Krieger ¹⁵⁵, S. Krishnamurthy ¹⁰³, M. Krivos ¹³³, K. Krizka ^{17a}, K. Kroeninger ⁴⁹,
 H. Kroha ¹¹⁰, J. Kroll ¹³¹, J. Kroll ¹²⁸, K.S. Krowpman ¹⁰⁷, U. Kruchonak ³⁸, H. Krüger ²⁴,
 N. Krumnack ⁸¹, M.C. Kruse ⁵¹, J.A. Krzysiak ⁸⁶, O. Kuchinskaia ³⁷, S. Kuday ^{3a}, D. Kuechler ⁴⁸,
 J.T. Kuechler ⁴⁸, S. Kuehn ³⁶, R. Kuesters ⁵⁴, T. Kuhl ⁴⁸, V. Kukhtin ³⁸, Y. Kulchitsky ^{37,a},
 S. Kuleshov ^{137d,137b}, M. Kumar ^{33g}, N. Kumari ¹⁰², A. Kupco ¹³¹, T. Kupfer ⁴⁹, A. Kupich ³⁷,
 O. Kuprash ⁵⁴, H. Kurashige ⁸⁴, L.L. Kurchaninov ^{156a}, Y.A. Kurochkin ³⁷, A. Kurova ³⁷,
 M. Kuze ¹⁵⁴, A.K. Kvam ¹⁰³, J. Kvita ¹²², T. Kwan ¹⁰⁴, K.W. Kwok ^{64a}, N.G. Kyriacou ¹⁰⁶,
 L.A.O. Laatu ¹⁰², C. Lacasta ¹⁶³, F. Lacava ^{75a,75b}, H. Lacker ¹⁸, D. Lacour ¹²⁷, N.N. Lad ⁹⁶,
 E. Ladygin ³⁸, B. Laforge ¹²⁷, T. Lagouri ^{137e}, S. Lai ⁵⁵, I.K. Lakomic ^{85a}, N. Lalloue ⁶⁰,
 J.E. Lambert ¹²⁰, S. Lammers ⁶⁸, W. Lampl ⁷, C. Lampoudis ^{152,f}, A.N. Lancaster ¹¹⁵,
 E. Lançon ²⁹, U. Landgraf ⁵⁴, M.P.J. Landon ⁹⁴, V.S. Lang ⁵⁴, R.J. Langenberg ¹⁰³,
 A.J. Lankford ¹⁶⁰, F. Lanni ³⁶, K. Lantzsch ²⁴, A. Lanza ^{73a}, A. Lapertosa ^{57b,57a},
 J.F. Laporte ¹³⁵, T. Lari ^{71a}, F. Lasagni Manghi ^{23b}, M. Lassnig ³⁶, V. Latonova ¹³¹,
 T.S. Lau ^{64a}, A. Laudrain ¹⁰⁰, A. Laurier ³⁴, S.D. Lawlor ⁹⁵, Z. Lawrence ¹⁰¹,
 M. Lazzaroni ^{71a,71b}, B. Le ¹⁰¹, B. Leban ⁹³, A. Lebedev ⁸¹, M. LeBlanc ³⁶, T. LeCompte ⁶,
 F. Ledroit-Guillon ⁶⁰, A.C.A. Lee ⁹⁶, G.R. Lee ¹⁶, L. Lee ⁶¹, S.C. Lee ¹⁴⁸, S. Lee ^{47a,47b},
 T.F. Lee ⁹², L.L. Leeuw ^{33c}, H.P. Lefebvre ⁹⁵, M. Lefebvre ¹⁶⁵, C. Leggett ^{17a}, K. Lehmann ¹⁴²,
 G. Lehmann Miotto ³⁶, M. Leigh ⁵⁶, W.A. Leight ¹⁰³, A. Leisos ^{152,v}, M.A.L. Leite ^{82c},
 C.E. Leitgeb ⁴⁸, R. Leitner ¹³³, K.J.C. Leney ⁴⁴, T. Lenz ²⁴, S. Leone ^{74a}, C. Leonidopoulos ⁵²,
 A. Leopold ¹⁴⁴, C. Leroy ¹⁰⁸, R. Les ¹⁰⁷, C.G. Lester ³², M. Levchenko ³⁷, J. Levêque ⁴,
 D. Levin ¹⁰⁶, L.J. Levinson ¹⁶⁹, M.P. Lewicki ⁸⁶, D.J. Lewis ⁴, A. Li ⁵, B. Li ^{62b}, C. Li ^{62a},
 C-Q. Li ^{62c}, H. Li ^{62a}, H. Li ^{62b}, H. Li ^{14c}, H. Li ^{62b}, J. Li ^{62c}, K. Li ¹³⁸, L. Li ^{62c},
 M. Li ^{14a,14d}, Q.Y. Li ^{62a}, S. Li ^{14a,14d}, S. Li ^{62d,62c,e}, T. Li ^{62b}, X. Li ¹⁰⁴, Z. Li ^{62b}, Z. Li ¹²⁶,
 Z. Li ¹⁰⁴, Z. Li ⁹², Z. Li ^{14a,14d}, Z. Liang ^{14a}, M. Liberatore ⁴⁸, B. Liberti ^{76a}, K. Lie ^{64c},
 J. Lieber Marin ^{82b}, K. Lin ¹⁰⁷, R.A. Linck ⁶⁸, R.E. Lindley ⁷, J.H. Lindon ², A. Linss ⁴⁸,
 E. Lipeles ¹²⁸, A. Lipniacka ¹⁶, A. Lister ¹⁶⁴, J.D. Little ⁴, B. Liu ^{14a}, B.X. Liu ¹⁴²,
 D. Liu ^{62d,62c}, J.B. Liu ^{62a}, J.K.K. Liu ³², K. Liu ^{62d,62c}, M. Liu ^{62a}, M.Y. Liu ^{62a}, P. Liu ^{14a},
 Q. Liu ^{62d,138,62c}, X. Liu ^{62a}, Y. Liu ^{14c,14d}, Y.L. Liu ¹⁰⁶, Y.W. Liu ^{62a}, M. Livan ^{73a,73b},
 J. Llorente Merino ¹⁴², S.L. Lloyd ⁹⁴, E.M. Lobodzinska ⁴⁸, P. Loch ⁷, S. Loffredo ^{76a,76b},
 T. Lohse ¹⁸, K. Lohwasser ¹³⁹, M. Lokajicek ^{131,*}, J.D. Long ¹⁶², I. Longarini ¹⁶⁰,












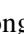



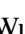

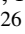



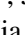


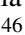

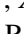



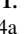








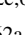


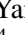

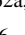

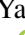
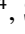

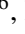


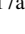

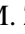

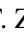


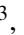




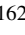

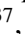


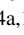


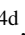
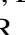

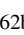
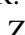
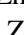


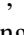
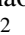


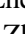
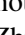

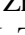



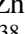

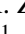
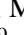


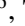
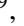

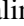
L. Longo [id70a,70b](#), R. Longo [id162](#), I. Lopez Paz [id67](#), A. Lopez Solis [id48](#), J. Lorenz [id109](#),
 N. Lorenzo Martinez [id4](#), A.M. Lory [id109](#), X. Lou [id47a,47b](#), X. Lou [id14a,14d](#), A. Lounis [id66](#), J. Love [id6](#),
 P.A. Love [id91](#), J.J. Lozano Bahilo [id163](#), G. Lu [id14a,14d](#), M. Lu [id80](#), S. Lu [id128](#), Y.J. Lu [id65](#),
 H.J. Lubatti [id138](#), C. Luci [id75a,75b](#), F.L. Lucio Alves [id14c](#), A. Lucotte [id60](#), F. Luehring [id68](#), I. Luise [id145](#),
 O. Lukianchuk [id66](#), O. Lundberg [id144](#), B. Lund-Jensen [id144](#), N.A. Luongo [id123](#), M.S. Lutz [id151](#),
 D. Lynn [id29](#), H. Lyons⁹², R. Lysak [id131](#), E. Lytken [id98](#), F. Lyu [id14a](#), V. Lyubushkin [id38](#),
 T. Lyubushkina [id38](#), M.M. Lyukova [id145](#), H. Ma [id29](#), L.L. Ma [id62b](#), Y. Ma [id96](#), D.M. Mac Donell [id165](#),
 G. Maccarrone [id53](#), J.C. MacDonald [id139](#), R. Madar [id40](#), W.F. Mader [id50](#), J. Maeda [id84](#), T. Maeno [id29](#),
 M. Maerker [id50](#), H. Maguire [id139](#), D.J. Mahon [id41](#), A. Maio [id130a,130b,130d](#), K. Maj [id85a](#),
 O. Majersky [id28a](#), S. Majewski [id123](#), N. Makovec [id66](#), V. Maksimovic [id15](#), B. Malaescu [id127](#),
 Pa. Malecki [id86](#), V.P. Maleev [id37](#), F. Malek [id60](#), D. Malito [id43b,43a](#), U. Mallik [id80](#), C. Malone [id32](#),
 S. Maltezos¹⁰, S. Malyukov³⁸, J. Mamuzic [id13](#), G. Mancini [id53](#), G. Manco [id73a,73b](#), J.P. Mandalia [id94](#),
 I. Mandić [id93](#), L. Manhaes de Andrade Filho [id82a](#), I.M. Maniatis [id169](#), J. Manjarres Ramos [id50](#),
 D.C. Mankad [id169](#), A. Mann [id109](#), B. Mansoulie [id135](#), S. Manzoni [id36](#), A. Marantis [id152,v](#),
 G. Marchiori [id5](#), M. Marcisovsky [id131](#), C. Marcon [id71a,71b](#), M. Marinescu [id20](#), M. Marjanovic [id120](#),
 E.J. Marshall [id91](#), Z. Marshall [id17a](#), S. Marti-Garcia [id163](#), T.A. Martin [id167](#), V.J. Martin [id52](#),
 B. Martin dit Latour [id16](#), L. Martinelli [id75a,75b](#), M. Martinez [id13,w](#), P. Martinez Agullo [id163](#),
 V.I. Martinez Outschoorn [id103](#), P. Martinez Suarez [id13](#), S. Martin-Haugh [id134](#), V.S. Martoiu [id27b](#),
 A.C. Martyniuk [id96](#), A. Marzin [id36](#), S.R. Maschek [id110](#), D. Mascione [id78a,78b](#), L. Masetti [id100](#),
 T. Mashimo [id153](#), J. Masik [id101](#), A.L. Maslennikov [id37](#), L. Massa [id23b](#), P. Massarotti [id72a,72b](#),
 P. Mastrandrea [id74a,74b](#), A. Mastroberardino [id43b,43a](#), T. Masubuchi [id153](#), T. Mathisen [id161](#),
 N. Matsuzawa¹⁵³, J. Maurer [id27b](#), B. Maček [id93](#), D.A. Maximov [id37](#), R. Mazini [id148](#), I. Maznas [id152,f](#),
 M. Mazza [id107](#), S.M. Mazza [id136](#), C. Mc Ginn [id29](#), J.P. Mc Gowan [id104](#), S.P. Mc Kee [id106](#),
 E.F. McDonald [id105](#), A.E. McDougall [id114](#), J.A. Mcfayden [id146](#), G. Mchedlidze [id149b](#),
 R.P. Mckenzie [id33g](#), T.C. Mclachlan [id48](#), D.J. Mclaughlin [id96](#), K.D. McLean [id165](#), S.J. McMahon [id134](#),
 P.C. McNamara [id105](#), C.M. Mcpartland [id92](#), R.A. McPherson [id165,aa](#), T. Megy [id40](#), S. Mehlhase [id109](#),
 A. Mehta [id92](#), B. Meirose [id45](#), D. Melini [id150](#), B.R. Mellado Garcia [id33g](#), A.H. Melo [id55](#),
 F. Meloni [id48](#), E.D. Mendes Gouveia [id130a](#), A.M. Mendes Jacques Da Costa [id20](#), H.Y. Meng [id155](#),
 L. Meng [id91](#), S. Menke [id110](#), M. Mentink [id36](#), E. Meoni [id43b,43a](#), C. Merlassino [id126](#),
 L. Merola [id72a,72b](#), C. Meroni [id71a](#), G. Merz¹⁰⁶, O. Meshkov [id37](#), J. Metcalfe [id6](#), A.S. Mete [id6](#),
 C. Meyer [id68](#), J-P. Meyer [id135](#), M. Michetti [id18](#), R.P. Middleton [id134](#), L. Mijović [id52](#),
 G. Mikenberg [id169](#), M. Mikesikova [id131](#), M. Mikuž [id93](#), H. Mildner [id139](#), A. Milic [id36](#),
 C.D. Milke [id44](#), D.W. Miller [id39](#), L.S. Miller [id34](#), A. Milov [id169](#), D.A. Milstead^{47a,47b}, T. Min^{14c},
 A.A. Minaenko [id37](#), I.A. Minashvili [id149b](#), L. Mince [id59](#), A.I. Mincer [id117](#), B. Mindur [id85a](#),
 M. Mineev [id38](#), Y. Mino [id87](#), L.M. Mir [id13](#), M. Miralles Lopez [id163](#), M. Mironova [id126](#),
 M.C. Missio [id113](#), T. Mitani [id168](#), A. Mitra [id167](#), V.A. Mitsou [id163](#), O. Miu [id155](#), P.S. Miyagawa [id94](#),
 Y. Miyazaki⁸⁹, A. Mizukami [id83](#), J.U. Mjörnmark [id98](#), T. Mkrtchyan [id63a](#), T. Mlinarevic [id96](#),
 M. Mlynarikova [id36](#), T. Moa [id47a,47b](#), S. Mobius [id55](#), K. Mochizuki [id108](#), P. Moder [id48](#), P. Mogg [id109](#),
 A.F. Mohammed [id14a,14d](#), S. Mohapatra [id41](#), G. Mokgatitswane [id33g](#), B. Mondal [id141](#), S. Mondal [id132](#),
 K. Mönig [id48](#), E. Monnier [id102](#), L. Monsonis Romero¹⁶³, J. Montejo Berlingen [id36](#), M. Montella [id119](#),
 F. Monticelli [id90](#), N. Morange [id66](#), A.L. Moreira De Carvalho [id130a](#), M. Moreno Llácer [id163](#),
 C. Moreno Martinez [id56](#), P. Morettini [id57b](#), S. Morgenstern [id167](#), M. Morii [id61](#), M. Morinaga [id153](#),
 A.K. Morley [id36](#), F. Morodei [id75a,75b](#), L. Morvaj [id36](#), P. Moschovakos [id36](#), B. Moser [id36](#),
 M. Mosidze^{149b}, T. Moskalets [id54](#), P. Moskvitina [id113](#), J. Moss [id31,p](#), E.J.W. Moyse [id103](#),
 O. Mtintsilana [id33g](#), S. Muanza [id102](#), J. Mueller [id129](#), D. Muenstermann [id91](#), R. Müller [id19](#),
 G.A. Mullier [id161](#), J.J. Mullin¹²⁸, D.P. Mungo [id155](#), J.L. Munoz Martinez [id13](#), D. Munoz Perez [id163](#),
 F.J. Munoz Sanchez [id101](#), M. Murin [id101](#), W.J. Murray [id167,134](#), A. Murrone [id71a,71b](#), J.M. Muse [id120](#),

M. Muškinja ^{17a}, C. Mwewa ²⁹, A.G. Myagkov ^{37,a}, A.J. Myers ⁸, A.A. Myers ¹²⁹, G. Myers ⁶⁸,
M. Myska ¹³², B.P. Nachman ^{17a}, O. Nackenhorst ⁴⁹, A. Nag ⁵⁰, K. Nagai ¹²⁶, K. Nagano ⁸³,
J.L. Nagle ^{29,an}, E. Nagy ¹⁰², A.M. Nairz ³⁶, Y. Nakahama ⁸³, K. Nakamura ⁸³, H. Nanjo ¹²⁴,
R. Narayan ⁴⁴, E.A. Narayanan ¹¹², I. Naryshkin ³⁷, M. Naseri ³⁴, C. Nass ²⁴, G. Navarro ^{22a},
J. Navarro-Gonzalez ¹⁶³, R. Nayak ¹⁵¹, A. Nayaz ¹⁸, P.Y. Nechaeva ³⁷, F. Nechansky ⁴⁸,
L. Nedic ¹²⁶, T.J. Neep ²⁰, A. Negri ^{73a,73b}, M. Negrini ^{23b}, C. Nellist ¹¹³, C. Nelson ¹⁰⁴,
K. Nelson ¹⁰⁶, S. Nemecek ¹³¹, M. Nessi ^{36,i}, M.S. Neubauer ¹⁶², F. Neuhaus ¹⁰⁰,
J. Neundorff ⁴⁸, R. Newhouse ¹⁶⁴, P.R. Newman ²⁰, C.W. Ng ¹²⁹, Y.S. Ng ¹⁸, Y.W.Y. Ng ⁴⁸,
B. Ngair ^{35e}, H.D.N. Nguyen ¹⁰⁸, R.B. Nickerson ¹²⁶, R. Nicolaidou ¹³⁵, J. Nielsen ¹³⁶,
M. Niemeyer ⁵⁵, N. Nikiforou ³⁶, V. Nikolaenko ^{37,a}, I. Nikolic-Audit ¹²⁷, K. Nikolopoulos ²⁰,
P. Nilsson ²⁹, I. Ninca ⁴⁸, H.R. Nindhito ⁵⁶, A. Nisati ^{75a}, N. Nishu ², R. Nisius ¹¹⁰,
J-E. Nitschke ⁵⁰, E.K. Nkadimeng ^{33g}, S.J. Noacco Rosende ⁹⁰, T. Nobe ¹⁵³, D.L. Noel ³²,
Y. Noguchi ⁸⁷, T. Nommensen ¹⁴⁷, M.A. Nomura ²⁹, M.B. Norfolk ¹³⁹, R.R.B. Norisam ⁹⁶,
B.J. Norman ³⁴, J. Novak ⁹³, T. Novak ⁴⁸, O. Novgorodova ⁵⁰, L. Novotny ¹³², R. Novotny ¹¹²,
L. Nozka ¹²², K. Ntekas ¹⁶⁰, N.M.J. Nunes De Moura Junior ^{82b}, E. Nurse ⁹⁶, F.G. Oakham ^{34,ak},
J. Ocariz ¹²⁷, A. Ochi ⁸⁴, I. Ochoa ^{130a}, S. Oerdek ¹⁶¹, J.T. Offermann ³⁹, A. Ogrodnik ^{85a},
A. Oh ¹⁰¹, C.C. Ohm ¹⁴⁴, H. Oide ⁸³, R. Oishi ¹⁵³, M.L. Ojeda ⁴⁸, Y. Okazaki ⁸⁷,
M.W. O'Keefe ⁹², Y. Okumura ¹⁵³, A. Olariu ^{27b}, L.F. Oleiro Seabra ^{130a}, S.A. Olivares Pino ^{137e},
D. Oliveira Damazio ²⁹, D. Oliveira Goncalves ^{82a}, J.L. Oliver ¹⁶⁰, M.J.R. Olsson ¹⁶⁰,
A. Olszewski ⁸⁶, J. Olszowska ^{86,*}, Ö.O. Öncel ⁵⁴, D.C. O'Neil ¹⁴², A.P. O'Neill ¹⁹,
A. Onofre ^{130a,130e}, P.U.E. Onyisi ¹¹, M.J. Oreglia ³⁹, G.E. Orellana ⁹⁰, D. Orestano ^{77a,77b},
N. Orlando ¹³, R.S. Orr ¹⁵⁵, V. O'Shea ⁵⁹, R. Ospanov ^{62a}, G. Otero y Garzon ³⁰, H. Otono ⁸⁹,
P.S. Ott ^{63a}, G.J. Ottino ^{17a}, M. Ouchrif ^{35d}, J. Ouellette ^{29,an}, F. Ould-Saada ¹²⁵, M. Owen ⁵⁹,
R.E. Owen ¹³⁴, K.Y. Oyulmaz ^{21a}, V.E. Ozcan ^{21a}, N. Ozturk ⁸, S. Ozturk ^{21d}, J. Pacalt ¹²²,
H.A. Pacey ³², K. Pachal ⁵¹, A. Pacheco Pages ¹³, C. Padilla Aranda ¹³, G. Padovano ^{75a,75b},
S. Pagan Griso ^{17a}, G. Palacino ⁶⁸, A. Palazzo ^{70a,70b}, S. Palestini ³⁶, M. Palka ^{85b}, J. Pan ¹⁷²,
T. Pan ^{64a}, D.K. Panchal ¹¹, C.E. Pandini ¹¹⁴, J.G. Panduro Vazquez ⁹⁵, H. Pang ^{14b}, P. Pani ⁴⁸,
G. Panizzo ^{69a,69c}, L. Paolozzi ⁵⁶, C. Papadatos ¹⁰⁸, S. Parajuli ⁴⁴, A. Paramonov ⁶,
C. Paraskevopoulos ¹⁰, D. Paredes Hernandez ^{64b}, T.H. Park ¹⁵⁵, M.A. Parker ³², F. Parodi ^{57b,57a},
E.W. Parrish ¹¹⁵, V.A. Parrish ⁵², J.A. Parsons ⁴¹, U. Parzefall ⁵⁴, B. Pascual Dias ¹⁰⁸,
L. Pascual Dominguez ¹⁵¹, V.R. Pascuzzi ^{17a}, F. Pasquali ¹¹⁴, E. Pasqualucci ^{75a}, S. Passaggio ^{57b},
F. Pastore ⁹⁵, P. Pasuwan ^{47a,47b}, P. Patel ⁸⁶, J.R. Pater ¹⁰¹, T. Pauly ³⁶, J. Pearkes ¹⁴³,
M. Pedersen ¹²⁵, R. Pedro ^{130a}, S.V. Peleganchuk ³⁷, O. Penc ³⁶, E.A. Pender ⁵², C. Peng ^{64b},
H. Peng ^{62a}, K.E. Pinski ¹⁰⁹, M. Penzin ³⁷, B.S. Peralva ^{82d}, A.P. Pereira Peixoto ⁶⁰,
L. Pereira Sanchez ^{47a,47b}, D.V. Perepelitsa ^{29,an}, E. Perez Codina ^{156a}, M. Perganti ¹⁰,
L. Perini ^{71a,71b,*}, H. Pernegger ³⁶, S. Perrella ³⁶, A. Perrevoort ¹¹³, O. Perrin ⁴⁰, K. Peters ⁴⁸,
R.F.Y. Peters ¹⁰¹, B.A. Petersen ³⁶, T.C. Petersen ⁴², E. Petit ¹⁰², V. Petousis ¹³²,
C. Petridou ^{152,f}, A. Petrukhin ¹⁴¹, M. Pettee ^{17a}, N.E. Pettersson ³⁶, A. Petukhov ³⁷,
K. Petukhova ¹³³, A. Peyaud ¹³⁵, R. Pezoa ^{137f}, L. Pezzotti ³⁶, G. Pezzullo ¹⁷², T.M. Pham ¹⁷⁰,
T. Pham ¹⁰⁵, P.W. Phillips ¹³⁴, M.W. Phipps ¹⁶², G. Piacquadio ¹⁴⁵, E. Pianori ^{17a},
F. Piazza ^{71a,71b}, R. Piegai ³⁰, D. Pietreanu ^{27b}, A.D. Pilkington ¹⁰¹, M. Pinamonti ^{69a,69c},
J.L. Pinfeld ², B.C. Pinheiro Pereira ^{130a}, C. Pitman Donaldson ⁹⁶, D.A. Pizzi ³⁴,
L. Pizzimento ^{76a,76b}, A. Pizzini ¹¹⁴, M.-A. Pleier ²⁹, V. Plesanovs ⁵⁴, V. Pleskot ¹³³, E. Plotnikova ³⁸,
G. Poddar ⁴, R. Poettgen ⁹⁸, L. Poggioli ¹²⁷, I. Pogrebnyak ¹⁰⁷, D. Pohl ²⁴, I. Pokharel ⁵⁵,
S. Polacek ¹³³, G. Polesello ^{73a}, A. Poley ^{142,156a}, R. Polifka ¹³², A. Polini ^{23b}, C.S. Pollard ¹⁶⁷,
Z.B. Pollock ¹¹⁹, V. Polychronakos ²⁹, E. Pompa Pacchi ^{75a,75b}, D. Ponomarenko ³⁷,
L. Pontecorvo ³⁶, S. Popa ^{27a}, G.A. Popeneciu ^{27d}, D.M. Portillo Quintero ^{156a}, S. Pospisil ¹³²,

P. Postolache [ID27c](#), K. Potamianos [ID126](#), I.N. Potrap [ID38](#), C.J. Potter [ID32](#), H. Potti [ID1](#), T. Poulsen [ID48](#),
 J. Poveda [ID163](#), M.E. Pozo Astigarraga [ID36](#), A. Prades Ibanez [ID163](#), M.M. Prapa [ID46](#), J. Pretel [ID54](#),
 D. Price [ID101](#), M. Primavera [ID70a](#), M.A. Principe Martin [ID99](#), R. Privara [ID122](#), M.L. Proffitt [ID138](#),
 N. Proklova [ID128](#), K. Prokofiev [ID64c](#), G. Proto [ID76a,76b](#), S. Protopopescu [ID29](#), J. Proudfoot [ID6](#),
 M. Przybycien [ID85a](#), J.E. Puddefoot [ID139](#), D. Pudzha [ID37](#), P. Puzo [ID66](#), D. Pyatiizbyantseva [ID37](#),
 J. Qian [ID106](#), D. Qichen [ID101](#), Y. Qin [ID101](#), T. Qiu [ID94](#), A. Quadt [ID55](#), M. Queitsch-Maitland [ID101](#),
 G. Quetant [ID56](#), G. Rabanal Bolanos [ID61](#), D. Rafanoharana [ID54](#), F. Ragusa [ID71a,71b](#), J.L. Rainbolt [ID39](#),
 J.A. Raine [ID56](#), S. Rajagopalan [ID29](#), E. Ramakoti [ID37](#), K. Ran [ID48,14d](#), N.P. Rapheeha [ID33g](#),
 V. Raskina [ID127](#), D.F. Rassloff [ID63a](#), S. Rave [ID100](#), B. Ravina [ID55](#), I. Ravinovich [ID169](#), M. Raymond [ID36](#),
 A.L. Read [ID125](#), N.P. Readioff [ID139](#), D.M. Rebutzi [ID73a,73b](#), G. Redlinger [ID29](#), K. Reeves [ID45](#),
 J.A. Reidelsturz [ID171](#), D. Reikher [ID151](#), A. Rej [ID141](#), C. Rembser [ID36](#), A. Renardi [ID48](#), M. Renda [ID27b](#),
 M.B. Rendel [ID110](#), F. Renner [ID48](#), A.G. Rennie [ID59](#), S. Resconi [ID71a](#), M. Ressegotti [ID57b,57a](#),
 E.D. Resseguie [ID17a](#), S. Rettie [ID36](#), J.G. Reyes Rivera [ID107](#), B. Reynolds [ID119](#), E. Reynolds [ID17a](#),
 M. Rezaei Estabragh [ID171](#), O.L. Rezanova [ID37](#), P. Reznicek [ID133](#), N. Ribaric [ID91](#), E. Ricci [ID78a,78b](#),
 R. Richter [ID110](#), S. Richter [ID47a,47b](#), E. Richter-Was [ID85b](#), M. Ridel [ID127](#), S. Ridouani [ID35d](#), P. Rieck [ID117](#),
 P. Riedler [ID36](#), M. Rijssenbeek [ID145](#), A. Rimoldi [ID73a,73b](#), M. Rimoldi [ID48](#), L. Rinaldi [ID23b,23a](#),
 T.T. Rinn [ID29](#), M.P. Rinnagel [ID109](#), G. Ripellino [ID144](#), I. Riu [ID13](#), P. Rivadeneira [ID48](#),
 J.C. Rivera Vergara [ID165](#), F. Rizatdinova [ID121](#), E. Rizvi [ID94](#), C. Rizzi [ID56](#), B.A. Roberts [ID167](#),
 B.R. Roberts [ID17a](#), S.H. Robertson [ID104,aa](#), M. Robin [ID48](#), D. Robinson [ID32](#), C.M. Robles Gajardo [ID137f](#),
 M. Robles Manzano [ID100](#), A. Robson [ID59](#), A. Rocchi [ID76a,76b](#), C. Roda [ID74a,74b](#), S. Rodriguez Bosca [ID63a](#),
 Y. Rodriguez Garcia [ID22a](#), A. Rodriguez Rodriguez [ID54](#), A.M. Rodríguez Vera [ID156b](#), S. Roe [ID36](#),
 J.T. Roemer [ID160](#), A.R. Roepe-Gier [ID120](#), J. Roggel [ID171](#), O. Røhne [ID125](#), R.A. Rojas [ID103](#),
 B. Roland [ID54](#), C.P.A. Roland [ID68](#), J. Roloff [ID29](#), A. Romaniouk [ID37](#), E. Romano [ID73a,73b](#),
 M. Romano [ID23b](#), A.C. Romero Hernandez [ID162](#), N. Rompotis [ID92](#), L. Roos [ID127](#), S. Rosati [ID75a](#),
 B.J. Rosser [ID39](#), E. Rossi [ID4](#), E. Rossi [ID72a,72b](#), L.P. Rossi [ID57b](#), L. Rossini [ID48](#), R. Rosten [ID119](#),
 M. Rotaru [ID27b](#), B. Rottler [ID54](#), C. Rougier [ID102,ae](#), D. Rousseau [ID66](#), D. Rousso [ID32](#), G. Rovelli [ID73a,73b](#),
 A. Roy [ID162](#), A. Rozanov [ID102](#), Y. Rozen [ID150](#), X. Ruan [ID33g](#), A. Rubio Jimenez [ID163](#), A.J. Ruby [ID92](#),
 V.H. Ruelas Rivera [ID18](#), T.A. Ruggeri [ID1](#), F. Rühr [ID54](#), A. Ruiz-Martinez [ID163](#), A. Rummler [ID36](#),
 Z. Rurikova [ID54](#), N.A. Rusakovich [ID38](#), H.L. Russell [ID165](#), J.P. Rutherford [ID7](#), K. Rybacki [ID91](#),
 M. Rybar [ID133](#), E.B. Rye [ID125](#), A. Ryzhov [ID37](#), J.A. Sabater Iglesias [ID56](#), P. Sabatini [ID163](#),
 L. Sabetta [ID75a,75b](#), H.F-W. Sadrozinski [ID136](#), F. Safai Tehrani [ID75a](#), B. Safarzadeh Samani [ID146](#),
 M. Safdari [ID143](#), S. Saha [ID104](#), M. Sahinsoy [ID110](#), M. Saimpert [ID135](#), M. Saito [ID153](#), T. Saito [ID153](#),
 D. Salamani [ID36](#), G. Salamanna [ID77a,77b](#), A. Salnikov [ID143](#), J. Salt [ID163](#), A. Salvador Salas [ID13](#),
 D. Salvatore [ID43b,43a](#), F. Salvatore [ID146](#), A. Salzburger [ID36](#), D. Sammel [ID54](#), D. Sampsonidis [ID152,f](#),
 D. Sampsonidou [ID62d,62c](#), J. Sánchez [ID163](#), A. Sanchez Pineda [ID4](#), V. Sanchez Sebastian [ID163](#),
 H. Sandaker [ID125](#), C.O. Sander [ID48](#), J.A. Sandesara [ID103](#), M. Sandhoff [ID171](#), C. Sandoval [ID22b](#),
 D.P.C. Sankey [ID134](#), T. Sano [ID87](#), A. Sansoni [ID53](#), L. Santi [ID75a,75b](#), C. Santoni [ID40](#), H. Santos [ID130a,130b](#),
 S.N. Santpur [ID17a](#), A. Santra [ID169](#), K.A. Saoucha [ID139](#), J.G. Saraiva [ID130a,130d](#), J. Sardain [ID7](#),
 O. Sasaki [ID83](#), K. Sato [ID157](#), C. Sauer [ID63b](#), F. Sauerburger [ID54](#), E. Sauvan [ID4](#), P. Savard [ID155,ak](#),
 R. Sawada [ID153](#), C. Sawyer [ID134](#), L. Sawyer [ID97](#), I. Sayago Galvan [ID163](#), C. Sbarra [ID23b](#), A. Sbrizzi [ID23b,23a](#),
 T. Scanlon [ID96](#), J. Schaarschmidt [ID138](#), P. Schacht [ID110](#), D. Schaefer [ID39](#), U. Schäfer [ID100](#),
 A.C. Schaffer [ID66,44](#), D. Schaile [ID109](#), R.D. Schamberger [ID145](#), E. Schanet [ID109](#), C. Scharf [ID18](#),
 M.M. Schefer [ID19](#), V.A. Schegelsky [ID37](#), D. Scheirich [ID133](#), F. Schenck [ID18](#), M. Schernau [ID160](#),
 C. Scheulen [ID55](#), C. Schiavi [ID57b,57a](#), Z.M. Schillaci [ID26](#), E.J. Schioppa [ID70a,70b](#), M. Schioppa [ID43b,43a](#),
 B. Schlag [ID100](#), K.E. Schleicher [ID54](#), S. Schlenker [ID36](#), J. Schmeing [ID171](#), M.A. Schmidt [ID171](#),
 K. Schmieden [ID100](#), C. Schmitt [ID100](#), S. Schmitt [ID48](#), L. Schoeffel [ID135](#), A. Schoening [ID63b](#),
 P.G. Scholer [ID54](#), E. Schopf [ID126](#), M. Schott [ID100](#), J. Schovancova [ID36](#), S. Schramm [ID56](#),

F. Schroeder ¹⁷¹, H-C. Schultz-Coulon ^{63a}, M. Schumacher ⁵⁴, B.A. Schumm ¹³⁶, Ph. Schune ¹³⁵,
 H.R. Schwartz ¹³⁶, A. Schwartzman ¹⁴³, T.A. Schwarz ¹⁰⁶, Ph. Schwemling ¹³⁵,
 R. Schwienhorst ¹⁰⁷, A. Sciandra ¹³⁶, G. Sciolla ²⁶, F. Scuri ^{74a}, F. Scutti ¹⁰⁵, C.D. Sebastiani ⁹²,
 K. Sedlaczek ⁴⁹, P. Seema ¹⁸, S.C. Seidel ¹¹², A. Seiden ¹³⁶, B.D. Seidlitz ⁴¹, C. Seitz ⁴⁸,
 J.M. Seixas ^{82b}, G. Sekhniaidze ^{72a}, S.J. Sekula ⁴⁴, L. Selem ⁴, N. Semprini-Cesari ^{23b,23a},
 S. Sen ⁵¹, D. Sengupta ⁵⁶, V. Senthilkumar ¹⁶³, L. Serin ⁶⁶, L. Serkin ^{69a,69b}, M. Sessa ^{77a,77b},
 H. Severini ¹²⁰, F. Sforza ^{57b,57a}, A. Sfyrta ⁵⁶, E. Shabalina ⁵⁵, R. Shaheen ¹⁴⁴,
 J.D. Shahinian ¹²⁸, D. Shaked Renous ¹⁶⁹, L.Y. Shan ^{14a}, M. Shapiro ^{17a}, A. Sharma ³⁶,
 A.S. Sharma ¹⁶⁴, P. Sharma ⁸⁰, S. Sharma ⁴⁸, P.B. Shatalov ³⁷, K. Shaw ¹⁴⁶, S.M. Shaw ¹⁰¹,
 Q. Shen ^{62c,5}, P. Sherwood ⁹⁶, L. Shi ⁹⁶, C.O. Shimmin ¹⁷², Y. Shimogama ¹⁶⁸, J.D. Shinner ⁹⁵,
 I.P.J. Shipsey ¹²⁶, S. Shirabe ⁶⁰, M. Shiyakova ^{38,y}, J. Shlomi ¹⁶⁹, M.J. Shochet ³⁹,
 J. Shojaii ¹⁰⁵, D.R. Shope ¹²⁵, S. Shrestha ^{119,ao}, E.M. Shrif ^{33g}, M.J. Shroff ¹⁶⁵, P. Sicho ¹³¹,
 A.M. Sickles ¹⁶², E. Sideras Haddad ^{33g}, A. Sidoti ^{23b}, F. Siegert ⁵⁰, Dj. Sijacki ¹⁵,
 R. Sikora ^{85a}, F. Sili ⁹⁰, J.M. Silva ²⁰, M.V. Silva Oliveira ³⁶, S.B. Silverstein ^{47a}, S. Simion ⁶⁶,
 R. Simoniello ³⁶, E.L. Simpson ⁵⁹, L.R. Simpson ¹⁰⁶, N.D. Simpson ⁹⁸, S. Simsek ^{21d},
 S. Sindhu ⁵⁵, P. Sinervo ¹⁵⁵, S. Singh ¹⁴², S. Singh ¹⁵⁵, S. Sinha ⁴⁸, S. Sinha ^{33g},
 M. Sioli ^{23b,23a}, I. Siral ³⁶, S.Yu. Sivoklov ^{37,*}, J. Sjölin ^{47a,47b}, A. Skaf ⁵⁵, E. Skorda ⁹⁸,
 P. Skubic ¹²⁰, M. Slawinska ⁸⁶, V. Smakhtin ¹⁶⁹, B.H. Smart ¹³⁴, J. Smiesko ³⁶, S.Yu. Smirnov ³⁷,
 Y. Smirnov ³⁷, L.N. Smirnova ^{37,a}, O. Smirnova ⁹⁸, A.C. Smith ⁴¹, E.A. Smith ³⁹,
 H.A. Smith ¹²⁶, J.L. Smith ⁹², R. Smith ¹⁴³, M. Smizanska ⁹¹, K. Smolek ¹³², A. Smykiewicz ⁸⁶,
 A.A. Snesarev ³⁷, H.L. Snoek ¹¹⁴, S. Snyder ²⁹, R. Sobie ^{165,aa}, A. Soffer ¹⁵¹,
 C.A. Solans Sanchez ³⁶, E.Yu. Soldatov ³⁷, U. Soldevila ¹⁶³, A.A. Solodkov ³⁷, S. Solomon ⁵⁴,
 A. Soloshenko ³⁸, K. Solovieva ⁵⁴, O.V. Solovyanov ⁴⁰, V. Solovyev ³⁷, P. Sommer ³⁶,
 A. Sonay ¹³, W.Y. Song ^{156b}, J.M. Sonneveld ¹¹⁴, A. Sopczak ¹³², A.L. Sopio ⁹⁶,
 F. Sopkova ^{28b}, V. Sothilingam ^{63a}, S. Sottocornola ⁶⁸, R. Soualah ^{116b}, Z. Soumami ^{35e},
 D. South ⁴⁸, S. Spagnolo ^{70a,70b}, M. Spalla ¹¹⁰, F. Spanò ⁹⁵, D. Sperlich ⁵⁴, G. Spigo ³⁶,
 M. Spina ¹⁴⁶, S. Spinali ⁹¹, D.P. Spiteri ⁵⁹, M. Spousta ¹³³, E.J. Staats ³⁴, A. Stabile ^{71a,71b},
 R. Stamen ^{63a}, M. Stamenkovic ¹¹⁴, A. Stampekis ²⁰, M. Standke ²⁴, E. Stanecka ⁸⁶,
 M.V. Stange ⁵⁰, B. Stanislaus ^{17a}, M.M. Stanitzki ⁴⁸, M. Stankaityte ¹²⁶, B. Stapf ⁴⁸,
 E.A. Starchenko ³⁷, G.H. Stark ¹³⁶, J. Stark ^{102,ae}, D.M. Staro ^{156b}, P. Staroba ¹³¹,
 P. Starovoitov ^{63a}, S. Stärz ¹⁰⁴, R. Staszewski ⁸⁶, G. Stavropoulos ⁴⁶, J. Steentoft ¹⁶¹,
 P. Steinberg ²⁹, A.L. Steinhebel ¹²³, B. Stelzer ^{142,156a}, H.J. Stelzer ¹²⁹, O. Stelzer-Chilton ^{156a},
 H. Stenzel ⁵⁸, T.J. Stevenson ¹⁴⁶, G.A. Stewart ³⁶, M.C. Stockton ³⁶, G. Stoicea ^{27b},
 M. Stolarski ^{130a}, S. Stonjek ¹¹⁰, A. Straessner ⁵⁰, J. Strandberg ¹⁴⁴, S. Strandberg ^{47a,47b},
 M. Strauss ¹²⁰, T. Strebler ¹⁰², P. Strizenec ^{28b}, R. Ströhmer ¹⁶⁶, D.M. Strom ¹²³, L.R. Strom ⁴⁸,
 R. Stroynowski ⁴⁴, A. Strubig ^{47a,47b}, S.A. Stucci ²⁹, B. Stugu ¹⁶, J. Stupak ¹²⁰, N.A. Styles ⁴⁸,
 D. Su ¹⁴³, S. Su ^{62a}, W. Su ^{62d,138,62c}, X. Su ^{62a,66}, K. Sugizaki ¹⁵³, V.V. Sulin ³⁷,
 M.J. Sullivan ⁹², D.M.S. Sultan ^{78a,78b}, L. Sultanaliyeva ³⁷, S. Sultansoy ^{3b}, T. Sumida ⁸⁷,
 S. Sun ¹⁰⁶, S. Sun ¹⁷⁰, O. Sunneborn Gudnadottir ¹⁶¹, M.R. Sutton ¹⁴⁶, M. Svatos ¹³¹,
 M. Swiatlowski ^{156a}, T. Swirski ¹⁶⁶, I. Sykora ^{28a}, M. Sykora ¹³³, T. Sykora ¹³³, D. Ta ¹⁰⁰,
 K. Tackmann ^{48,x}, A. Taffard ¹⁶⁰, R. Tafirout ^{156a}, J.S. Tafoya Vargas ⁶⁶, R.H.M. Taibah ¹²⁷,
 R. Takashima ⁸⁸, K. Takeda ⁸⁴, E.P. Takeva ⁵², Y. Takubo ⁸³, M. Talby ¹⁰², A.A. Talyshv ³⁷,
 K.C. Tam ^{64b}, N.M. Tamir ¹⁵¹, A. Tanaka ¹⁵³, J. Tanaka ¹⁵³, R. Tanaka ⁶⁶, M. Tanasini ^{57b,57a},
 J. Tang ^{62c}, Z. Tao ¹⁶⁴, S. Tapia Araya ^{137f}, S. Tapprogge ¹⁰⁰, A. Tarek Abouelfadl Mohamed ¹⁰⁷,
 S. Tarem ¹⁵⁰, K. Tariq ^{62b}, G. Tarna ^{102,27b}, G.F. Tartarelli ^{71a}, P. Tas ¹³³, M. Tasevsky ¹³¹,
 E. Tassi ^{43b,43a}, A.C. Tate ¹⁶², G. Tateno ¹⁵³, Y. Tayalati ^{35e,z}, G.N. Taylor ¹⁰⁵, W. Taylor ^{156b},
 H. Teagle ⁹², A.S. Tee ¹⁷⁰, R. Teixeira De Lima ¹⁴³, P. Teixeira-Dias ⁹⁵, J.J. Teoh ¹⁵⁵,

K. Terashi ¹⁵³, J. Terron ⁹⁹, S. Terzo ¹³, M. Testa ⁵³, R.J. Teuscher ^{155,aa}, A. Thaler ⁷⁹,
 O. Theiner ⁵⁶, N. Themistokleous ⁵², T. Thevenaux-Pelzer ¹⁸, O. Thielmann ¹⁷¹, D.W. Thomas⁹⁵,
 J.P. Thomas ²⁰, E.A. Thompson ⁴⁸, P.D. Thompson ²⁰, E. Thomson ¹²⁸, E.J. Thorpe ⁹⁴,
 Y. Tian ⁵⁵, V. Tikhomirov ^{37,a}, Yu.A. Tikhonov ³⁷, S. Timoshenko³⁷, E.X.L. Ting ¹, P. Tipton ¹⁷²,
 S. Tisserant ¹⁰², S.H. Tlou ^{33g}, A. Tnourji ⁴⁰, K. Todome ^{23b,23a}, S. Todorova-Nova ¹³³, S. Todt⁵⁰,
 M. Togawa ⁸³, J. Tojo ⁸⁹, S. Tokár ^{28a}, K. Tokushuku ⁸³, O. Toldaiev ⁶⁸, R. Tombs ³²,
 M. Tomoto ^{83,111}, L. Tompkins ^{143,r}, K.W. Topolnicki ^{85b}, P. Tornambe ¹⁰³, E. Torrence ¹²³,
 H. Torres ⁵⁰, E. Torró Pastor ¹⁶³, M. Toscani ³⁰, C. Tosciri ³⁹, M. Tost ¹¹, D.R. Tovey ¹³⁹,
 A. Traeet¹⁶, I.S. Trandafir ^{27b}, T. Trefzger ¹⁶⁶, A. Tricoli ²⁹, I.M. Trigger ^{156a},
 S. Trincaz-Duvoid ¹²⁷, D.A. Trischuk ²⁶, B. Trocmé ⁶⁰, A. Trofymov ⁶⁶, C. Troncon ^{71a},
 L. Truong ^{33c}, M. Trzebinski ⁸⁶, A. Trzupiek ⁸⁶, F. Tsai ¹⁴⁵, M. Tsai ¹⁰⁶, A. Tsiamis ^{152,f},
 P.V. Tsiareshka³⁷, S. Tsigaridas ^{156a}, A. Tsirigotis ^{152,v}, V. Tsiskaridze ¹⁴⁵, E.G. Tskhadadze^{149a},
 M. Tsopoulou ^{152,f}, Y. Tsujikawa ⁸⁷, I.I. Tsukerman ³⁷, V. Tsulaia ^{17a}, S. Tsuno ⁸³, O. Tsur¹⁵⁰,
 D. Tsybychev ¹⁴⁵, Y. Tu ^{64b}, A. Tudorache ^{27b}, V. Tudorache ^{27b}, A.N. Tuna ³⁶, S. Turchikhin ³⁸,
 I. Turk Cakir ^{3a}, R. Turra ^{71a}, T. Turtuvshin ^{38,ab}, P.M. Tuts ⁴¹, S. Tzamarias ^{152,f}, P. Tzanis ¹⁰,
 E. Tzovara ¹⁰⁰, K. Uchida¹⁵³, F. Ukegawa ¹⁵⁷, P.A. Ulloa Poblete ^{137c}, E.N. Umaka ²⁹,
 G. Unal ³⁶, M. Unal ¹¹, A. Undrus ²⁹, G. Unel ¹⁶⁰, J. Urban ^{28b}, P. Urquijo ¹⁰⁵, G. Usai ⁸,
 R. Ushioda ¹⁵⁴, M. Usman ¹⁰⁸, Z. Uysal ^{21b}, L. Vacavant ¹⁰², V. Vacek ¹³², B. Vachon ¹⁰⁴,
 K.O.H. Vadla ¹²⁵, T. Vafeiadis ³⁶, A. Vaitkus ⁹⁶, C. Valderanis ¹⁰⁹, E. Valdes Santurio ^{47a,47b},
 M. Valente ^{156a}, S. Valentinetti ^{23b,23a}, A. Valero ¹⁶³, A. Vallier ^{102,ae}, J.A. Valls Ferrer ¹⁶³,
 D.R. Van Arneman ¹¹⁴, T.R. Van Daalen ¹³⁸, P. Van Gemmeren ⁶, M. Van Rijnbach ^{125,36},
 S. Van Stroud ⁹⁶, I. Van Vulpen ¹¹⁴, M. Vanadia ^{76a,76b}, W. Vandelli ³⁶, M. Vandenbroucke ¹³⁵,
 E.R. Vandewall ¹²¹, D. Vannicola ¹⁵¹, L. Vannoli ^{57b,57a}, R. Vari ^{75a}, E.W. Varnes ⁷,
 C. Varni ^{17a}, T. Varol ¹⁴⁸, D. Varouchas ⁶⁶, L. Varriale ¹⁶³, K.E. Varvell ¹⁴⁷, M.E. Vasile ^{27b},
 L. Vaslin⁴⁰, G.A. Vasquez ¹⁶⁵, F. Vazeille ⁴⁰, T. Vazquez Schroeder ³⁶, J. Veatch ³¹,
 V. Vecchio ¹⁰¹, M.J. Veen ¹⁰³, I. Veliscek ¹²⁶, L.M. Veloce ¹⁵⁵, F. Veloso ^{130a,130c},
 S. Veneziano ^{75a}, A. Ventura ^{70a,70b}, A. Verbytskyi ¹¹⁰, M. Verducci ^{74a,74b}, C. Vergis ²⁴,
 M. Verissimo De Araujo ^{82b}, W. Verkerke ¹¹⁴, J.C. Vermeulen ¹¹⁴, C. Vernieri ¹⁴³,
 P.J. Verschuuren ⁹⁵, M. Vessella ¹⁰³, M.C. Vetterli ^{142,ak}, A. Vgenopoulos ^{152,f},
 N. Viaux Maira ^{137f}, T. Vickey ¹³⁹, O.E. Vickey Boeriu ¹³⁹, G.H.A. Viehhauser ¹²⁶, L. Vignani ^{63b},
 M. Villa ^{23b,23a}, M. Villaplana Perez ¹⁶³, E.M. Villhauer⁵², E. Vilucchi ⁵³, M.G. Vincter ³⁴,
 G.S. Virdee ²⁰, A. Vishwakarma ⁵², C. Vittori ^{23b,23a}, I. Vivarelli ¹⁴⁶, V. Vladimirov¹⁶⁷,
 E. Voevodina ¹¹⁰, F. Vogel ¹⁰⁹, P. Vokac ¹³², J. Von Ahnen ⁴⁸, E. Von Toerne ²⁴,
 B. Vormwald ³⁶, V. Vorobel ¹³³, K. Vorobev ³⁷, M. Vos ¹⁶³, K. Voss ¹⁴¹, J.H. Vosseveld ⁹²,
 M. Vozak ¹¹⁴, L. Vozdecky ⁹⁴, N. Vranjes ¹⁵, M. Vranjes Milosavljevic ¹⁵, M. Vreeswijk ¹¹⁴,
 R. Vuillermet ³⁶, O. Vujinovic ¹⁰⁰, I. Vukotic ³⁹, S. Wada ¹⁵⁷, C. Wagner¹⁰³, W. Wagner ¹⁷¹,
 S. Wahdan ¹⁷¹, H. Wahlberg ⁹⁰, R. Wakasa ¹⁵⁷, M. Wakida ¹¹¹, V.M. Walbrecht ¹¹⁰,
 J. Walder ¹³⁴, R. Walker ¹⁰⁹, W. Walkowiak ¹⁴¹, A.M. Wang ⁶¹, A.Z. Wang ¹⁷⁰, C. Wang ^{62a},
 C. Wang ^{62c}, H. Wang ^{17a}, J. Wang ^{64a}, R.-J. Wang ¹⁰⁰, R. Wang ⁶¹, R. Wang ⁶,
 S.M. Wang ¹⁴⁸, S. Wang ^{62b}, T. Wang ^{62a}, W.T. Wang ⁸⁰, X. Wang ^{14c}, X. Wang ¹⁶²,
 X. Wang ^{62c}, Y. Wang ^{62d}, Y. Wang ^{14c}, Z. Wang ¹⁰⁶, Z. Wang ^{62d,51,62c}, Z. Wang ¹⁰⁶,
 A. Warburton ¹⁰⁴, R.J. Ward ²⁰, N. Warrack ⁵⁹, A.T. Watson ²⁰, H. Watson ⁵⁹, M.F. Watson ²⁰,
 G. Watts ¹³⁸, B.M. Waugh ⁹⁶, A.F. Webb ¹¹, C. Weber ²⁹, H.A. Weber ¹⁸, M.S. Weber ¹⁹,
 S.M. Weber ^{63a}, C. Wei^{62a}, Y. Wei ¹²⁶, A.R. Weidberg ¹²⁶, J. Weingarten ⁴⁹, M. Weirich ¹⁰⁰,
 C. Weiser ⁵⁴, C.J. Wells ⁴⁸, T. Wenaus ²⁹, B. Wendland ⁴⁹, T. Wengler ³⁶, N.S. Wenke¹¹⁰,
 N. Wermes ²⁴, M. Wessels ^{63a}, K. Whalen ¹²³, A.M. Wharton ⁹¹, A.S. White ⁶¹, A. White ⁸,
 M.J. White ¹, D. Whiteson ¹⁶⁰, L. Wickremasinghe ¹²⁴, W. Wiedenmann ¹⁷⁰, C. Wiel ⁵⁰,

M. Wielers ¹³⁴, C. Wigglesworth ⁴², L.A.M. Wiik-Fuchs ⁵⁴, D.J. Wilbern¹²⁰, H.G. Wilkens ³⁶, D.M. Williams ⁴¹, H.H. Williams¹²⁸, S. Williams ³², S. Willocq ¹⁰³, P.J. Windischhofer ¹²⁶, F. Winklmeier ¹²³, B.T. Winter ⁵⁴, J.K. Winter ¹⁰¹, M. Wittgen¹⁴³, M. Wobisch ⁹⁷, R. Wölker ¹²⁶, J. Wollrath¹⁶⁰, M.W. Wolter ⁸⁶, H. Wolters ^{130a,130c}, V.W.S. Wong ¹⁶⁴, A.F. Wongel ⁴⁸, S.D. Worm ⁴⁸, B.K. Wosiek ⁸⁶, K.W. Woźniak ⁸⁶, K. Wraight ⁵⁹, J. Wu ^{14a,14d}, M. Wu ^{64a}, M. Wu ¹¹³, S.L. Wu ¹⁷⁰, X. Wu ⁵⁶, Y. Wu ^{62a}, Z. Wu ^{135,62a}, J. Wuerzinger ¹²⁶, T.R. Wyatt ¹⁰¹, B.M. Wynne ⁵², S. Xella ⁴², L. Xia ^{14c}, M. Xia ^{14b}, J. Xiang ^{64c}, X. Xiao ¹⁰⁶, M. Xie ^{62a}, X. Xie ^{62a}, S. Xin ^{14a,14d}, J. Xiong ^{17a}, I. Xiotidis¹⁴⁶, D. Xu ^{14a}, H. Xu^{62a}, H. Xu ^{62a}, L. Xu ^{62a}, R. Xu ¹²⁸, T. Xu ¹⁰⁶, W. Xu ¹⁰⁶, Y. Xu ^{14b}, Z. Xu ^{62b}, Z. Xu ^{14a}, B. Yabsley ¹⁴⁷, S. Yacoob ^{33a}, N. Yamaguchi ⁸⁹, Y. Yamaguchi ¹⁵⁴, H. Yamauchi ¹⁵⁷, T. Yamazaki ^{17a}, Y. Yamazaki ⁸⁴, J. Yan ^{62c}, S. Yan ¹²⁶, Z. Yan ²⁵, H.J. Yang ^{62c,62d}, H.T. Yang ^{62a}, S. Yang ^{62a}, T. Yang ^{64c}, X. Yang ^{62a}, X. Yang ^{14a}, Y. Yang ⁴⁴, Z. Yang ^{62a,106}, W.-M. Yao ^{17a}, Y.C. Yap ⁴⁸, H. Ye ^{14c}, H. Ye ⁵⁵, J. Ye ⁴⁴, S. Ye ²⁹, X. Ye ^{62a}, Y. Yeh ⁹⁶, I. Yeletsikh ³⁸, B.K. Yeo ^{17a}, M.R. Yexley ⁹¹, P. Yin ⁴¹, K. Yorita ¹⁶⁸, S. Younas ^{27b}, C.J.S. Young ⁵⁴, C. Young ¹⁴³, Y. Yu ^{62a}, M. Yuan ¹⁰⁶, R. Yuan ^{62b,1}, L. Yue ⁹⁶, X. Yue ^{63a}, M. Zaazoua ^{35e}, B. Zabinski ⁸⁶, E. Zaid⁵², T. Zakareishvili ^{149b}, N. Zakharchuk ³⁴, S. Zambito ⁵⁶, J.A. Zamora Saa ^{137d,137b}, J. Zang ¹⁵³, D. Zanzi ⁵⁴, O. Zaplatilek ¹³², S.V. Zeißner ⁴⁹, C. Zeitnitz ¹⁷¹, J.C. Zeng ¹⁶², D.T. Zenger Jr ²⁶, O. Zenin ³⁷, T. Ženiš ^{28a}, S. Zenz ⁹⁴, S. Zerradi ^{35a}, D. Zerwas ⁶⁶, M. Zhai ^{14a,14d}, B. Zhang ^{14c}, D.F. Zhang ¹³⁹, J. Zhang ^{62b}, J. Zhang ⁶, K. Zhang ^{14a,14d}, L. Zhang ^{14c}, P. Zhang ^{14a,14d}, R. Zhang ¹⁷⁰, S. Zhang ¹⁰⁶, T. Zhang ¹⁵³, X. Zhang ^{62c}, X. Zhang ^{62b}, Y. Zhang ^{62c,5}, Z. Zhang ^{17a}, Z. Zhang ⁶⁶, H. Zhao ¹³⁸, P. Zhao ⁵¹, T. Zhao ^{62b}, Y. Zhao ¹³⁶, Z. Zhao ^{62a}, A. Zhemchugov ³⁸, X. Zheng ^{62a}, Z. Zheng ¹⁴³, D. Zhong ¹⁶², B. Zhou¹⁰⁶, C. Zhou ¹⁷⁰, H. Zhou ⁷, N. Zhou ^{62c}, Y. Zhou⁷, C.G. Zhu ^{62b}, C. Zhu ^{14a,14d}, H.L. Zhu ^{62a}, H. Zhu ^{14a}, J. Zhu ¹⁰⁶, Y. Zhu ^{62c}, Y. Zhu ^{62a}, X. Zhuang ^{14a}, K. Zhukov ³⁷, V. Zhulanov ³⁷, N.I. Zimine ³⁸, J. Zinsser ^{63b}, M. Ziolkowski ¹⁴¹, L. Živković ¹⁵, A. Zoccoli ^{23b,23a}, K. Zoch ⁵⁶, T.G. Zorbas ¹³⁹, O. Zormpa ⁴⁶, W. Zou ⁴¹, L. Zwalinski ³⁶.

¹Department of Physics, University of Adelaide, Adelaide; Australia.

²Department of Physics, University of Alberta, Edmonton AB; Canada.

³(^a)Department of Physics, Ankara University, Ankara; (^b)Division of Physics, TOBB University of Economics and Technology, Ankara; Türkiye.

⁴LAPP, Université Savoie Mont Blanc, CNRS/IN2P3, Annecy; France.

⁵APC, Université Paris Cité, CNRS/IN2P3, Paris; France.

⁶High Energy Physics Division, Argonne National Laboratory, Argonne IL; United States of America.

⁷Department of Physics, University of Arizona, Tucson AZ; United States of America.

⁸Department of Physics, University of Texas at Arlington, Arlington TX; United States of America.

⁹Physics Department, National and Kapodistrian University of Athens, Athens; Greece.

¹⁰Physics Department, National Technical University of Athens, Zografou; Greece.

¹¹Department of Physics, University of Texas at Austin, Austin TX; United States of America.

¹²Institute of Physics, Azerbaijan Academy of Sciences, Baku; Azerbaijan.

¹³Institut de Física d'Altes Energies (IFAE), Barcelona Institute of Science and Technology, Barcelona; Spain.

¹⁴(^a)Institute of High Energy Physics, Chinese Academy of Sciences, Beijing; (^b)Physics Department, Tsinghua University, Beijing; (^c)Department of Physics, Nanjing University, Nanjing; (^d)University of Chinese Academy of Science (UCAS), Beijing; China.

¹⁵Institute of Physics, University of Belgrade, Belgrade; Serbia.

¹⁶Department for Physics and Technology, University of Bergen, Bergen; Norway.

- ^{17(a)}Physics Division, Lawrence Berkeley National Laboratory, Berkeley CA;^(b)University of California, Berkeley CA; United States of America.
- ¹⁸Institut für Physik, Humboldt Universität zu Berlin, Berlin; Germany.
- ¹⁹Albert Einstein Center for Fundamental Physics and Laboratory for High Energy Physics, University of Bern, Bern; Switzerland.
- ²⁰School of Physics and Astronomy, University of Birmingham, Birmingham; United Kingdom.
- ^{21(a)}Department of Physics, Bogazici University, Istanbul;^(b)Department of Physics Engineering, Gaziantep University, Gaziantep;^(c)Department of Physics, Istanbul University, Istanbul;^(d)Istinye University, Sariyer, Istanbul; Türkiye.
- ^{22(a)}Facultad de Ciencias y Centro de Investigaciones, Universidad Antonio Nariño, Bogotá;^(b)Departamento de Física, Universidad Nacional de Colombia, Bogotá; Colombia.
- ^{23(a)}Dipartimento di Fisica e Astronomia A. Righi, Università di Bologna, Bologna;^(b)INFN Sezione di Bologna; Italy.
- ²⁴Physikalisches Institut, Universität Bonn, Bonn; Germany.
- ²⁵Department of Physics, Boston University, Boston MA; United States of America.
- ²⁶Department of Physics, Brandeis University, Waltham MA; United States of America.
- ^{27(a)}Transilvania University of Brasov, Brasov;^(b)Horia Hulubei National Institute of Physics and Nuclear Engineering, Bucharest;^(c)Department of Physics, Alexandru Ioan Cuza University of Iasi, Iasi;^(d)National Institute for Research and Development of Isotopic and Molecular Technologies, Physics Department, Cluj-Napoca;^(e)University Politehnica Bucharest, Bucharest;^(f)West University in Timisoara, Timisoara;^(g)Faculty of Physics, University of Bucharest, Bucharest; Romania.
- ^{28(a)}Faculty of Mathematics, Physics and Informatics, Comenius University, Bratislava;^(b)Department of Subnuclear Physics, Institute of Experimental Physics of the Slovak Academy of Sciences, Kosice; Slovak Republic.
- ²⁹Physics Department, Brookhaven National Laboratory, Upton NY; United States of America.
- ³⁰Universidad de Buenos Aires, Facultad de Ciencias Exactas y Naturales, Departamento de Física, y CONICET, Instituto de Física de Buenos Aires (IFIBA), Buenos Aires; Argentina.
- ³¹California State University, CA; United States of America.
- ³²Cavendish Laboratory, University of Cambridge, Cambridge; United Kingdom.
- ^{33(a)}Department of Physics, University of Cape Town, Cape Town;^(b)iThemba Labs, Western Cape;^(c)Department of Mechanical Engineering Science, University of Johannesburg, Johannesburg;^(d)National Institute of Physics, University of the Philippines Diliman (Philippines);^(e)University of South Africa, Department of Physics, Pretoria;^(f)University of Zululand, KwaDlangezwa;^(g)School of Physics, University of the Witwatersrand, Johannesburg; South Africa.
- ³⁴Department of Physics, Carleton University, Ottawa ON; Canada.
- ^{35(a)}Faculté des Sciences Ain Chock, Réseau Universitaire de Physique des Hautes Energies - Université Hassan II, Casablanca;^(b)Faculté des Sciences, Université Ibn-Tofail, Kénitra;^(c)Faculté des Sciences Semlalia, Université Cadi Ayyad, LPHEA-Marrakech;^(d)LPMR, Faculté des Sciences, Université Mohamed Premier, Oujda;^(e)Faculté des sciences, Université Mohammed V, Rabat;^(f)Institute of Applied Physics, Mohammed VI Polytechnic University, Ben Guerir; Morocco.
- ³⁶CERN, Geneva; Switzerland.
- ³⁷Affiliated with an institute covered by a cooperation agreement with CERN.
- ³⁸Affiliated with an international laboratory covered by a cooperation agreement with CERN.
- ³⁹Enrico Fermi Institute, University of Chicago, Chicago IL; United States of America.
- ⁴⁰LPC, Université Clermont Auvergne, CNRS/IN2P3, Clermont-Ferrand; France.
- ⁴¹Nevis Laboratory, Columbia University, Irvington NY; United States of America.
- ⁴²Niels Bohr Institute, University of Copenhagen, Copenhagen; Denmark.

- ^{43(a)}Dipartimento di Fisica, Università della Calabria, Rende; ^(b)INFN Gruppo Collegato di Cosenza, Laboratori Nazionali di Frascati; Italy.
- ⁴⁴Physics Department, Southern Methodist University, Dallas TX; United States of America.
- ⁴⁵Physics Department, University of Texas at Dallas, Richardson TX; United States of America.
- ⁴⁶National Centre for Scientific Research "Demokritos", Agia Paraskevi; Greece.
- ^{47(a)}Department of Physics, Stockholm University; ^(b)Oskar Klein Centre, Stockholm; Sweden.
- ⁴⁸Deutsches Elektronen-Synchrotron DESY, Hamburg and Zeuthen; Germany.
- ⁴⁹Fakultät Physik, Technische Universität Dortmund, Dortmund; Germany.
- ⁵⁰Institut für Kern- und Teilchenphysik, Technische Universität Dresden, Dresden; Germany.
- ⁵¹Department of Physics, Duke University, Durham NC; United States of America.
- ⁵²SUPA - School of Physics and Astronomy, University of Edinburgh, Edinburgh; United Kingdom.
- ⁵³INFN e Laboratori Nazionali di Frascati, Frascati; Italy.
- ⁵⁴Physikalisches Institut, Albert-Ludwigs-Universität Freiburg, Freiburg; Germany.
- ⁵⁵II. Physikalisches Institut, Georg-August-Universität Göttingen, Göttingen; Germany.
- ⁵⁶Département de Physique Nucléaire et Corpusculaire, Université de Genève, Genève; Switzerland.
- ^{57(a)}Dipartimento di Fisica, Università di Genova, Genova; ^(b)INFN Sezione di Genova; Italy.
- ⁵⁸II. Physikalisches Institut, Justus-Liebig-Universität Giessen, Giessen; Germany.
- ⁵⁹SUPA - School of Physics and Astronomy, University of Glasgow, Glasgow; United Kingdom.
- ⁶⁰LPSC, Université Grenoble Alpes, CNRS/IN2P3, Grenoble INP, Grenoble; France.
- ⁶¹Laboratory for Particle Physics and Cosmology, Harvard University, Cambridge MA; United States of America.
- ^{62(a)}Department of Modern Physics and State Key Laboratory of Particle Detection and Electronics, University of Science and Technology of China, Hefei; ^(b)Institute of Frontier and Interdisciplinary Science and Key Laboratory of Particle Physics and Particle Irradiation (MOE), Shandong University, Qingdao; ^(c)School of Physics and Astronomy, Shanghai Jiao Tong University, Key Laboratory for Particle Astrophysics and Cosmology (MOE), SKLPPC, Shanghai; ^(d)Tsung-Dao Lee Institute, Shanghai; China.
- ^{63(a)}Kirchhoff-Institut für Physik, Ruprecht-Karls-Universität Heidelberg, Heidelberg; ^(b)Physikalisches Institut, Ruprecht-Karls-Universität Heidelberg, Heidelberg; Germany.
- ^{64(a)}Department of Physics, Chinese University of Hong Kong, Shatin, N.T., Hong Kong; ^(b)Department of Physics, University of Hong Kong, Hong Kong; ^(c)Department of Physics and Institute for Advanced Study, Hong Kong University of Science and Technology, Clear Water Bay, Kowloon, Hong Kong; China.
- ⁶⁵Department of Physics, National Tsing Hua University, Hsinchu; Taiwan.
- ⁶⁶IJCLab, Université Paris-Saclay, CNRS/IN2P3, 91405, Orsay; France.
- ⁶⁷Centro Nacional de Microelectrónica (IMB-CNM-CSIC), Barcelona; Spain.
- ⁶⁸Department of Physics, Indiana University, Bloomington IN; United States of America.
- ^{69(a)}INFN Gruppo Collegato di Udine, Sezione di Trieste, Udine; ^(b)ICTP, Trieste; ^(c)Dipartimento Politecnico di Ingegneria e Architettura, Università di Udine, Udine; Italy.
- ^{70(a)}INFN Sezione di Lecce; ^(b)Dipartimento di Matematica e Fisica, Università del Salento, Lecce; Italy.
- ^{71(a)}INFN Sezione di Milano; ^(b)Dipartimento di Fisica, Università di Milano, Milano; Italy.
- ^{72(a)}INFN Sezione di Napoli; ^(b)Dipartimento di Fisica, Università di Napoli, Napoli; Italy.
- ^{73(a)}INFN Sezione di Pavia; ^(b)Dipartimento di Fisica, Università di Pavia, Pavia; Italy.
- ^{74(a)}INFN Sezione di Pisa; ^(b)Dipartimento di Fisica E. Fermi, Università di Pisa, Pisa; Italy.
- ^{75(a)}INFN Sezione di Roma; ^(b)Dipartimento di Fisica, Sapienza Università di Roma, Roma; Italy.
- ^{76(a)}INFN Sezione di Roma Tor Vergata; ^(b)Dipartimento di Fisica, Università di Roma Tor Vergata, Roma; Italy.
- ^{77(a)}INFN Sezione di Roma Tre; ^(b)Dipartimento di Matematica e Fisica, Università Roma Tre, Roma; Italy.

- ⁷⁸(*a*) INFN-TIFPA; (*b*) Università degli Studi di Trento, Trento; Italy.
- ⁷⁹Universität Innsbruck, Department of Astro and Particle Physics, Innsbruck; Austria.
- ⁸⁰University of Iowa, Iowa City IA; United States of America.
- ⁸¹Department of Physics and Astronomy, Iowa State University, Ames IA; United States of America.
- ⁸²(*a*) Departamento de Engenharia Elétrica, Universidade Federal de Juiz de Fora (UFJF), Juiz de Fora; (*b*) Universidade Federal do Rio De Janeiro COPPE/EE/IF, Rio de Janeiro; (*c*) Instituto de Física, Universidade de São Paulo, São Paulo; (*d*) Rio de Janeiro State University, Rio de Janeiro; Brazil.
- ⁸³KEK, High Energy Accelerator Research Organization, Tsukuba; Japan.
- ⁸⁴Graduate School of Science, Kobe University, Kobe; Japan.
- ⁸⁵(*a*) AGH University of Science and Technology, Faculty of Physics and Applied Computer Science, Krakow; (*b*) Marian Smoluchowski Institute of Physics, Jagiellonian University, Krakow; Poland.
- ⁸⁶Institute of Nuclear Physics Polish Academy of Sciences, Krakow; Poland.
- ⁸⁷Faculty of Science, Kyoto University, Kyoto; Japan.
- ⁸⁸Kyoto University of Education, Kyoto; Japan.
- ⁸⁹Research Center for Advanced Particle Physics and Department of Physics, Kyushu University, Fukuoka ; Japan.
- ⁹⁰Instituto de Física La Plata, Universidad Nacional de La Plata and CONICET, La Plata; Argentina.
- ⁹¹Physics Department, Lancaster University, Lancaster; United Kingdom.
- ⁹²Oliver Lodge Laboratory, University of Liverpool, Liverpool; United Kingdom.
- ⁹³Department of Experimental Particle Physics, Jožef Stefan Institute and Department of Physics, University of Ljubljana, Ljubljana; Slovenia.
- ⁹⁴School of Physics and Astronomy, Queen Mary University of London, London; United Kingdom.
- ⁹⁵Department of Physics, Royal Holloway University of London, Egham; United Kingdom.
- ⁹⁶Department of Physics and Astronomy, University College London, London; United Kingdom.
- ⁹⁷Louisiana Tech University, Ruston LA; United States of America.
- ⁹⁸Fysiska institutionen, Lunds universitet, Lund; Sweden.
- ⁹⁹Departamento de Física Teórica C-15 and CIAFF, Universidad Autónoma de Madrid, Madrid; Spain.
- ¹⁰⁰Institut für Physik, Universität Mainz, Mainz; Germany.
- ¹⁰¹School of Physics and Astronomy, University of Manchester, Manchester; United Kingdom.
- ¹⁰²CPPM, Aix-Marseille Université, CNRS/IN2P3, Marseille; France.
- ¹⁰³Department of Physics, University of Massachusetts, Amherst MA; United States of America.
- ¹⁰⁴Department of Physics, McGill University, Montreal QC; Canada.
- ¹⁰⁵School of Physics, University of Melbourne, Victoria; Australia.
- ¹⁰⁶Department of Physics, University of Michigan, Ann Arbor MI; United States of America.
- ¹⁰⁷Department of Physics and Astronomy, Michigan State University, East Lansing MI; United States of America.
- ¹⁰⁸Group of Particle Physics, University of Montreal, Montreal QC; Canada.
- ¹⁰⁹Fakultät für Physik, Ludwig-Maximilians-Universität München, München; Germany.
- ¹¹⁰Max-Planck-Institut für Physik (Werner-Heisenberg-Institut), München; Germany.
- ¹¹¹Graduate School of Science and Kobayashi-Maskawa Institute, Nagoya University, Nagoya; Japan.
- ¹¹²Department of Physics and Astronomy, University of New Mexico, Albuquerque NM; United States of America.
- ¹¹³Institute for Mathematics, Astrophysics and Particle Physics, Radboud University/Nikhef, Nijmegen; Netherlands.
- ¹¹⁴Nikhef National Institute for Subatomic Physics and University of Amsterdam, Amsterdam; Netherlands.
- ¹¹⁵Department of Physics, Northern Illinois University, DeKalb IL; United States of America.

¹¹⁶(*a*) New York University Abu Dhabi, Abu Dhabi; (*b*) University of Sharjah, Sharjah; United Arab Emirates.

¹¹⁷Department of Physics, New York University, New York NY; United States of America.

¹¹⁸Ochanomizu University, Otsuka, Bunkyo-ku, Tokyo; Japan.

¹¹⁹Ohio State University, Columbus OH; United States of America.

¹²⁰Homer L. Dodge Department of Physics and Astronomy, University of Oklahoma, Norman OK; United States of America.

¹²¹Department of Physics, Oklahoma State University, Stillwater OK; United States of America.

¹²²Palacký University, Joint Laboratory of Optics, Olomouc; Czech Republic.

¹²³Institute for Fundamental Science, University of Oregon, Eugene, OR; United States of America.

¹²⁴Graduate School of Science, Osaka University, Osaka; Japan.

¹²⁵Department of Physics, University of Oslo, Oslo; Norway.

¹²⁶Department of Physics, Oxford University, Oxford; United Kingdom.

¹²⁷LPNHE, Sorbonne Université, Université Paris Cité, CNRS/IN2P3, Paris; France.

¹²⁸Department of Physics, University of Pennsylvania, Philadelphia PA; United States of America.

¹²⁹Department of Physics and Astronomy, University of Pittsburgh, Pittsburgh PA; United States of America.

¹³⁰(*a*) Laboratório de Instrumentação e Física Experimental de Partículas - LIP, Lisboa; (*b*) Departamento de Física, Faculdade de Ciências, Universidade de Lisboa, Lisboa; (*c*) Departamento de Física, Universidade de Coimbra, Coimbra; (*d*) Centro de Física Nuclear da Universidade de Lisboa, Lisboa; (*e*) Departamento de Física, Universidade do Minho, Braga; (*f*) Departamento de Física Teórica y del Cosmos, Universidad de Granada, Granada (Spain); (*g*) Departamento de Física, Instituto Superior Técnico, Universidade de Lisboa, Lisboa; Portugal.

¹³¹Institute of Physics of the Czech Academy of Sciences, Prague; Czech Republic.

¹³²Czech Technical University in Prague, Prague; Czech Republic.

¹³³Charles University, Faculty of Mathematics and Physics, Prague; Czech Republic.

¹³⁴Particle Physics Department, Rutherford Appleton Laboratory, Didcot; United Kingdom.

¹³⁵IRFU, CEA, Université Paris-Saclay, Gif-sur-Yvette; France.

¹³⁶Santa Cruz Institute for Particle Physics, University of California Santa Cruz, Santa Cruz CA; United States of America.

¹³⁷(*a*) Departamento de Física, Pontificia Universidad Católica de Chile, Santiago; (*b*) Millennium Institute for Subatomic physics at high energy frontier (SAPHIR), Santiago; (*c*) Instituto de Investigación Multidisciplinario en Ciencia y Tecnología, y Departamento de Física, Universidad de La Serena; (*d*) Universidad Andres Bello, Department of Physics, Santiago; (*e*) Instituto de Alta Investigación, Universidad de Tarapacá, Arica; (*f*) Departamento de Física, Universidad Técnica Federico Santa María, Valparaíso; Chile.

¹³⁸Department of Physics, University of Washington, Seattle WA; United States of America.

¹³⁹Department of Physics and Astronomy, University of Sheffield, Sheffield; United Kingdom.

¹⁴⁰Department of Physics, Shinshu University, Nagano; Japan.

¹⁴¹Department Physik, Universität Siegen, Siegen; Germany.

¹⁴²Department of Physics, Simon Fraser University, Burnaby BC; Canada.

¹⁴³SLAC National Accelerator Laboratory, Stanford CA; United States of America.

¹⁴⁴Department of Physics, Royal Institute of Technology, Stockholm; Sweden.

¹⁴⁵Departments of Physics and Astronomy, Stony Brook University, Stony Brook NY; United States of America.

¹⁴⁶Department of Physics and Astronomy, University of Sussex, Brighton; United Kingdom.

¹⁴⁷School of Physics, University of Sydney, Sydney; Australia.

- ¹⁴⁸Institute of Physics, Academia Sinica, Taipei; Taiwan.
- ¹⁴⁹^(a)E. Andronikashvili Institute of Physics, Iv. Javakhishvili Tbilisi State University, Tbilisi;^(b)High Energy Physics Institute, Tbilisi State University, Tbilisi;^(c)University of Georgia, Tbilisi; Georgia.
- ¹⁵⁰Department of Physics, Technion, Israel Institute of Technology, Haifa; Israel.
- ¹⁵¹Raymond and Beverly Sackler School of Physics and Astronomy, Tel Aviv University, Tel Aviv; Israel.
- ¹⁵²Department of Physics, Aristotle University of Thessaloniki, Thessaloniki; Greece.
- ¹⁵³International Center for Elementary Particle Physics and Department of Physics, University of Tokyo, Tokyo; Japan.
- ¹⁵⁴Department of Physics, Tokyo Institute of Technology, Tokyo; Japan.
- ¹⁵⁵Department of Physics, University of Toronto, Toronto ON; Canada.
- ¹⁵⁶^(a)TRIUMF, Vancouver BC;^(b)Department of Physics and Astronomy, York University, Toronto ON; Canada.
- ¹⁵⁷Division of Physics and Tomonaga Center for the History of the Universe, Faculty of Pure and Applied Sciences, University of Tsukuba, Tsukuba; Japan.
- ¹⁵⁸Department of Physics and Astronomy, Tufts University, Medford MA; United States of America.
- ¹⁵⁹United Arab Emirates University, Al Ain; United Arab Emirates.
- ¹⁶⁰Department of Physics and Astronomy, University of California Irvine, Irvine CA; United States of America.
- ¹⁶¹Department of Physics and Astronomy, University of Uppsala, Uppsala; Sweden.
- ¹⁶²Department of Physics, University of Illinois, Urbana IL; United States of America.
- ¹⁶³Instituto de Física Corpuscular (IFIC), Centro Mixto Universidad de Valencia - CSIC, Valencia; Spain.
- ¹⁶⁴Department of Physics, University of British Columbia, Vancouver BC; Canada.
- ¹⁶⁵Department of Physics and Astronomy, University of Victoria, Victoria BC; Canada.
- ¹⁶⁶Fakultät für Physik und Astronomie, Julius-Maximilians-Universität Würzburg, Würzburg; Germany.
- ¹⁶⁷Department of Physics, University of Warwick, Coventry; United Kingdom.
- ¹⁶⁸Waseda University, Tokyo; Japan.
- ¹⁶⁹Department of Particle Physics and Astrophysics, Weizmann Institute of Science, Rehovot; Israel.
- ¹⁷⁰Department of Physics, University of Wisconsin, Madison WI; United States of America.
- ¹⁷¹Fakultät für Mathematik und Naturwissenschaften, Fachgruppe Physik, Bergische Universität Wuppertal, Wuppertal; Germany.
- ¹⁷²Department of Physics, Yale University, New Haven CT; United States of America.
- ^a Also Affiliated with an institute covered by a cooperation agreement with CERN.
- ^b Also at An-Najah National University, Nablus; Palestine.
- ^c Also at Borough of Manhattan Community College, City University of New York, New York NY; United States of America.
- ^d Also at Bruno Kessler Foundation, Trento; Italy.
- ^e Also at Center for High Energy Physics, Peking University; China.
- ^f Also at Center for Interdisciplinary Research and Innovation (CIRI-AUTH), Thessaloniki ; Greece.
- ^g Also at Centro Studi e Ricerche Enrico Fermi; Italy.
- ^h Also at CERN, Geneva; Switzerland.
- ⁱ Also at Département de Physique Nucléaire et Corpusculaire, Université de Genève, Genève; Switzerland.
- ^j Also at Departament de Física de la Universitat Autònoma de Barcelona, Barcelona; Spain.
- ^k Also at Department of Financial and Management Engineering, University of the Aegean, Chios; Greece.
- ^l Also at Department of Physics and Astronomy, Michigan State University, East Lansing MI; United States of America.
- ^m Also at Department of Physics and Astronomy, University of Louisville, Louisville, KY; United States of America.

- ⁿ Also at Department of Physics, Ben Gurion University of the Negev, Beer Sheva; Israel.
- ^o Also at Department of Physics, California State University, East Bay; United States of America.
- ^p Also at Department of Physics, California State University, Sacramento; United States of America.
- ^q Also at Department of Physics, King's College London, London; United Kingdom.
- ^r Also at Department of Physics, Stanford University, Stanford CA; United States of America.
- ^s Also at Department of Physics, University of Fribourg, Fribourg; Switzerland.
- ^t Also at Department of Physics, University of Thessaly; Greece.
- ^u Also at Department of Physics, Westmont College, Santa Barbara; United States of America.
- ^v Also at Hellenic Open University, Patras; Greece.
- ^w Also at Institutio Catalana de Recerca i Estudis Avancats, ICREA, Barcelona; Spain.
- ^x Also at Institut für Experimentalphysik, Universität Hamburg, Hamburg; Germany.
- ^y Also at Institute for Nuclear Research and Nuclear Energy (INRNE) of the Bulgarian Academy of Sciences, Sofia; Bulgaria.
- ^z Also at Institute of Applied Physics, Mohammed VI Polytechnic University, Ben Guerir; Morocco.
- ^{aa} Also at Institute of Particle Physics (IPP); Canada.
- ^{ab} Also at Institute of Physics and Technology, Ulaanbaatar; Mongolia.
- ^{ac} Also at Institute of Physics, Azerbaijan Academy of Sciences, Baku; Azerbaijan.
- ^{ad} Also at Institute of Theoretical Physics, Ilia State University, Tbilisi; Georgia.
- ^{ae} Also at L2IT, Université de Toulouse, CNRS/IN2P3, UPS, Toulouse; France.
- ^{af} Also at Lawrence Livermore National Laboratory, Livermore; United States of America.
- ^{ag} Also at National Institute of Physics, University of the Philippines Diliman (Philippines); Philippines.
- ^{ah} Also at RWTH Aachen University, III. Physikalisches Institut A, Aachen; Germany.
- ^{ai} Also at Technical University of Munich, Munich; Germany.
- ^{aj} Also at The Collaborative Innovation Center of Quantum Matter (CICQM), Beijing; China.
- ^{ak} Also at TRIUMF, Vancouver BC; Canada.
- ^{al} Also at Università di Napoli Parthenope, Napoli; Italy.
- ^{am} Also at University of Chinese Academy of Sciences (UCAS), Beijing; China.
- ^{an} Also at University of Colorado Boulder, Department of Physics, Colorado; United States of America.
- ^{ao} Also at Washington College, Maryland; United States of America.
- ^{ap} Also at Yeditepe University, Physics Department, Istanbul; Türkiye.
- * Deceased